THE SYNTHESIS, CHARACTERIZATION, AND USE OF A PROTEIN-CYSTEINE PROTEINASE INHIBITOR COMPLEX FOR THE STUDY OF ENDOSOME/LYSOSOME FUSION

by

Adele K. Mountz

Dissertation to the Faculty of the
Virginia Polytechnic Institute and State University

in partial fulfillment of the requirements for the degree of

DOCTOR OF PHILOSOPHY

in

Biochemistry and Anaerobic Microbiology

APPROVED:

R. W. Mason , Chairman

W. E. Newton

N. Castagnoli

E. M. Gregory

D. R. Bevan

May, 1994
Blacksburg, Virginia

THE SYNTHESIS, CHARACTERIZATION, AND USE OF A PROTEIN-CYSTEINE PROTEINASE INHIBITOR COMPLEX FOR THE STUDY OF ENDOSOME/LYSOSOME FUSION

by

Adele K. Mountz

(ABSTRACT)

The cysteine proteinases cathepsins B, L, and S are lysosomal enzymes responsible for the degradation of endocytosed proteins. Their presence in human cell monocytic lines THP1 and U937 was detected by the use of the membrane-permeable, irreversible, active-site directed inhibitor Fmoc-(^{125}I)Tyr-Ala-CHN_2 followed by immunoprecipitation of the enzymes, SDS-PAGE, and autoradiography. All three enzymes were detected in THP1 cells; only after differentiation of U937 cells to macrophage-like cells were the enzymes detectable. Both cell lines show multiple forms of cathepsin S, at 35 kDa, 28 kDa, and 26 kDa, suggesting the presence of an active pro-form of cathepsin S as well as the processing of cathepsin S into single- and two-chain forms. This is the first evidence for an active pro-form of a cysteine proteinase and for the processing of cathepsin S to a two-chain enzyme form. Multiple forms of cathepsin L were analyzed by iso-electric focusing followed by denaturing polyacrylamide gel electrophoresis. The multiple forms are not due to the presence of carbohydrate chains on the protein.

The inhibitor Fmoc-Tyr-Ala-CHN_2 was synthesized and its inhibitory properties against cathepsins B, L, and S were determined. Both *in vitro* and *in vivo* studies show that this inhibitor is an effective reagent for studying lysosomal cysteine proteinases. In order to be useful in the study of the delivery of lysosomal enzymes to vesicles containing recently internalized compounds, the deblocked peptidyl diazomethane inhibitor NH_2-Tyr-Ala-CHN_2 was cross-linked to bovine serum albumin (BSA) using the heterobifunctional cross-linking agent sulfo-SANPAH. This non-reducible cross-linked complex was used to characterize the inhibitory properties of the protein-inhibitor complex against cathepsins B, L, S and papain *in vitro* and *in vivo*.

ACKNOWLEDGEMENTS

I would like to thank my advisor Dr. R.W. Mason and the members of my committee for their guidance and support. I would also like to thank all the co-workers in the laboratory for our many discussions, both scientific and social. A special thanks to Barbara Spence for our talks about life in general.

I would like especially to thank my family for their love and support through out my entire education.

And most of all, I would like to thank my best friend and fiancee, Shawn Addington, for putting up with me through out this ordeal. I'll be there for you, too.

This work was supported by NSF grant # MCB 9304109 and the Council for Tobacco Research, Inc.

TABLE OF CONTENTS

LIST OF FIGURES

LIST OF TABLES

LIST OF ABBREVIATIONS

ammediol	2-amino-2-methyl-propanediol
APS	ammonium persulfate
BOC	t-butyloxycarbonyl
Brij-35	polyoxyethylene 23-laurylether
BSA	bovine serum albumin
CD-MPR	cation dependent mannose 6-phosphate receptor
CH_2N_2	diazomethane
$-CHN_2$	diazomethyl group
CI-MPR	cation independent mannose 6-phosphate receptor
CM-BSA	carboxymethyl cysteine bovine serum albumin
DAB	3,3'-diaminobenzidine tetrahydrochloride
DMEM	Dulbecco's modified essential medium
DMSO	dimethyl sulfoxide
DTNB	5,5'-dithiobis[2-nitrobenzoate]
DTT	dithiothreitol
E-64	L-trans-epoxysuccinyl-leucylamido [4-guanidino] butane
E-64d	ethyl(+)-(2S,3S)-3-[(S)-methyl-1-(3-methyl-1-(3-methylbutyl-carbomyl)-butylcarbamoyl]-2-oxirane carboxylate
EDTA	ethylenediamine tetraacetic acid
EP-475	L-trans-epoxysuccinyl-leucylamido[3-methyl] butane
FBS	fetal bovine serum
Fmoc-	9-fluorenylmethyloxycarbonyl
FU	fluorescence units

h	hour(s)
HPLC	high pressure liquid chromatography
hrp	horseradish peroxidase
IEF	isoelectric focusing
IgG	immunoglobulin G
kDa	kilo-Dalton
KNIH 3T3	Kirsten-virus transformed NIH-3T3 mouse fibroblasts
M	molar
MHC	major histocompatability complex
min	minute(s)
MPR	mannose 6-phosphate receptor
MS	mass spectrometry
MS-MS	tandem mass spectrometry
NHMec	7-amino-4-methylcoumarin
NIH	National Institutes of Health
NP-40	nonidet P-40
NTB	2-nitro-5-thiobenzoate
NTSB	2-nitro-5-thiosulfobenzoate
PAS	protein-A Sepharose
PBS	phosphate buffered saline
PGS	protein-G Sepharose
PLC	prelysosomal compartment
PMA	12-O-tetradecanoylphorbol-13-acetate
PNGase F	protein N-glycosidase F
PTH	parathyroid hormone
RCM	radial compression matrix

s	second(s)
SDS	sodium dodecyl sulfate
SDS-PAGE	sodium dodecyl sulfate polyacrylamide gel electrophoresis
sulfo-SADP	sulfosuccinimidyl (4-azidophenyldithio) proprionate
sulfo-SANPAH	sulfosuccinimidyl 6-(4'azido-2'-nitrophenylamino) hexanoate
TC	tubulovesicular compartment
TEMED	N,N,N',N'-tetramethylethylenediamine
TfR	transferrin receptor
TGN	trans Golgi network
THF	tetrahydrofuran
TRIS	2-amino-2-(hydroxymethyl)-1,3-propanediol
Z-	carboxybenzyl

CHAPTER 1 LITERATURE REVIEW

Cells internalize compounds from the extracellular environment via the process of endocytosis. Once inside the cell in membrane-bound vesicles, substances destined to be degraded are transported to lysosomes, either by passing through pre-existing late endosomes or by the maturation of the vesicle in which the substances reside into late endosomes and lysosomes. Exactly when internalized compounds first meet active lysosomal hydrolases is not clear. Immunocytochemical methods detect both active and inactive (pro-) forms of lysosomal enzymes. Identification of lysosomal hydrolases present in vesicles separated by subcellular fractionation procedures is clouded by incomplete separation of endosomes, lysosomes, and microsomes. The internalization of compounds that can tag specific active lysosomal proteinases would clearly identify which, if any, of the proteinases are present in endocytic vesicles. This thesis describes the synthesis and characterization of a prototype of such a compound. A protein carrier molecule was covalently cross-linked to a specific active-site-directed inhibitor of cysteine proteinases and the complex analyzed for its ability to interact irreversibly with the lysosomal cysteine proteinases cathepsins B, L, and S. Cellular forms of these enzymes were also identified by the use of a membrane permeable form of the

inhibitor.

1.1 Endocytosis

Endocytosis is the process by which substances in the extracellular environment are internalized by cells into membrane-bound vesicles. Three general routes have been described: phagocytosis ("cell eating", or the uptake of large particles such as whole bacteria by macrophages); pinocytosis ("cell drinking", or the nonspecific uptake of small substances); and receptor-mediated endocytosis (an extracellular ligand specifically binds a cell surface receptor and the receptor-ligand complex is internalized into small vesicles). Pinocytosis occurs during both phagocytosis and receptor-mediated endocytosis. Not all substances taken into cells by receptor-mediated endocytosis are internalized at the same rate. One class of receptors is clustered in specific regions of the plasma membrane, in clathrin-coated pits, and these are rapidly internalized once ligand is bound. A second type of receptor aggregates in coated pits only after ligand has bound to the receptor. A third type does not aggregate into coated pits, regardless of the presence of bound ligand; receptor-ligand complexes are internalized nonetheless.

Many receptors of the type located in coated pits contain an essential Tyr residue in a tight loop in their cytoplasmic

tails located 6 or 7 amino acid residues from the transmembrane domain (Collawn et al. 1990; Chen 1990; Ktistakis et al. 1990). This motif is thought to be recognized by the clathrin assembly protein AP2 (Pearse 1988; Glickman 1989; Beltzer and Speiss 1991; Smythe et al. 1992). AP2 is hypothesized to mediate the assembly of clathrin triskilions into the polygonal coat lattice below receptors to be internalized. GTP-binding proteins have also been shown to be involved in coated pit assembly, invagination, and budding (Carter et al. 1993). Once formed, clathrin is removed from the vesicle by the heat shock protein hsc70 (DeLuca-Flaherty et al. 1990).

The vesicles formed by invagination and budding of clathrin-coated pits fuse with each other and with larger early endosomes after the clathrin coat has been removed. The factors required for such endocytic membrane fusions are not fully characterized, although they are thought to be very similar to those required for membrane fusion events in the transport of proteins from the endoplasmic reticulum to the Golgi body and for fusion events in protein transfer from one section of the Golgi to the next (Hunziker et al. 1992). AP2 is implicated in the aggregation of the uncoated vesicles for lateral fusion events and for fusion with endosomes (Beck et al. 1992). Small GTP binding proteins (Bucci et al. 1992; van der Sluijs et al. 1992; Wessling-Resnick et al. 1990), an ADP-

ribosylation factor (Lenhard et al. 1992), N-ethylmaleimide sensitive factors (Wessling-Resnick et al. 1990), and endosomal membrane proteins (Emans et al. 1993) all seem to be involved in the fusion mechanism.

1.1.1 Acidification

Early endosomes have an acidic pH of 6.0 - 6.2 (Gruenberg 1989), which facilitates the uncoupling of ligand from receptors, freeing the receptors to recycle to the plasma membrane. The decreased pH is achieved by the activity of a H^+-ATPase. Known as the V-ATPase, it is distinct from other cellular ATPases based on sensitivity (or lack there of) to a variety of reagents such as N-ethylmaleimide, vanadate, oligomycin, aurovertin, dicyclohexylcarbodiimide, and balifomycin. It contains two domains: the cytoplasmic V_1 domain, which contains the ATP binding site, and the transmembrane V_0 domain, which houses the proton channel. It has been immunolocalized to endosomes, lysosomes, parts of the Golgi complex, the plasma membrane, and small vesicles just inside the plasma membrane (Marquez-Sterling et al. 1991). Acidification of internalized vesicles does not occur, however, until they reach the endosome responsible for uncoupling of ligands from receptors (early endosome, or "CURL"), even though the V-ATPase is present. Many models for control of the V-ATPase have been proposed, including changes

in subunit composition, changes in the number of V-ATPases present in a given compartment, control of coupling of ATP hydrolysis and protein translocation, inactivity of separated V_1 and V_0 domains, and the control of the Cl^- channel present in the vesicles necessary for maintaining electrical neutrality across the membrane (reviewed in Forac 1992a,b). Additional studies suggest also that a Na^+ flux is necessary (Gaete et al. 1991). Casciola-Rosen et al. (1992) have identified a Na^+/K^+-ATPase present in early and late endosomes and they propose that it may be important in the regulation of vesicular pH.

1.1.2 Late Endosomes

After dissociation of ligands from their receptors, the receptors and bulk membrane are recycled back to the plasma membrane (Mayor et al. 1993) while the fluid content proceeds towards late endosomes and lysosomes. Late endosomes are described as being more dense and more acidic (pH 5.5 -6.0, Gruenberg 1989) than early endosomes. They are located towards the perinuclear region of the cell as compared to the proximity of early endosomes to the cell periphery. Late endosomes have been described as multi-vesicular bodies because they often appear to contain internal membrane swirls. Other names for late endosomes include "endolysosome" and the "prelysosomal compartment" (PLC). These structures are

distinct from lysosomes even though they contain lysosomal membrane markers because they contain mannose 6-phosphate receptors. Parks et al. (1991) have identified the membrane glycoprotein plpg 57 as a distinct marker for late endosomes. The protein rab7 is also a marker for late endosomes as it is not seen in early endosomes or lysosomes.

1.1.3 Maturation versus Vesicle Delivery Models

Two different hypotheses exist as to how contents of early endosomes end up in late endosomes and lysosomes: the maturation model and the vesicle delivery model (Helenius et al. 1983). The maturation model suggests that each early endosome matures to a late endosome and to a lysosome, with vesicles delivering lysosomal proteins to the endosome over time, such that the vesicle eventually acquires a full battery of lysosomal proteins. The endosomal contents are not selectively removed for transport to another compartment.

The vesicle delivery model, however, states that there are pre-existing cellular compartments to which internalized compounds are shuttled. An internalized ligand buds from the early endosome into a small delivery vesicle, which then fuses with another pre-existing organelle (the late endosome). The partially digested ligand is then removed from this organelle and transferred to the lysosome for complete degradation.

The primary difference between the two models is that the

maturation model states that the internalized compounds never leave the vesicle in which they were originally internalized, while the hydrolytic enzyme content and membrane components of the vesicle changes. The delivery model suggests that the internalized molecules are removed from early endosomes and delivered to a pre-existing late endosome. Recently, a number of studies have concluded that early endosomes mature into late endosomes and lysosomes (Stoorvogel et al. 1991; Dunn and Mafield 1992; Roederer et al. 1990; Casciola-Rosen et al. 1991). Racoosin and Swansen (1993), however, present data suggesting that the initial stages of endocytosis occur by a maturation process, while the last step occurs by vesicle delivery of endosomal contents to a pre-existing, stable lysosome.

1.2 Lysosome Biogenesis

Lysosomes are subcellular organelles with a high density and low internal pH (4.5 to 5.0). They are the site of complete degradation of internalized ligands and are accessible to fluid-phase markers. Their biogenesis can best be described by the biosynthesis of lysosomal hydrolases.

1.2.1 Co-translational Insertion of Lysosomal Proteins into the Endoplasmic Reticulum

Proteins destined for lysosomes are co-translationally

inserted into the endoplasmic reticulum (ER). Such proteins contain an N-terminal signal (pre-) sequence, which directs their recognition and, thus, insertion through the ER membrane by proteins of the signal recognition particle (SRP) (Walter and Blobel 1980). The SRP, after binding to the recently translated peptide signal sequence from ribosome-bound mRNA, inhibits further translation. It then carries the ribosome complex to the ER and docks with resident ER membrane proteins (Gilmore et al. 1982 a,b; Meyer et al. 1982), anchoring the ribosome and nascent chain to the organelle. The SRP then leaves the ER-bound ribosome, removing the translational inhibition. Once internalized, the N-terminal signal sequence is proteolytically removed (Conner et al. 1987). The rest of the polypeptide chain continues to be inserted as it is translated. Folding of the polypeptide occurs during and after insertion and is facilitated by chaperone proteins. Disulfide bonds also form during or soon after protein synthesis and insertion through the ER membrane.

1.2.2 Glycosylation

Once the entire folded peptide is inside the ER, it is glycosylated at Asn sites in the sequence Asn-X-Ser/Thr, where X represents any amino acid except Pro or Asp (Marshall 1972). A common precursor branched oligosaccharide complex containing three glucose, nine mannose, and two N-acetylglucosamine

residues is transferred en bloc to the Asn in the above motif by the enzyme oligosaccharide transferase from a dolichol phosphate lipid anchor. Immediately following the transfer, the three glucose residues are removed by two different enzymes: glucosidase I (Atkinson and Lee 1984) and glucosidase II (Hubbard and Robins 1979). Up to 4 mannose residues can be removed by ER mannosidases. Resident ER proteins persist in the high mannose oligosaccharide form.

Further oligosaccharide processing occurs as proteins are transported from the ER to the cis Golgi via non-clathrin coated vesicles in an ATP-dependent manner (Farquhar and Palade 1981). The mechanism of vesicle fusion between the ER and Golgi components is similar to that involved in vesicle fusion along the endocytic pathway, although the specific proteins involved differ. Resident ER proteins contain a C-terminal sequence Lys-Asp-Glu-Leu ("KDEL") (reviewed by Pelham et al. 1990); proteins lacking this motif proceed through the Golgi complex by default, while proteins containing the "KDEL" sequence are retrieved and transported back to the ER.

Some lysosomal enzymes contain "complex" carbohydrate chains, in which the remaining mannose residues have been removed and N-acetylglucosamine, galactose, and sialic acid added. Other lysosomal enzymes contain oligosaccharides of the high mannose type as found in the ER. In the Golgi complex, most soluble lysosomal enzymes are phosphorylated on

carbon-6 of a terminal mannose residue. The enzyme UDP-N-acetyl glucosamine : lysosomal enzyme N-acetyl glucosamine phosphotransferase catalyzes the addition of N-acetyl glucosamine phosphate via a phosphodiester bond to the mannose residue; the enzyme N-acetyl glucosamine-1-phosphodiester α-N-acetyl glucosaminidase then removes N-acetyl glucosamine, leaving the phosphate attached to the mannose residue of the oligosaccharide chain. The transferase seems to modify selectively only proteins destined for lysosomes. It has been suggested that the transferase recognizes some unidentified conformational feature of lysosomal enzymes (Kornfeld 1987).

1.2.3 Mannose 6-Phosphate Receptors

The presence of mannose 6-phosphate on soluble lysosomal enzymes is the primary feature of these enzymes that targets them for lysosomal delivery. Two classes of mannose 6-phosphate receptor (MPR) have been identified: the 215 kDa or cation-independent MPR (CI-MPR, Sahagian et al. 1981), and the 46 kDa or cation-dependent MPR (CD-MPR, Hoflack and Kornfeld 1985). Both receptor types have been immunolocalized to the trans Golgi network (TGN), early and late endosomes, and the plasma membrane. Klumperman et al. (1993) have found, however, that the CD-MPR and CI-MPR have different endosomal distributions. The CD-MPR is more rapidly segregated into more electron-dense tubules and vesicles associated with endosomes

than is the CI-MPR, implying that the CD-MPR is more rapidly recycled to the TGN. Studies of the sequence of the CI-MPR revealed 99% identity with the insulin-like growth factor II (IGF II) receptor (Morgan et al. 1987; Oshima et al. 1988). Biochemical studies have shown that the same receptor binds both mannose 6-phosphate and IGF II at different binding sites (Keiss et al. 1988; MacDonald 1988; Waheed 1989). Both the CD- and CI-MPR bind to mannose 6-phosphate with high affinity at pH 6-7, but with low affinity at pH 5.5 (Fisher et al. 1980, Hoflack et al. 1987, Tong et al. 1989a,b); the receptors release their ligand at low pH once delivered to early or late endosomes. Chao et al. (1990) have evidence that the CD-MPR is also involved with the enhanced secretion of newly synthesized lysosomal enzymes either by transporting them directly to the plasma membrane or by releasing their bound ligand in early endosomes. The bound ligand is reeleased due to the lowered pH, where the free ligands can cycle to the plasma membrane in the small vesicles that are returning plasma membrane receptor molecules. Hoflack and Lobel (1993) have reviewed the structure and function of both the CI- and CD-MPR.

1.2.4 Additional Targeting Mechanisms

Lysosomal membrane proteins are thought to be targeted to lysosomes by sequences in their cytoplasmic tails. The

protein lgp120 (lgp A) is reported to contain a Gly-Tyr motif similar to the plasma membrane receptor internalization motif (Section 1.1.1; Harter and Mellman 1992) as does the protein lamp 1 (Carlsson and Fukuda 1992). The exact path taken in the delivery of lysosomal membrane proteins is not clear. Mathews et al. (1992) report that LEP 100 is initially targeted to either the plasma membrane or early endosomes before proceeding to lysosomes. The cytoplasmic domain is most likely recognized by the same adaptor proteins as plasma membrane receptors and internalized by a similar mechanism. Other reports (Harter and Mellman 1992; Green et al. 1987), however, suggest that lysosomal membrane proteins are segregated from plasma membrane-destined proteins at the TGN, and that the delivery to the plasma membrane of lysosomal membrane proteins is not necessary or kinetically possible. Carlsson and Fukada (1992) suggest that both initial plasma membrane and lysosomal targeting occur, with the majority, but not all, of lysosomal membrane proteins being delivered to lysosomes.

1.2.5 An Alternative View

In a recent study, Rabinowitz et al. (1992) suggested a different model for the delivery of endocytosed compounds for degradation. They propose that internalized ligands first enter coated pits, which fuse with a large pre-existing

tubulo-vesicular endosome. From there, endosomal carrier vesicles bud off and transport the internalized molecules to a large tubular compartment equivalent to the PLC, where degradation occurs (the functional lysosome). Dense spherical lysosomal vesicles which contain hydrolytic enzymes and degradation products pinch off the TC. These vesicles are hypothesized to be only storage sites for the degradative hydrolases.

1.3 Lysosomal Cysteine Proteinases

Lysosomes are the site of degradation of compounds internalized from the extracellular milieu. These organelles of acidic lumenal pH (4.5-5.0) contain hydrolytic enzymes such as glycosidases, phosphatases, lipases, and proteinases. Proteinases, in general, are classified with respect to the enzyme site at which catalysis occurs. The major classes are metallo-proteinases, in which a metal ion, usually Zn^{+2}, is involved in the catalytic mechanism; aspartic; serine; and cysteine proteinases. Cathepsins B, H, L, and S are the most fully characterized of the lysosomal cysteine proteinases (EC # 3.4.22).

1.3.1 Catalytic Mechanism and Active Site Structure

Cathepsins B, H, L, and S are members of a family of sequence- and mechanism- related proteinases found in a wide

variety of species including plants, animals, and microorganisms. The best-studied cysteine proteinase is papain (EC 3.4.22.2), derived from the unripe papaya fruit latex (Carica papaya). The catalytic mechanism of papain is thought to be identical to that of lysosomal cysteine proteinases based on sequence homologies. The essential cysteine residue (Cys 25 in papain) and the role of its sulfhydryl group in catalysis was first demonstrated by Finkle and Smith (1958). A nearby histidine residue (His 159) aids in catalysis by forming an ion pair between the sulfhydryl proton and histidine imidazole group, generating a thiolate ion ($R\text{-}S^-$) (Polgar 1973). The sulfhydryl in cysteine normally has an pKa of 8, but the proximity of His 159 in the enzyme active site drops the pKa to 4, thus facilitating the proton transfer. Conversely, the pKa of the histidine side chain rises to 8.0. Papain and related cathepsins B and L therefore have a pH optima ranging from 4 to 8. As shown in Figure 1.1, the thiolate ion attacks the carbonyl carbon of the scissile peptide bond, initially forming a tetrahedral acylated enzyme intermediate (Lowe and Williams 1965). The oxy-anion then re-forms the carbonyl with a proton transferred from the imidazole group to the neighboring amino group, cleaving the bond with the amino group. Water enters the active site where His 159 abstracts a proton and the remaining hydroxyl groups attacks the carbonyl carbon, forming a

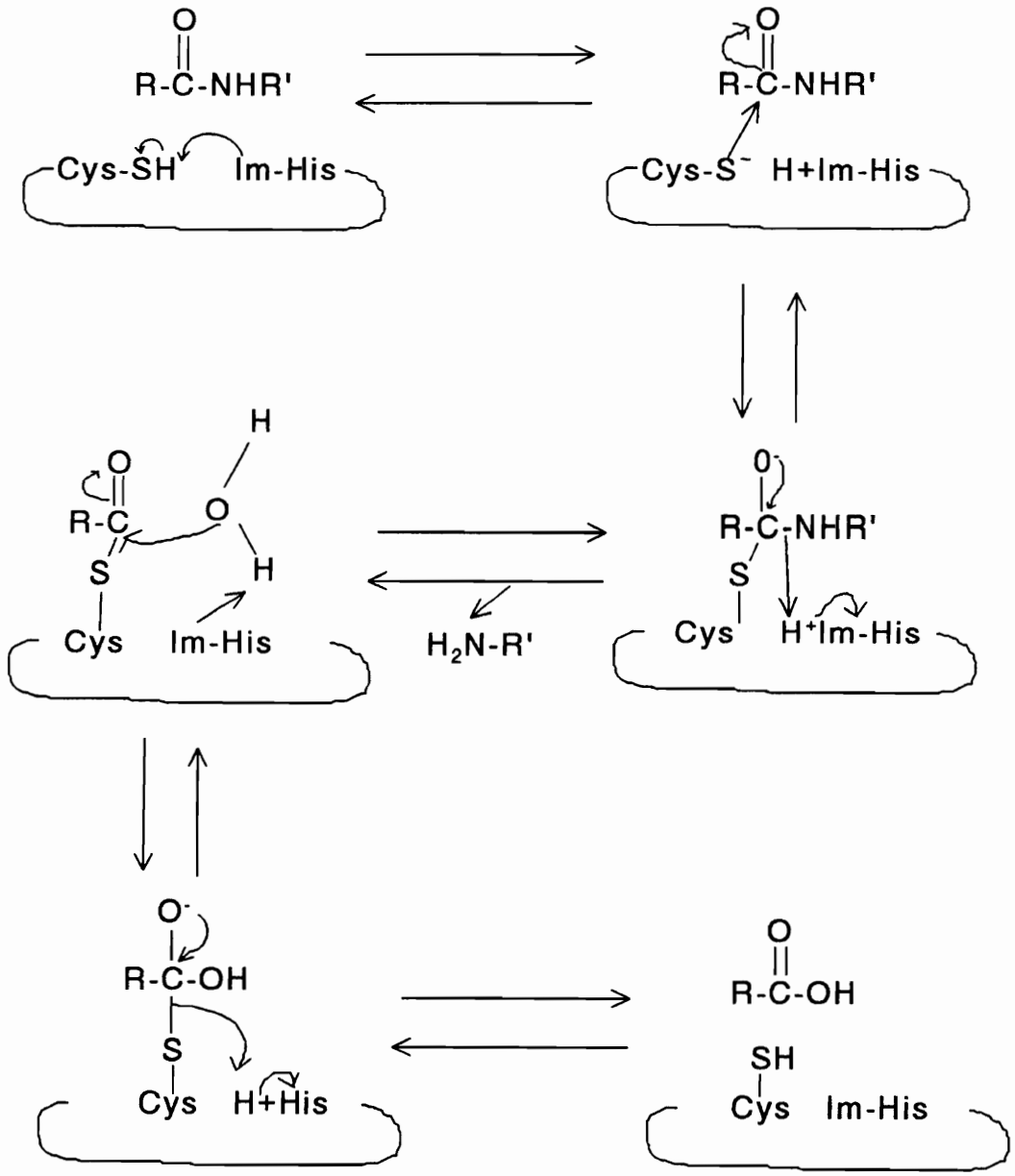

Figure 1.1 The Catalytic Mechanism of Cysteine Proteinases (taken from Rich 1986)

tetrahedral oxy-anion intermediate. Re-formation of the carbonyl bond to oxygen causes breakage of the bond to the cysteine sulfur, freeing the N-terminal peptide from the active site. The resulting thiolate ion abstracts the proton from His 159, returning the active site to its initial conformation.

Both papain and cathepsin B have been crystallized and their structures defined (Kamphuis 1985; Musil et al. 1991). The overall folding pattern and arrangements of active site residues are similar, even though cathepsin B contains small insertion loops on the surface. These loops can occlude specific substrate binding sites, explaining the dipeptidyl carboxypeptidase activity of cathepsin B and its insensitivity to inhibition by cystatin-like proteins.

Although cathepsins L, H, and S have not been crystallized, a great deal of information has been deduced about their active site structures based on synthetic substrate and inhibitor specificities. A general model of proteinase active site, proposed by Schechter and Berger (1967) (Figure 1.2), included up to 7 sub-sites in the enzyme (S_n to S_n') for binding specific amino acid residues in the substrate (P_n to P_n'). P' sites are located on the C-terminal side of the scissile bond accommodated by the S' subsites of the enzyme.

As reviewed by Mason and Wilcox (1993), the active sites

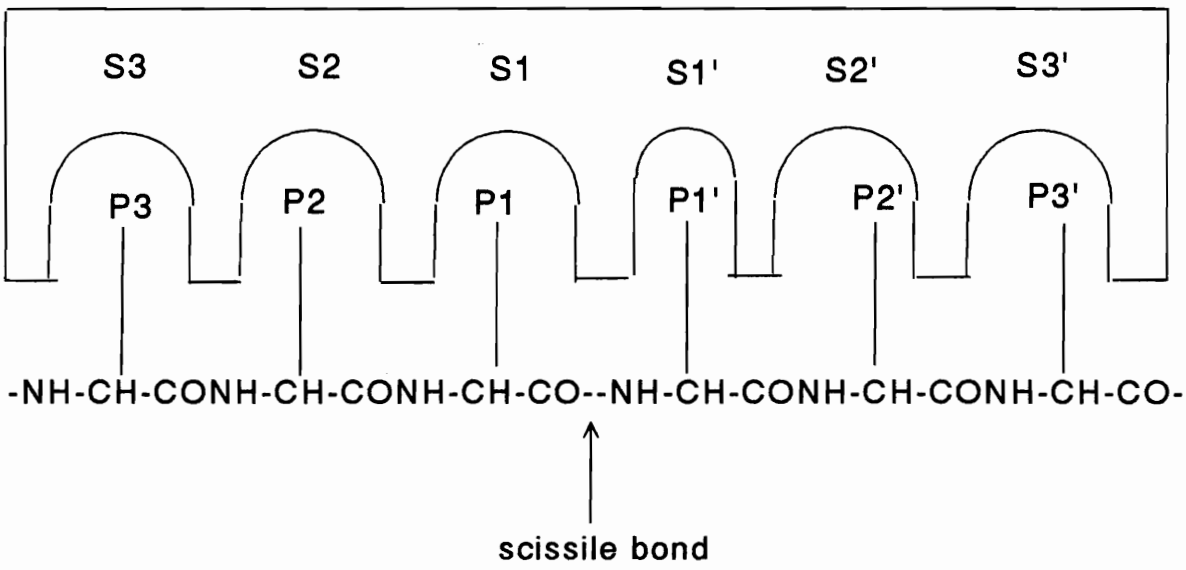

Figure 1.2 The Schechter & Berger (1967) Model for the Active Site of Papain

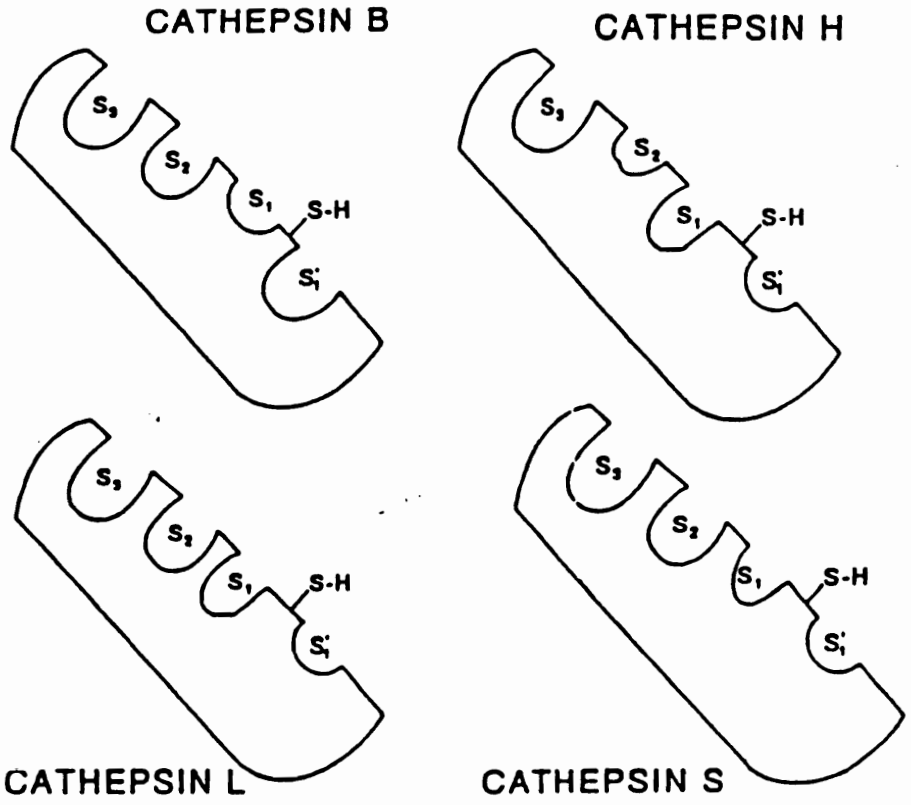

Figure 1.3 Peptide Binding Subsites in Cathepsins B, H, L, and S

of cathepsins B, H, L, and S have been modeled (Figure 1.3). Cathepsin B prefers large amino acids in the P_2 and P_3 positions, while discriminating against large bulky groups at P_1. Studies of the exopeptidase activity of cathepsin B show the ability of the enzyme to bind large residues in the S_1' site. Thus, cathepsin B seems to accommodate large groups in the S_2, S_3, and S_1' sites, while only small residues can fit into the S_1 site. Cathepsin H can be differentiated from the other lysosomal cysteine proteinases based on its inability to accommodate large residues at P_2, implying a small S_2 site (Xin et al. 1992). It also has a small S_1' site. Cathepsin L is unique in having large pockets in S_3, S_2, and S_1 sites. The subtle differences in size of the S_1 and S_2 sites in cathepsin S (with S_2 more restricted in cathepsin S) is likely responsible for its lower activity against the synthetic substrate carboxybenzyl-Phe-Arg-N-methylcoumarin (Z-Phe-Arg-NHMec) than cathepsin L and its decreased sensitivity to the inhibitor carboxybenzyl-Phe-Phe-CHN_2. Cathepsin S is also unique in that it can hydrolyze insoluble elastin at both acidic and neutral pH (Xin et al. 1992). Table 1.1 describes the minimal criteria necessary to distinguish cathepsins B, H, L, and S from each other. Differences in active site structures have been used to design affinity chromatography columns for cathepsin B (Rich et al. 1986 b).

Table 1.1 Minimal Criteria to Distinguish Between Cathepsins B, H, L, and S

enzyme	Z-Arg-Arg-NHMec	Z-Phe-Arg NHMec	Arg-NHMec	Bz-Phe-Val-Arg-NHMec	Z-Leu-Leu-Tyr-CHN_2	Z-Tyr-Ala-CHN_2
B	++ pH6.0	+++	+	ND	-	I
H	+	+	++ pH6.8	ND	I	-
L	+	+++	+	+	I	I
S	+	++	+	+++	I	I

\+ low activity
++ moderate activity
+++ high activity
I inhibitory
\- weakly or not inhibitory
ND not determined
Z carboxybenzyl
NHMec N-methyl-coumarin

*adapted from Mason and Wilcox (1993)

1.3.2 Biosynthesis of Lysosomal Cysteine Proteinases

Being lysosomal enzymes, cathepsins B, H, L, and S are co-translationally inserted into the ER as directed by their signal (pre-) sequences (Gal and Gottesman 1988; Joseph et al. 1988; Portnoy et al. 1986; Chan et al. 1986; Ishidoh et al. 1987). Transit through the ER results in proteolytic removal of the signal sequence and addition of N-linked high mannose oligosaccharides (see Section 1.2); lysosomal targeting of these enzymes has been shown to occur primarily by the MPR pathway. These enzymes must remain inactive during transit to lysosomes to prevent degradation of the biosynthetic machinery. After removal of the signal (pre-) sequence, the enzymes are present in the ER as inactive pro-enzymes. A synthetic peptide corresponding to the pro-region of cathepsin B is a slow-binding reversible inhibitor of cathepsin B (Fox et al. 1992). This peptide blocks access of substrates to the enzyme active site, binding across the active-site in a pH dependent manner, with tighter binding at higher pH. It does not, however, inhibit other cysteine proteinases, such as papain. Removal of the N-terminal pro-sequence during transport to lysosomes results in activation of the enzymes. Cathepsins B, H, and L undergo further proteolytic processing in lysosomes to two-chain forms (see Figure 1.4 and Table 1.2) of identical catalytic activity, with the two chains linked by disulfide bonds.

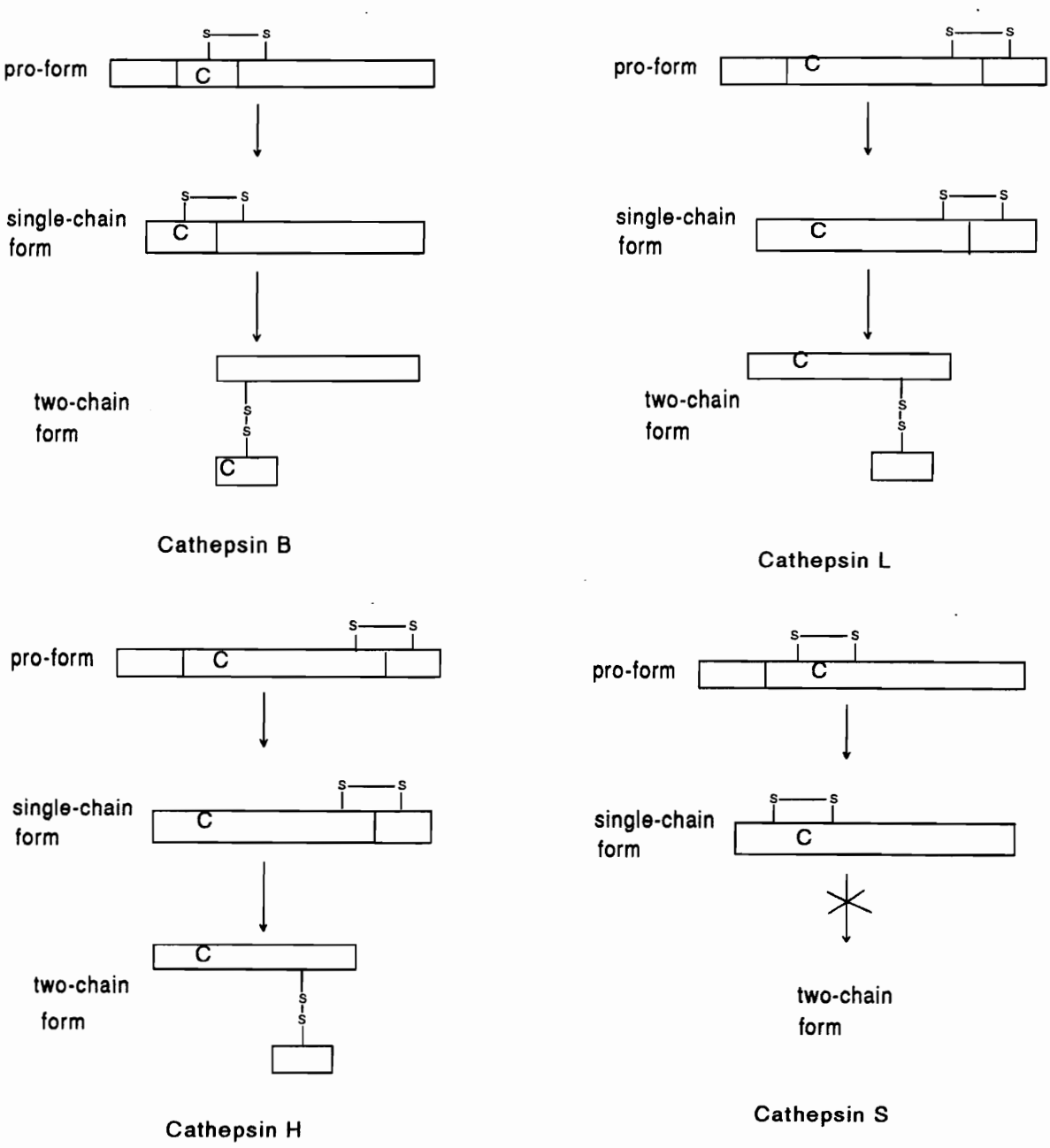

Figure 1.4 Biosynthetic Forms of Cathepsins B, H, L, and S

"C" represents the active site cysteine residue.

Table 1.2 Biosynthetic Forms of Cathepsins B, H, L, and S

	B	H	L	S
Pro-form (kDa)	39-46	41	39	36
single-chain (kDa)	29-35	28	29-35	24-28
two-chain: heavy (kDa)	24-25	22	20-30	NA
two-chain: light (kDa)	5	6	5	NA

1.3.2.1 Cathepsin B

The biosynthetic forms of cathepsin B have been demonstrated in a variety of mammalian cells and tissues. Human fibroblasts contain pro-cathepsin B of 44.5 kDa, which is later processed to 46 kDa (addition of oligosaccharide chains) and 33 kDa (proteolytic processing) forms (Hanewinkel et al. 1987). HepG2 cells (human hepatocarcinoma) produce pro-cathepsin B of 44 kDa, which is processed to the 33 kDa single chain and the 24 + 5 kDa two-chain form (Mach et al. 1992). The active site Cys is present in the light chain of the two-chain form. Rat macrophages have a pro-cathepsin B of 39 kDa, single chain of 29 kDa, and a heavy chain of the two-chain form of 25 kDa (Kominami et al. 1988). KNIH 3T3 mouse fibroblasts have pro-cathepsin B of 39 kDa with a stable mature form of 35 kDa (Mason et al. 1989a). Differences in molecular mobilities of pro-, single-, and two-chain forms may represent different glycosylation patterns in different tissues and species. Mach et al. (1992) have demonstrated that in HepG2 cells the conversion of pro-cathepsin B to the single chain form is not sensitive to the cysteine proteinase inhibitors Z-Phe-Phe-CHN_2 or Z-Phe-Ala-CHN_2, while processing of the single chain to the two chain form is. This selective sensitivity implies that either cathepsin B or L may be responsible for the cleavage of the single- to the two-chain form, but not responsible for the removal of the pro-peptide.

1.3.2.2. Cathepsin H

Rat liver shows pro-cathepsin H at 41 kDa which is processed to the single chain form of 28 kDa (Nishimura and Kato 1987). Incubation up to 60 min failed to convert the single-chain to the two-chain form (22 + 6 kDa) and suggests that the conversion may occur more slowly and may be species and tissue dependent.

1.3.2.3. Cathepsin L

Cathepsin L in NIH 3T3 mouse fibroblasts is synthesized as an inactive 39 kDa pro-form and subsequently processed to active 29 kDa and 20 + 5 kDa single- and two-chain forms, respectively (Gal et al. 1985). Rat hepatocytes produce pro-cathepsin L of 39 kDa which is processed to 30 kDa and 25 + 5 kDa (Nishimura et al. 1988). The active site cysteine is in the heavy chain of the two-chain form. KNIH 3T3 mouse fibroblasts oversecrete pro-cathepsin L of 39 kDa, which rapidly autolyses at pH 3.0 to 35 kDa and 30 kDa (Mason et al. 1987). Sensitivity of cathepsin L processing to Z-Phe-Ala-CHN_2 and E-64, both potent irreversible inhibitors of select cysteine proteinases, suggests that cathepsin L or a closely related protein may be responsible for the processing events. Recently, Mason and Massey (1992) have demonstrated the autoactivation of pro-cathepsin L from KNIH 3T3 mouse fibroblasts at pH 5.0 and 6.0 in the presence of negatively-

charged surfaces, indicating that a small percentage of the pro-enzyme population exists in an active conformation. Salminen and Gottesman (1990) have also demonstrated that active cathepsin L is probably essential for its own processing in cultured fibroblasts.

1.3.2.4 Cathepsin S

The biosynthesis of cathepsin S is not yet fully elucidated. The human mature single chain form is 24 kDa, similar to that of the heavy-chain of two-chain cathepsin L (Kirschke et al. 1986). Shi et al. (1992), however, report that human alveolar cathepsin S has a molecular weight of 28 kDa. No further proteolytic cleavage of cathepsin S has been reported to date. The pre-pro-form of the enzyme is reported to be 331 residues (Shi et al. 1992), and contains only 1 N-linked glycosylation site, located in the pro-peptide region.

1.4 Inhibitors of Cysteine Proteinases

Much of the work to characterize the active site subsite specificities of cathepsins B, H, L, and S was performed using active-site directed peptide inhibitors. These include the epoxy-succinyl peptides, peptidyl halo-methanes, peptide aldehydes, and peptidyl diazomethanes.

Pseudo-first order kinetics are observed for inhibition of cysteine proteinases by irreversible inhibitors (epoxy-

succinyl peptides, peptidyl halo-methanes, and peptidyl diazomethanes; Knight 1986). The extent of inhibition is dependent on both time and inhibitor concentration. The enzyme and inhibitor first associate in a reversible manner, based on the binding of the peptidyl moiety in the S_n subsites (k_{on}). Once in the proper orientation, the active site cysteine sulfhydryl is irreversibly modified ($k_{inactivation}$). Both k_{on} and $k_{inactivation}$ contribute to the pseudo-first order rate constant $k_{2apparent}$ (k_{2app}). This constant can be calculated from the observed rate (k_{obs}) and inhibitor concentration, as described by Geuggenheim (1926) and Tian and Tsou (1982), where $k_{2app} = k_{obs}/[I]$ (see Section 2.2.11).

1.4.1 Epoxy-Succinyl Peptides

The family of epoxy-succinyl peptides irreversibly inhibits cysteine proteinases in a 1:1 ratio by addition of the active site cysteine to the C2 carbon of the epoxide ring (Varughese et al. 1988). The peptide portion of the inhibitor binds in the S subsites of the enzyme. E-64 (L-trans-epoxysuccinyl-leucylamido [4-guanidino] butane) was originally isolated from Aspergillus japonicus and has been synthesized by Hanada et al. (1978a,b). Barrett et al. (1982) demonstrated the inactivation of cathepsins B, H, and L by E-64, even in the presence of low molecular weight thiols.

E-64 and the related inhibitor EP-475 (L-trans-

epoxysuccinyl-leucylamido[3-methyl]butane) were used in whole animal studies to determine the involvement of lysosomal cysteine proteinases in protein turnover. E-64 has been used *in vivo* for treatment of muscular dystrophy in animal models; the inhibitor was able to reach lysosomes (Hashida *et al*. 1980; Node *et al*. 1981), but had little effect on muscle protein degradation. E-64 and EP-475 can not block labeling of lysosomal cysteine proteinases in intact cells by the membrane permeable inhibitor Z-iodoTyr-Ala-CHN_2, and are thus membrane impermeable (see Section 1.4.4; Wilcox and Mason, 1992). E-64 and EP-475 enter cells and lysosomes by pinocytosis. Their membrane impermeability was predicted based on molecular charge (Mehdi 1991). E-64 contains a positively charged guanidino group and a negatively charged carbonyl group where as EP-475 contains only the negatively charged carbonyl group. E-64d (EST, Loxistatin) is a membrane-permeable analog of EP-475 (Tamai *et al.* 1986); its ability to enter cells and interact with proteins (lysosomal cysteine proteinases as well as other proteins) has been demonstrated by Shoji-Kasai *et al.* (1989), Wilcox and Mason (1992), and McGowan *et al*. (1989).

1.4.2 Peptide Aldehydes

Peptide aldehydes are tight binding, substrate transition state analogs, that reversibly inhibit cysteine proteinases (Rich 1986). The most widely used peptide aldehyde is

leupeptin (N-blocked leucyl-leucyl arginal; Umezawa 1972). It has been shown to inhibit cathepsin B (Knight 1980) and cathepsin L (Mason et al. 1985). At first, leupeptin was thought to be membrane permeable (Simon et al. 1977), but it has recently been shown to be membrane impermeable (Wilcox and Mason 1992).

1.4.3 Peptidyl Halo-Methanes

The peptidyl halo-methyl ketone inhibitors irreversibly alkylate both serine and cysteine proteinases at their active site His or Cys residue, respectively. The chloromethyl ketones have been most widely studied. Fluoromethyl derivatives of related peptides have been compared to chloromethyl ketone inhibitors with respect to their inhibition of chymotrypsin and cathepsin B (Rauber et al. 1986). With cathepsin B, the fluoromethyl ketones had lower rates of inactivation than did the chloromethyl ketones due to a slower rate of covalent bond formation. The use of chloromethyl ketones has not been pursued in in vivo applications for medicine because they are not selective, as demonstrated by their reactivity with both serine and cysteine proteinases.

1.4.4 Peptidyl Diazomethanes

In contrast to the halo-methyl derivatives, the peptidyl

diazomethanes are active-site directed, irreversible inhibitors of only cysteine proteinases. They alkylate the active site cysteine by a mechanism similar to that of substrate catalysis (Figure 1.5). The thiolate ion attacks the ketone carbonyl, forming a tetrahedral intermediate. Upon re-formation of the carbonyl bond, the bond from the cysteine sulfur atom to the carbonyl carbon shifts to the diazomethyl carbon, resulting in the abstraction of the imidazole proton on the active site histidine by the diazomethyl carbon and release of $N_2(g)$.

These inhibitors were designed by Shaw and Greene (1981) and, depending on the peptidyl moiety, can be used to discriminate between calpain II (a cytosolic, Ca^{2+}-dependent cysteine proteinase), cathepsin B, and cathepsin L (Crawford et al. 1988; Shaw 1984). Z-Tyr-Ala-CHN_2 reacts 40-times faster with cathepsin L than with cathepsin B and does not react with calpain II. Z-Leu-Leu-Tyr-CHN_2 reacts rapidly with cathepsin L and calpain II, but very slowly with cathepsin B. Boc-Val-Lys(ϵ-Z)-Leu-Tyr-CHN_2 reacts more rapidly with calpain II than with cathepsins B or L. Z-(^{125}I)Tyr-Ala-CHN_2 has been used as a probe for cysteine proteinases in human tissues (Mason et al. 1989b) and in whole cells (Wilcox and Mason 1992). The peptidyl diazomethane inhibitors are also membrane permeable (Wilcox and Mason 1992). In addition to reactivity of cathepsins B and L with peptidyl diazomethane

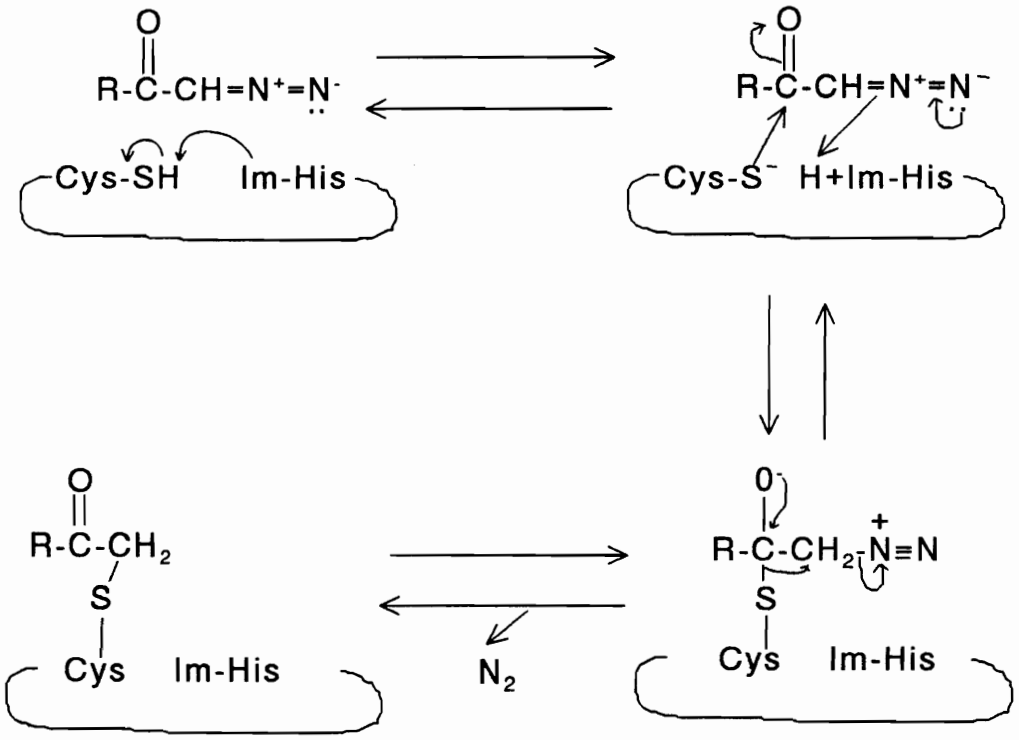

Figure 1.5 Mechanism of Inhibition of Cysteine Proteinases by Peptidyl Diazomethane Inhibitors

inhibitors, cathepsin H was inhibited by Z-Leu-Leu-Tyr-CHN_2 but not Z-Tyr-Ala-CHN_2 (Xin et al. 1992). Z-Phe-Phe-CHN_2 inhibits lysosomal protein degradation in isolated rat hepatocytes (Grinde 1983).

1.5 Location of Biosynthetic Forms of Lysosomal Hydrolases

Cathepsins B, H, L, and S are thought to mature to active forms during their transport to lysosomes. Inactive pro-forms are hypothesized to be in the ER, Golgi complex, and vesicles recently derived from the Golgi, while two-chain forms have been demonstrated in lysosomes. The site of the initial processing of the pro-forms to single-chain forms has not been established. Evidence exists that active proteinases are present in the prelysosomal compartment and that newly synthesized lysosomal proteinases are delivered to early and late endosomes. The acidic pH of both early and late endosomes could promote autoactivation and catalytic activity of activating proteinases.

The membrane-bound nerve growth factor receptor (NGFR) is processed to an extracellular, soluble form after transit through endosomes in A875 human melanoma cells (Zupan et al. 1991), implying the presence of proteinases in endosomes. This process is retarded by treatment with weak bases, monensin, and the ATPase inhibitor bafilomycin A, all of which

dissipate endosomal/lysosomal proton gradients. No individual proteinase was identified as the processing enzyme, as a variety of serine-, cysteine-, aspartic-, and metallo-proteinase inhibitors were unsuccessful in stopping the complete proteolytic processing of NGFR.

Mayorga et al. (1989) found that proteolysis of immune complexes of anti-dinitrophenol monoclonal IgG and radiolabeled dinitrophenol modified BSA (bovine serum albumin) in J774 macrophages did not occur until 5 minutes after internalization, suggesting that the initial vesicles into which compounds are internalized do not contain proteinases. Fusion of these vesicles with light density proteinase-containing vesicles (in a cytosol, energy, and membrane-association-protein dependent manner) triggers the processing of internalized ligands. These experiments involved separation of subcellular vesicles by Percoll fractionation after incubation of cells with the IgG-BSA complex. Subcellular fractionation techniques are not capable of completely separating early endosomes from late endosomes or microsomes.

Renfrew and Hubbard (1991) report sequential processing of epidermal growth factor (EGF) in early and late endosomes of rat liver based on subcellular fractionation techniques. The initial processing event occurs in early endosomes by the action of a carboxypeptidase B-like enzyme. Late endosomes

contain trypsin-like and carboxypeptidase B-like enzymes, both of which process EGF to its second and third biosynthetic forms. The late endosomal processing, slowed by lower temperatures, is most likely due to poor delivery of EGF to these sites. As mentioned above, the results may be skewed due to incomplete separation of endosomes and microsomes by subcellular fractionation methods employed in the study.

In an extensive study of rat hepatocytic endocytic compartments using subcellular fractionation and lactoperoxidase-mediated iodination, Casciola-Rosen et al. (1992) provide evidence that cathepsin D, an aspartic proteinase, but not cathepsin L, β-glucuronidase, or lpg 120, is present in early endosomes in precursor forms (56 kDa, 44 kDa, and 38 kDa), while mature cathepsin D (34 kDa) is found only in lysosomes. Cathepsin L was present in minute amounts in late endosomal fractions but in large amounts in lysosomal fractions. The proteins were isolated from subcellular fractions by immunoprecipitation with specific antibodies.

In an earlier study of rat liver cell intracellular hydrolase-containing compartments, the same group (Casciola-Rosen et al. 1991) suggested that selective activation and/or delivery of hydrolases occurs along the endocytic pathway. They perfused rat liver with small synthetic substrates for aryl sulfatase, acid phosphatase, and β-glucosaminidase for various times and at various temperatures. Hydrolysis

products are membrane permeable and are rapidly released into the perfusant where the cleavage products are detected fluorometrically. Aryl sulfatase and acid phosphatase are active in prelysosomal compartments (early or late endosomes), while β-glucosaminidase is active only in lysosomes, based on the appearance of the fluorescent product in the perfusate after short or long lag periods and perfusions at reduced temperatures. Reduced temperatures reportedly prevent endosome/lysosome fusion.

Ludwig et al. (1991) used a CI-MPR affinity column to capture mannose 6-phosphate-containing lysosomal enzymes after in situ labeling of the enzymes. The enzymes were labeled with lactoperoxidase that had been internalized for various times. In NRK (normal rat kidney) cells, 20-40% of the total cellular lysosomal hydrolases that contain mannose 6-phosphate are present in early endocytic vesicles, including early endosomes. Early endosomes are characterized as containing a low amount of CI-MPR and accessible to fluid phase markers between 5 and 15 minutes after internalization. However, most phosphorylated lysosomal enzymes were present in late endocytic structures. Late endosomes are rich in CI-MPR and contain fluid phase markers after 30-60 minutes incubation periods. These vesicles are distinct from the CI-MPR negative lysosomes. Cathepsin D that had been metabolically labeled by pulse-chase procedures was a transient resident of early

endosomes. Cathepsin D was detected using internalized anti-cathepsin D antibody.

Rijnboutt et al. (1992) localized the 51-55 kDa cathepsin D proenzyme in the TGN of HepG2 cells. In these studies, cathepsin D was detected by cross-linking mediated by horseradish peroxidase-DAB chemistry. Reaction of the reagent with proteins forms an insoluble complex. Disappearance of cathepsin D on Western blots implies the presence of cathepsin D in the DAB-hrp insoluble conjugates. Processing of the proenzyme to the active 44 kDa form occurred in compartments (endosomes) fully accessible to the fluid phase marker horseradish peroxidase; only 20% of transferrin-bound TfR was present in these vesicles. Processing of cathepsin D to the mature 31 kDa form occurred in vesicles that were accessible to the fluid phase marker but inaccessible to the TfR (lysosomes).

Parathyroid hormone in macrophage endosomes is cleaved to its bioactive form in a pepstatin-sensitive manner (Diment et al. 1989), implying that the cleavage is the result of cathepsin D activity. The cleavage is reported to be endosomal, as detected by the release of cleavage products after a brief incubation of cells with ^{125}I-PTH (residues 1-84).

In rabbit alveolar macrophages cathepsin D has also been immunolocalized to endosomes, lysosomes, and small vesicles at

the cell periphery. No cathepsin D was found on the plasma membrane (Rodman et al. 1990), suggesting that the cathepsin D in endosomes did not originate from plasma membrane forms but was delivered to early endosomes by the small peripheral, vesicles that contain cathepsin D.

Cathepsin D is not the only proteinase to be identified in endosomes. Cathepsin B may be involved in the intracellular processing of exogenous IgG by U937 cells (Santoro et al. 1993). The degradation products of IgG in these cells resembles that performed by pure cathepsin B in vitro, but not by cathepsin D, L, or by a mix of the two with cathepsin B. The site of degradation was identified as late endosomes by analysis of the ability of subcellular fractions to degrade added IgG. Data presented in the study do not, however, warrant such conclusions. The authors conclude that proteolysis has occurred in fractions containing plasma membrane and endosomes and in fractions containing lysosomes and mitochondria; the degradation products are not evident in the photographs accompanying the text.

A leupeptin-sensitive proteolytic event is required for the removal of the MHC (major histocompatibility complex) Class II invariant chain in a transformed B lymphoid cell line (Neefjes and Ploegh 1992). The invariant chain must be removed for the complex to bind 8-10 amino acid peptides for antigen presentation. Leupeptin also inhibits surface

deposition of newly synthesized Class II molecules, presumably by inhibiting the proteolytic digestion of antigens to presentable peptides (Blum and Cresswell 1988; Puri and Factorovich 1988; Vidard et al. 1992; Michalek et al. 1992).

1.6 The Use of Membrane-Impermeable Inhibitors for the Identification of Endosomal Proteinases

As described in Section 1.5, a great deal of evidence exists that newly synthesized lysosomal enzymes are delivered to early and late endosomes and that these vesicles are the sites of initial digestion of substances internalized by receptor-mediated endocytosis. Many of the studies described above rely on immunocytochemical identification of lysosomal enzymes, which can detect both active and inactive (pro-) forms of lysosomal enzymes. Subcellular fractionation methods can also be problematic, as complete separation of early from late endosomes and microsomes is not possible. Different forms of lysosomal enzymes (pro-, single-, or two-chain forms of the enzymes) may be distributed differently in early and late endosomes; microsomes contain pro-forms of the enzymes. These differences would be clouded by contamination of early endosome fractions with late endosomes and microsomes.

While the aspartic proteinase cathepsin D has clearly been demonstrated in endosomes, it is not clear whether active forms of cathepsin B, H, L, or S are present. To investigate

the involvement of lysosomal cysteine proteinases (and their biosynthetic forms) in endocytic proteolysis, membrane-impermeable forms of the peptidyl diazomethane inhibitors can be used. It is proposed that a protein-radiolabeled inhibitor conjugate may be selectively internalized by cells via receptor-mediated endocytosis and thus irreversibly label any active forms of cathepsins B, H, L, or S. Incubation of such a complex with cells for various times and at lowered temperatures, followed by analysis by immunoprecipitation, SDS-PAGE, and autoradiography, could identify which, if any, of the lysosomal cysteine proteinases are present in endocytic vesicles. The use of a reducible cross-linking agent between the protein and inhibitor, followed by similar analyses under reducing conditions can demonstrate the biosynthetic forms of cathepsins B or L present, as determined by the labeling of single or two-chain forms of the enzymes. Labeling of two-chain forms would implicate fully processed enzymes present in mature lysosomes, while single-chain labeling would imply that the enzymes are delivered to the endosomes by a vesicle more recently derived from the TGN. No labeling would indicate the absence of active forms of the enzymes, implying either the absence of the enzymes themselves or the presence of inactive pro-forms. In such a case, pretreatment of the cells with unlabeled, membrane-permeable forms of the inhibitors (to block labeling of already

synthesized enzymes) followed by a brief incubation in the absence of inhibitor (to allow synthesis of new enzymes), incubation of the cells with the protein-inhibitor complex with tunicamycin (to block protein synthesis), and subsequent treatment of the cells at pH 3.0 to induce autoactivation of the enzymes present, could lead to the detection of inactive pro-forms.

The membrane-permeable peptidyl diazomethane inhibitor, Fmoc-(^{125}I)Tyr-Ala-CHN_2, was initially used to characterize the active forms of cathepsins B, L, and S in human monocytic cell lines. Immunoprecipitated cathepsin L, isolated after cell labeling with the radio-iodinated inhibitor, was further analyzed by 2-dimensional electrophoresis (IEF/SDS-PAGE) to characterize the different biosynthetic forms present in cells.

This project addresses the synthesis and characterization of protein-inhibitor complexes internalized by cells via endocytosis. Bovine serum albumin (BSA) was cross linked to (^{125}I)Tyr-Ala-CHN_2 using both reducible and nonreducible cross linking agents. The nonreducible complex was used to characterize the inhibitory activity both in vitro and in initial studies with intact cells.

CHAPTER 2: MATERIALS AND METHODS

2.1 MATERIALS

All chemicals were purchased from Fisher Scientific (Pittsburg, PA) or Sigma Chemical Company (St. Louis, MO) and were ACS or HPLC grade. Electrophoresis chemicals were purchased from Bio-Rad (Hercules, CA); ampholines, PAS, and PGS were purchased from Pharmacia Biotech Inc.(Piscataway, NJ). Kodak X-Omat X-ray film and ammediol (2-amino-a-methyl-1,3-propanediol) came from Kodak Chemicals (Rochester, NY). Cell culture reagents were purchased from Gibco BRL (Gaithersburg, MD), fetal bovine serum from Hy-Clone Laboratories, Inc. (Logan, UH). Fmoc-Tyr-Ala-OH was purchased from Bachem (Switzerland). Cross-linking agents were purchased from Pierce Chemical Company (Rockford, IL).

2.1.1 Cell Lines

KNIH 3T3 fibroblasts (Kirsten-virus transformed NIH 3T3 fibroblasts) were obtained from Dr. M.M. Gottesman (NIH, Bethesda, MD). THP1 and U937 cell lines were purchased from the American Type Culture Collection (Rockville, MD).

2.1.2 Antisera

2.1.2.1 Sources

Sheep anti-human cathepsin B was provided by Dr. D.J.

Buttle (Strangeways Research Laboratory, Cambridge, U.K.); rabbit anti-human cathepsin L was raised as previously described (Mason 1986). Rabbit anti-bovine cathepsin S (IgG fraction, 1 mg/mL protein) was provided by Dr. H. Kirschke (Halle, Germany). Rabbit anti-mouse cathepsin L was a gift from Dr. M. M. Gottesman, (NIH, Bethesda, MD). Rabbit anti-papaya was raised in rabbits using whole papaya protein (Sigma). The first injection consisted of 1 mL of a 0.5 mg/mL solution (total protein) in 50% Freund's complete adjuvant; 2 subsequent injections, each at three week intervals, consisted of similar injections prepared in Freund's incomplete adjuvant. Two weeks following the last injection, total blood was removed by heart puncture; cells were pelleted by centrifugation and the whole serum used.

2.1.2.2 Titration of Anti-Papaya Serum

Assay tubes containing 25 μL of 25 μg/mL papain (0.625 μg) were diluted to 500 μL with 10 mM Tris-HCl, pH 7.5. To this was added a range of dilutions of anti-serum (no serum, no dilution, 1:2, 1:4, 1:8, 1:16, 1:32, and 1:64; two tubes with each antibody dilution). Being a whole serum preparation, the antibody solution also contains serum cysteine proteinase inhibitors such as cystatins. Thus, the degree of inhibition of papain activity by removal by the anti-papain was calculated both with and without 10 % protein-

A Sepharose (PAS) present. Thus, to one set of anti-serum dilutions was added 30 μL of 10% PAS; no PAS was added to the second set. The solutions were incubated overnight on a rotary mixer at 4°C. The PAS-containing tubes were centrifuged to pellet the antibody-bound papain. The samples without PAS and the supernatants from those samples with PAS were assessed for papain activity (Section 2.2.6). Figure 2.1.a shows these results. As seen for the samples without PAS, the 1:4 dilution returns the fluorescence reading to that without antibody (about 95 fluorescence units). Therefore, the effective concentration of inhibitors in the serum preparation is less than the concentration of papain in the 1:4 dilution. In the set containing PAS, the 1:4 dilution gives nearly complete inhibition. Since the effective concentration of inhibitors is zero, the inhibition is due solely to the removal of papain by specific antibody in the serum. The antibody itself does not inhibit the enzyme, as demonstrated by a return of the fluorescence values to 100 in samples without PAS.

A linear titration was then performed in which the antiserum was diluted 1:2 in water. A series of dilutions of this solution was set up such that each tube contained 0, 10, 20, 30, 40, 60, 80, or 100 μL of the 1:2 dilution; the total volume was brought to 100 μL with water. Separate tubes were prepared containing 25 μL of 25 μg/mL papain (0.625 μg) and

a. Determination of initial dilution

anti-serum	FU PAS	FU +PAS
none	94.7	67.2
1:0	30.2	4.9
1 : 2	69.3	7.0
1 : 4	96.1	13.0
1: 8	100.7	44.3
1: 16	105.4	73.1
1: 32	105.2	80.2
1: 64	99.2	84.2

b. Titration with 1:2 dilution

µL dil.	flu. +PAS
0	65.0
10	53.1
20	54.3
30	50.1
40	32.8
60	19.9
80	16.1
100	14.1

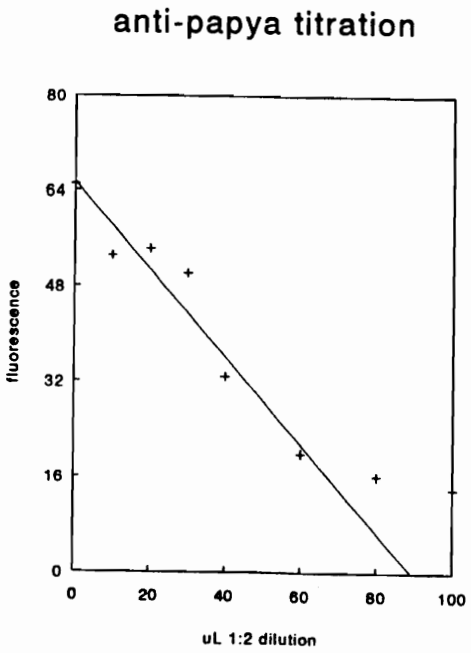

Figure 2.1 Titration of Rabbit Anti-papaya Immune Serum
a. An anti-serum dilution (10 µL) was added to 0.625 µg papain in 0.5 mL 10 mM Tris-HCl, pH 7.5. To one set was added 30 µL 10 % Protein-A Sepharose; to the other set nothing was added. After incubation over night at 4°C on a rotary mixer, the PAS was pelleted and 50 µL of the supernatant assessed for papain activity. Likewise, 50 µL of the set without PAS was also assessed for papain activity (Section 2.2.6). The 1:4 dilution of serum without PAS returned the fluorescence reading to that without serum added. With PAS present, the papain is nearly completely removed.
b. Anti-serum was diluted 1:2 and then 0 to 100 µL brought to 100 µL with water. An aliquot of these dilutions (10 µL) was added to papain in Tris-HCl as above. PAS was included in one set and excluded in the other. Immunoprecipitation occurred over 4 hours at 4°C on a rotary mixer. Samples were then assessed as above. The fluorescence values were plotted against µL dilution; the x-intercept represents the volume of antisera which contains an equimolar amount of anti-papain and papain. Thus, 86.7 µL of the 1:2 dilution contains 2.5 pmoles specific IgG, or 87 µg/mL anti-papain in the undiluted stock.

475 μL 10 mM Tris, pH 7.5 To each tube was added 10 μL of the antiserum dilution and 30 μL 10 % PAS. To determine the amount of proteinase inhibitors present in the antiserum, a parallel experiment was performed without the PAS, as before. The immunoprecipitation was carried out over 4 h at 4°C on a rotary mixer. The PAS was pelleted by centrifugation, and 50 μL of each sample assessed for papain activity as before. Figure 2.1.b shows the results. The x-intercept was calculated to be 86.7 μL. No inhibition was seen in samples without PAS. Since 2.5 pmoles papain was present in the assay, the volume of antisera for which no activity was seen in the assay (the x-intercept) represents the situation where papain and anti-papain are present in equimolar amounts. Thus, 8.67 μL (10 μL of the 86.7 μL dilution) of the 1:2 antiserum dilution contains 2.5 pmoles anti-papain, giving 0.29 pmole anti-papain per μL of the 1:2 dilution, and 0.58 pmole/μL antiserum (87 μg anti-papain / mL anti-serum).

2.1.3 Inhibitors

Z-Tyr-Ala-CHN_2 and Z-Leu-Leu-Tyr-CHN_2 were kindly provided by Elliot Shaw. E-64 (L-trans-epoxysuccinyl-leucylamino [4-guanidino] butane) was provided by Dr. Hanada, Taisho Pharmaceuticals, Tokyo, Japan. Fmoc-Tyr-Ala-CHN_2 was synthesized as described in Section 2.4.3.

2.2 GENERAL METHODS

2.2.1 Glassware and Water

All glassware was thoroughly washed with mild detergent and rinsed in tap water, followed by two rinses in distilled deionized water. Distilled, deionized water was prepared by passing distilled water through a Barnstead cartridge to remove organic contaminants and then two Barnstead mixed bed ion exchange resin cartridges to deionize. Distilled, deionized water was used for all buffer solutions and tissue culture media.

2.2.2 Protein Determination

Protein amount was determined by the BioRad Protein Assay as described by the manufacturer.

2.2.3 SDS-PAGE

2.2.3.1 Bury System

Denaturing polyacrylamide gel electrophoresis (SDS-PAGE) was performed as described by Bury (1986). This system provides better resolution than the Laemmli system for proteins whose masses range between 5 kDa and 30 kDa. Buffers used in this system are described in Table 2.1. All reagents were prepared, stored at 4°C, and warmed to room temperature before use.

BioRad Protean II System was used with 20 cm gel length

Table 2.1 SDS-PAGE Reagents

Buffer A (resolving gel)	440 mM ammediol (4.63 g) 188 mM HCl (18.72 mL of 1M) pH 8.96 water to 100 mL
Buffer B (stacking gel)	336 mM ammediol (3.51 g) 248 mM HCl (24.67 mL of 1M) pH 8.37 water to 100 mL
Buffer C (upper reservoir)	164 mM ammediol (17.0 g) 160 mM glycine (12.0 g) 0.4 % SDS (4.0 g) pH 9.39 water to 1000 mL
Buffer D (lower reservoir)	250 mM ammediol (26.28 g) 200 mM HCl (200 mL of 1M) pH 8.23 water to 1000 mL
Buffer E (sample buffer)	2 % SDS (0.2 g) 9 M urea (5.4 g) 1 mL of 0.1% bromophenol blue 5.0 mL of buffer B 4.0 mL glycerol immediately before use, add 10 μL 2-mercaptoethanol to 1 mL
10 % APS	1 g APS to 10 mL water; aliquot 100 μL into small tubes; store at -20 C; thaw prior to use
25 % acrylamide	24.35 g acrylamide 0.65 g bis-acrylamide water to 100 mL
50 % sucrose	50 g sucrose water to 100 mL
Stain	0.01 % Coomassie Brilliant Blue G250,(1g) 50 % Methanol (500 mL) 20 % glacial acetic acid (200 mL) water to 1000 mL
Destain	30% methanol (750 mL) 1% formic acid (25 mL of 88%) water to 2000 mL

and 0.75 mm spacers for 2-dimensional and some 1-dimensional analyses. Many additional 1-dimensional analyses were performed on BioRad mini gel apparatus with 0.75 mm spacers. Gel apparati were set up as described by the manufacturers. Resolving gels of 12.5% acrylamide were used with 4% stacking gels; Table 2.2 details gel composition. Gel ingredients were mixed, degassed for 5 minutes and then 10% ammonium persulfate and TEMED were added. The solution was carefully pipetted between the gel plates, overlaid with water and allowed to polymerize for 45 minutes to 1 hour.

After polymerization was complete, the overlay was decanted and the stacking gel solution applied. Depending on the type of analyses to be performed, either a multi-well comb or a comb designed for IEF tube gel inlay was used. The stacking gel was allowed to polymerize and the combs removed.

The upper reservoir was filled with a 1:4 dilution (into water) of buffer C; the lower reservoir was filled with a 1:4 dilution of buffer D. Samples were solubilized in buffer E (or diluted with an equal volume for samples in solution) and 10 μL loaded into the appropriate well. The gel was exposed to an electric field (250 V, constant voltage) until the tracking dye (bromophenol blue in buffer E) was 1 cm or less from the bottom of the gel plates. The gels were then carefully removed from the plates and stained for protein for 30 minutes followed by destaining until the background was

Table 2.2 SDS-PAGE Gel Composition (for four 20 cm gels)

Resolving Gel:	32 mL 25% acrylamide solution 16 mL buffer A 14 mL 50% sucrose 1.7 mL water degas 5 minutes 0.26 mL freshly prepared 10% ammonium persulfate 0.026 mL TEMED
Stacking Gel:	8 mL 25 % acrylamide solution 10.8 mL buffer B 10.8 mL 50 % sucrose 12.7 mL water degas 5 minutes 0.1 mL 10 % ammonium persulfate 0.05 mL TEMED

clear. For mini gel analyses, the volumes used were adjusted accordingly. Protein molecular weight markers used were bovine serum albumin (66 kDa), ovalbumin (45 kDa), muscle glyceraldehyde-3-phosphate dehydrogenase(36 kDa), bovine carbonic anhydrase (29 kDa), trypsinogen (24 kDa), soybean trypsin inhibitor (20.1 kDa), and bovine α-lactalbumin (14.2 kDa) as present in Sigma Chemical Company's Dalton Mark VII markers.

2.2.3.2 Laemmli System

For analysis of samples of higher molecular weights (66 kDa and above), a variation of the Laemmli gel system (Laemmli 1970) was used. All reagents (Table 2.3) were prepared, stored at 4°C, and warmed to room temperature before use. Bio-Rad Protean II and Bio-Rad mini gel apparati were assembled and used as described in section 2.2.3.1. Resolving gels of 7.5 % acrylamide and stacking gels of 3.5 % were used. Table 2.4 details gel compositions. There is no need to degas the gel solutions before adding TEMED and APS. The running buffer was used for both upper and lower reservoirs without pH adjustment. Molecular weight markers used were rabbit muscle myosin (205 kDa), β-galactosidase (116 kDa), phosphorylase b (97.4 kDa), bovine serum albumin (66 kDa), ovalbumin (45 kDa), and carbonic anhydrase (29 kDa).

Table 2.3 Laemmli Gel Reagents

Acrylamide/ bis-acrylamide (30.0:0.8)	30 g acrylamide 0.8 g bis-acrylamide water to 100 mL filter over Whatman paper store in dark bottle
Separating Buffer (1.5 M Tris-HCl)	18.17 g Tris-HCl pH 8.8 with HCl water to 100 mL
Stacking Buffer (0.5 M Tris-HCl)	6.06 g Tris-HCl pH 6.8 with HCl water to 100 mL
10 % SDS	10 g SDS to 100 mL water filter over Whatman paper (store at room temp.)
10 % ammonium persulfate	1 g ammonium persulfate water to 10 mL aliquot into small tubes (0.5 mL/tube) store at -20 C; thaw as needed do not refreeze excess
Running Buffer (0.05 M Tris-HCl, 0.5 M glycine, 0.1 % SDS)	24.0 g Tris-HCl 115.2 g glycine 40 mL 10 % SDS water to 4L do not adjust pH

Table 2.4 Laemmli Gel Composition
(all volumes in mL)

Separating Gel

	5.0%	7.5%	9.0%	10.5%	12.5%	15.0%	18.0%
water	23.3	19.6	17.4	15.1	12.1	8.3	3.9
1.5 M Tris-HCl	11.25	11.25	11.25	11.25	11.25	11.25	11.25
acryl	7.5	11.25	13.5	15.75	18.75	22.5	27.0
10% SDS	0.45	0.45	0.45	0.45	0.45	0.45	0.45
gly-cerol	2.3	2.3	2.3	2.3	2.3	2.3	2.3
TEMED	0.03	0.03	0.03	0.03	0.03	0.03	0.03
10% APS	0.30	0.30	0.30	0.30	0.30	0.30	0.30

Stacking Gel

	3.0%	3.5%	4.5%	5.0%	6.0%	7.5%	9.0%
water	9.45	9.20	8.70	8.40	7.95	7.25	6.45
0.5M Tris-HCl	3.75	3.75	3.75	3.75	3.75	3.75	3.75
acryl	1.50	1.75	2.25	2.50	3.00	3.70	4.50
10 % SDS	0.15	0.15	0.15	0.15	0.15	0.15	0.15
TEMED	0.015	0.015	0.015	0.015	0.015	0.015	0.015
10% APS	0.20	0.20	0.20	0.20	0.20	0.20	0.20

2.2.4 Isoelectric Focusing

Two-dimensional electrophoresis was performed by first separating proteins by their isoelectric point and then by molecular size (SDS-PAGE). Isoelectric focusing was performed in 0.75 mm ID glass tubes on the BioRad Protean II gel system. Table 2.5 lists buffer solutions and gel components.

Glass tubes were thoroughly cleaned in chromic acid overnight, rinsed with water, then treated for 2 hours with saturated KOH in ethanol, rinsed again with water, and dried. Tubes were treated with dimethyldichlorosilane periodically to ease removal of gels.

The acrylamide gel solution was prepared and degassed with stirring for 30 minutes. After the addition of 10% ammonium persulfate and TEMED, the solution was pulled into the tubes (12 cm total, leaving 2-3 cm empty at the top) by the use of 1 cc syringes with tip adapters cut from plastic disposable Pasteur pipets. Once the gels were polymerized, the tops were overlaid with 10 μL IEF sample buffer, both ends were sealed with parafilm, and they were stored upright at room temperature in an air tight container.

Four tubes were placed in the Protean II apparatus with the tube support. Using a 3 cc syringe with a bent 22 gauge needle, the lower ends of the tubes were filled with 0.02 M NaOH, removing all air bubbles, covered with a small nylon sheet secured by a small rubber band, and immersed in 0.02 M

Table 2.5 IEF Buffers and Gel Components

0.02 M NaOH (lower reservoir)	1.6 g NaOH water to 2000 mL
0.01 M H_3PO_4 (upper reservoir)	0.5 mL of 85% phosphoric acid water to 730 mL
10 % NP-40	4 g (liquid) NP-40 water to 40 mL
8% acrylamide solution	3.67 g urea 1.45 mL 25 % acrylamide 1.35 mL 10% NP-40 1.3 mL water 0.267 mL pH 4-6.5 ampholines 0.067 mL pH 3-10 ampholines degas 30 minutes with stirring 6.7 μL 10% ammonium persulfate 4.7 μL TEMED
Sample Overlay	9.0 g urea 0.5 mL pH 4-6.5 ampholines 0.125 mL pH 3-10 ampholines water to 25 mL *aliquot to 0.25 mL/tube *store at -20°C
IEF Sample Buffer	28.5 g urea 1.0 g NP-40 2.0 mL pH 4-6.5 ampholines 0.5 mL pH 3-10 ampholines 2.5 mL 5% 2-mercaptoethanol water to 50 mL *aliquot to 0.5 mL/tube *store at -20°C

NaOH (lower reservoir solution). Samples prepared from cell lysates were dissolved in 100 or 50 μL IEF sample buffer and 10 μL loaded onto each tube gel with a Hamilton syringe. SDS-PAGE markers (5 μL) were also added to each tube to use as internal IEF markers (see Table 2.6). Finally, each tube was filled to the top with sample overlay solution, and 0.01 M phosphoric acid added to the upper reservoir. The anode was connected to the upper reservoir and the cathode to the lower reservoir, and the samples exposed to an electric field between 3000 and 3600 volt*hours (usually 7 hours at 500 volts). The apparatus was then disassembled and the gels removed from the tubes by water pressure from a 10 mL syringe with a plastic pasteur pipet adaptor. The gels were placed into the long horizontal well in SDS-PAGE gels (Section 2.2.3) and SDS-PAGE was performed as described.

2.2.5 Gel Drying and Autoradiography

Destained gels were photographed using Polaroid Instant film as described by the film manufacturers, and dried onto Whatman filter paper (Type 1) using a heated gel drier under aspiration vacuum. Dried gels were placed in an autoradiography cassette with an intensifying screen and a sheet of Kodak X-Omat X-ray film in between the screen and the gel. The film was exposed at -70°C for a specified amount of time (usually 1 week), removed from the freezer, and warmed to

Table 2.6 Marker Proteins

protein	molecular weight (kDa)	pI
bovine serum albumin	66	4.6
ovalbumin	45	---
glyceraldehyde-3-phosphate dehydrogenase	36	8.3/8.5
bovine carbonic anhydrase	29	5.4/5.9
trypsinogen	24	9.3
soybean trypsin inhibitor	20.1	4.5
α-lactalbumin	14.2	4.0

room temperature. Autoradiographs were developed for 5 minutes, rinsed 30 s in water, fixed for 5 minutes, and rinsed again in water. The dried autoradiographs were then photographed.

2.2.6 Fluorometric Assay of Cathepsin L and Papain

This method is based on that of Barrett and Kirschke (1981). Reagents needed are listed in Table 2.7.

The enzyme sample was brought to 500 μL with 0.01% Brij-35; 250 μL activity buffer (pH 5.5) was added and the solution allowed to preincubate 5 minutes at 37°C to fully activate the enzyme. A 250 μL volume of 20 μM Z-Phe-Arg-NHMec was added to each assay tube to start the reaction (final concentration of substrate is 5 μM). The assay proceeded for 10 minutes at 37°C and was stopped by the addition of 2 mL stop reagent. Assays involving multiple samples had substrate added at 5 second intervals; likewise, stop reagent was added 10 minutes later at the same timed interval, guaranteeing that each sample reacted for only 10 minutes. Fluorescence was determined using a Perkin-Elmer Luminescence Spectrometer LS-50 with excitation and emission wavelengths set at 360 nm and 460 nm, respectively. Slit widths were 2.5 mm and the machine blanked with water and and calibrated to 100 fluorescence units with 0.33 μM coumarin. A reading of 100 corresponds to 0.1 mUnits of enzyme activity, where one enzyme unit is the

Table 2.7 Fluorometric Assay Reagents

0.01% Brij-35	1 mL of 5% Brij-35 water to 500 mL
Activity Buffers	400 mM sodium acetate 4 mM EDTA 0.1% sodium azide pH 5.5 *prior to use: bring to 4 mM DTT
	400 mM sodium phosphate 4 mM EDTA 0.1% sodium azide pH 7.5 *prior to use: bring to 4 mM DTT
Substrates	20 μM Z-Phe-Arg-NHMec (cathepsin L and papain) 20 μM Z-Arg-Arg-NHMec (cathepsin B) *prepared from 2 mM stock solutions
Stop Reagent	100 mM monochloroacetic acid 100 mM acetic acid pH 4.3 using NaOH
Coumarin Standard	0.33 μM in water prepared from 100 μM stock

amount of enzyme needed to produce 1 μM product per minute .

2.2.7 Fluorometric Assay of Cathepsin B

The assay for cathepsin B is the same as that for cathepsin L, except that the activity buffer is 400 mM sodium phosphate, 4 mM EDTA, 0.1% azide (pH 6.0), and the substrate was 20 μM Z-Arg-Arg-NHMec.

2.2.8 E-64 Titration of Papain

Commercial papain (in suspension, 25 mg/mL) was diluted to 0.25 mg/mL in 0.1% Brij-35. A 50 μM stock solution of E-64 in DMSO was diluted to 1-10 μM. Additions to borosilicate glass tubes were made in the given order: 25 μL papain (0.25 mg/mL), 50 μL activity buffer (+DTT, pH 5.5), and 25 μL of the respective concentration of E-64. Samples were incubated for 30 minutes at 37°C, diluted to 5 mL with 0.1% Brij-35, and mixed well. An aliquot (50 μL) of each sample was then assayed as described in Section 2.2.6. Fluorescence values were plotted against concentration of E-64 (see Figure 2.2). A line of best fit was drawn through the first four or five data points (non-zero activity points); the x-intercept of this line represents the concentration of papain in the 0.25 mg/mL solution. This is based on the irreversible reaction of E-64 with the enzyme in a 1:1stoichiometry. Thus, the concentration of E-64 at which zero activity is produced

μM E-64	fluorescence
0	44.6
1	38.5
2	22.1
3	12.2
4	2.5
6	2.5
8	2.5
10	2.5

m = -11.05
b = 46.08
r = 0.992
x int = -b/m
= 4.17 μM

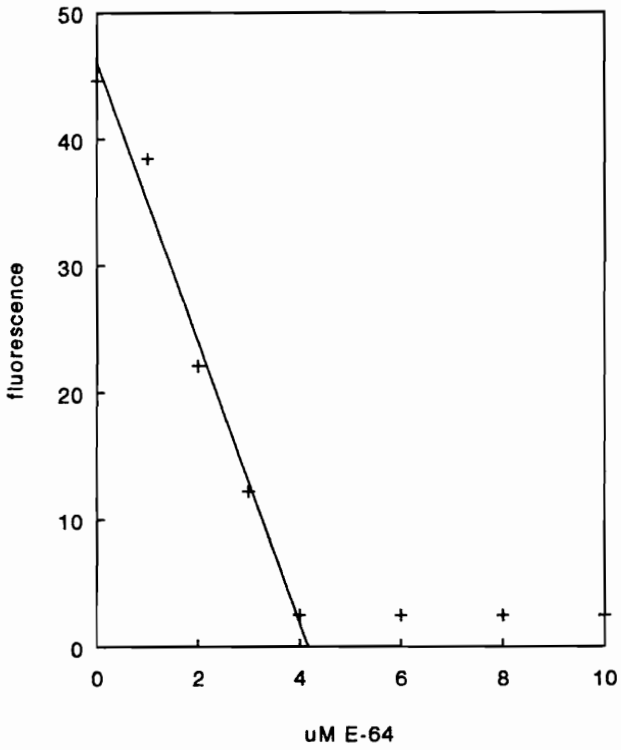

Figure 2.2 E-64 Titration of Papain

Papain (25 μL of 0.25 mg/mL) was incubated for 30 minutes at 37°C with 50 μL 400 mM sodium acetate activity buffer (pH 5.5) 4 mM DTT, and varying concentrations of E-64. The solution was diluted to 5 mL, and then 50 μL was assessed for remaining papain activity (Section 2.2.6). The fluorescence values were plotted against concentration of E-64 present. The x-intercept of the resulting line represents the concentration of E-64 that inhibits all the papain present. Given that the inhibitor interacts 1:1 with the enzyme, the x-intercept also represents the concentration in μM of papain present in the incubation solution.

equals the concentration of papain.

2.2.9 Determination of Unknown Inhibitor Concentration

Inhibitor dilutions were prepared such that 1-100 μL of inhibitor solution is brought to 100 μL total volume with solvent (usually 85% acetonitrile / 15% methanol). An aliquot (25 μL) of each dilution is added to an assay tube containing 25 μL papain (0.25 mg/mL) and 50 μL 400 mM sodium acetate, 4 mM DTT (pH 5.5); samples are incubated and assayed in parallel with an E-64 titration of papain (Section 2.2.8). Sample fluorescence is plotted against volume of stock inhibitor incubated with papain (see Figure 2.3) A line of best fit is drawn through the linear portion of the curve. The x-intercept of this line gives the volume in which the concentration of inhibitor is equal to that of papain present, as determined by the concurrent papain titration. Thus, the concentration of inhibitor in the stock solution can be calculated.

2.2.10 Continuous Rate Assays

The enzyme sample was added to 1.5 mL 0.01 % Brij-35 and 0.75 mL activity buffer (+DTT). The solution was incubated in the sample holder of the fluorimeter (heated by circulating water at 37°C) for 5 minutes and then 0.75 mL substrate was added. The data were collected over 1000 seconds (interval =

μL I	set A	set B	set C
0	52.6	47.9	51.6
10	48.2	44.3	46.5
20	35.7	37.1	34.6
30	28.9	28.0	30.2
40	24.8	23.7	24.6
60	15.4	10.8	13.7
80	5.6	6.2	6.9
100	4.9	4.2	4.8

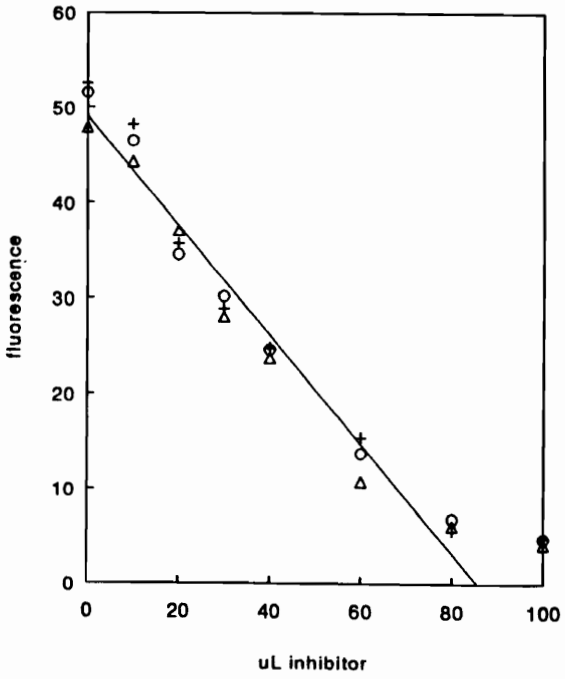

m = -0.564
b = 48.46
r =r0.991
x int = -b/m
= 85.9

$$\frac{4.17\ \mu M}{85.9\ \mu L} = \frac{X}{100\ \mu L}$$

X = 4.85 μM

Figure 2.3 Determination of Inhibitor Concentration

The inhibitor (0, 10 μL, 20 μL, etc.) was diluted to 100 μL and 25 μL incubated with 25 μL papain (0.25 mg/mL) and 50 μL 400 mM sodium acetate, pH 5.5, 4 mM DTT, for 30 minutes at 37°C. The solution was diluted to 5 mL and 50 μL assessed for papain activity (Section 2.2.6). The fluorescence values were plotted against volume inhibitor present in the dilutions; the x-intercept of the resulting line represents the volume of inhibitor at which all the papain present is inhibited. When performed along side an E-64 titration of papain (Section 2.2.8) using the same solution of papain, the concentration of inhibitor present can be determined. Provided that the inhibitor under study interacts with the enzyme in a 1:1 manner, the concentration of papain determined by E-64 titration is equal to that of inhibitor in the volume determined by the x-intercept above. By calculating the ratio of papain to volume inhibitor , the concentration of 100 μL inhibitor (no dilution) is found.

0.5 sec) and the fluorescence plotted against time. The slope of the line generated represents enzyme activity.

2.2.11 Determination of k_{2app}

A continuous rate assay was initiated as described in Section 2.2.10. Once a linear rate was achieved, a known concentration of inhibitor was added. The rate of substrate hydrolysis eventually becomes zero for irreversible inhibitors. The fluorescence data were analyzed by the Geuggenheim method (1926; also Tian and Tsou 1982), in which the data (fluorescence values) were separated in half, corresponding to two equal time periods (for example, fluorescence values for 200 to 500 sec and 501 to 800 sec). The fluorescence values for the first half (early time periods) were subtracted from the second half, and the natural log of the difference was determined (see Figure 2.4). The natural log values were then plotted against time; the slope of the resulting line represents the k_{obs} of the reaction. Using the equation

$$k_{2app} = k_{obs}/[I]$$

the k_{2app} was determined for a known concentration of irreversible inhibitor. k_{2app} represents the rate of irreversible modification of the enzyme by the inhibitor.

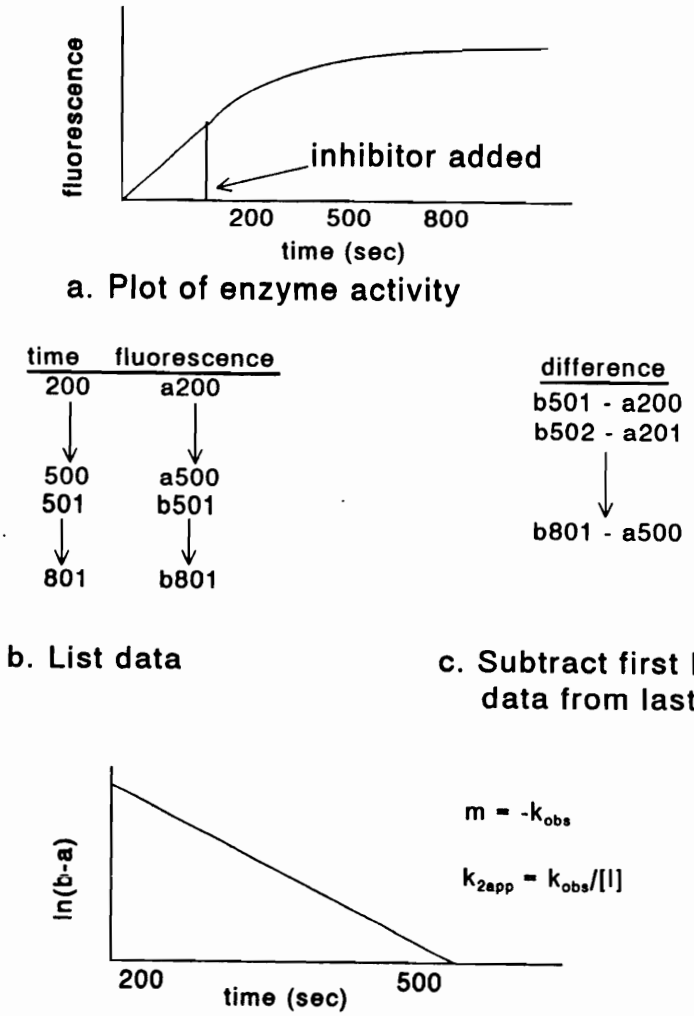

Figure 2.4 Determination of k_{2app}

The determination of k_{2app} was based on that of Geuggenheim (1926) and also Tian and Tsou (1982). a) A continuous rate assay of the enzyme under study was started (Section 2.2.10). Once the enzyme had reached a linear rate, a known concentration of inhibitor (vertical line) was added and the reaction allowed to proceed until the rate was nearly zero. b) The time and fluorescence data was then analyzed by splitting the fluorescence data into two halves and c) subtracting the earlier values from the later. d) The natural log of the difference was plotted against time; the slope of the resulting line is equal to $-k_{obs}$ and $k_{obs}/[I]$ is equal to k_{2app}.

2.2.12 Immunoprecipitation of Cathepsin L

Cellular extracts were prepared by solubilization of cell pellets in 0.5 mL of 10 mM Tris-HCl, 1 mM EDTA (pH 7.5) followed by three rounds of freezing in a dry ice / methanol bath and thawing in a 37° C water bath. The extract was treated with 10 μL non-specific rabbit IgG and 30 μL 10 % (w/v) protein A-Sepharose for 2 hours at room temperature on a rotary mixer. Following centrifugation, the pellet was discarded and to the supernatant was added 10 μL rabbit anti-human cathepsin L and 30 μL 10 % protein A-Sepharose. This was incubated for 2 hours at room temperature as before. Following centrifugation, the supernatant was discarded and the pellet (containing immunoprecipitated cathepsin L) was washed 2 times in 0.5 mL phosphate buffered saline and retained for further use.

2.2.13 Immunoprecipitation of Cathepsin S and Papain

Immunoprecipitations of cathepsin S and papain were performed similarly to that of cathepsin L. For cathepsin S, the extraact was pretreated with 10 μL non-immune IgG and 30 μL 10% protein-A Sepharose; the immunoprecipitation of cathepsin S utilized 10 μL rabbit anti-bovine cathepsin S and 30 μL 10% protein-A Sepharose. Likewise for papain, the preincubation utilized rabbit IgG and the immunoprecipitation rabbit serum containing anti-papaya IgG.

2.2.14 Immunoprecipitation of Cathepsin B

Cathepsin B was immunoprecipitated in much the same manner as the other enzymes except that the sample had to be denatured in order to be recognized by the antibody. Cell lysates were prepared in 10 mM Tris-HCl, 1 mM EDTA, 0.2 % SDS, 1% Triton X-100 (pH 7.5) and subjected to three rounds of rapid freezing and thawing. The lysate was treated with 10 μL rabbit (anti-sheep) IgG and 30 μL 10% protein A-Sepharose for 2 hours at room temperature to remove interfering proteins. Following centrifugation, the pellet was discarded; to the supernatant was added 5 μL 0.1% SDS and the sample boiled for 15 minutes and cooled to room temperature. Affinity purified sheep anti-human cathepsin B IgG (10 μL) and 30 μL 10 % protein G-Sepharose were added and incubated for 2 hours at room temperature. Following centrifugation, the resulting pellet was washed twice in PBS and retained for further analyses.

2.2.15 TCA Precipitation of Proteins

A 20 % (w/v) solution of trichloroacetic acid (TCA) was prepared and chilled on ice. Equal volumes of sample (for example, cell lysate) and 20 % TCA were mixed and kept on ice for either 30 minutes or 1 hour. The precipitated proteins were pelleted by centrifugation at 14000 rpm for 10 minutes and the resulting pellet washed twice in ice cold acetone.

After acetone was removed by evaporation, the pellet was dissolved in SDS-sample buffer (buffer E) (Section 2.1.3).

2.2.16 Radiolabeling of Peptide Inhibitors

Tyrosine residues of the peptide inhibitors were radiolabeled with $Na^{125}I$ using Iodobeads (Pierce). The inhibitor (50 μL of 1 mM solution in acetonitrile) was diluted with 50 μL 100 mM sodium phosphate, pH 7.0. One Iodobead (Pierce) was washed 5 minutes in 100 mM sodium phosphate, dried, and transferred to a tube containing 50 μL of the same buffer. $Na^{125}I$ (10 μL, or 1 mCi) was added to the Iodobead and allowed to incubate for 5 minutes at room temperature. The inhibitor was added and the incubation continued for 15 minutes at room temperature. The incubation mixture was diluted to 500 μL with 50 % acetonitrile / 50 % 100 mM sodium phosphate, (pH 7.0), (v/v) and divided into 20 μL aliquots. Each aliquot contained 40 μCi ^{125}I-Tyr (0.1 mM inhibitor, 2 nmole). Mono-iodinated inhibitor was not purified from non-iodinated or di-iodinated inhibitor, as the mono-iodinated inhibitor was present in limiting amounts (1 mono-iodinated inhibitor molecule in 100, 0.02 nmole) and would be difficult to completely retrieve following HPLC purification.

2.2.17 Measurement of Radioactivity

Radioactive iodine was determined in a LKB/Wallac

CompuGamma gamma counter (energy levels 35-102). Radioactive samples were measured for 60 seconds for the number of counts per minute (cpm),and the cpm were corrected to disintegrations per minute (dpm), given an instrument efficiency of 70 % and the equation

$$\% \text{ efficiency} = (\text{cpm}/\text{dpm})*100.$$

2.3 CELL CULTURE METHODS

The cell lines used in the study, their origin, and growth media used are shown in Table 2.8. All cell work was performed in a laminar flow hood with a HEPA filter and the working surface was irradiated with UV light for 5 minutes and then swabbed with 70 % ethanol before use. Aseptic technique was practiced for all culture procedures. Media were warmed to 37° C before use.

2.3.1 Growth Media Preparation

All glassware was sterilized by autoclaving for 30 minutes. All solutions were filter-sterilized (0.2 μm filters, Gibco).

2.3.1.1 DMEM: Dulbecco's modified essential medium was prepared from pre-weighed sterile powder (containing 4.5 g/L glucose) by dissolving in 1 L distilled deionized water. Sodium bicarbonate was added according to manufacturer's instructions, and the pH adjusted to 7.4 with HCl. The

Table 2.8 Cell Lines Used in the Study

cell line	origin	media
KNIH 3T3	Kirsten -virus transformed NIH mouse fibroblasts	DMEM
THP1 (w/o PMA*)	human monocytes	RPMI-1640
(w/PMA)	human macrophage-like	RPMI-1640
U937 (w/o PMA‡)	human histocytic lymphoma	RPMI-1640
(w/PMA)	macrophage-like	RPMI-1640

* PMA (phorbol ester, 12-o-tetradecanoylphorbol-13-acetate) treatment of THP1 cells with PMA induced differentiation to macrophage-like cells (Miller and Koeffler 1986)

‡ treatment of U937 cells with PMA induces production of cathepsin B (Ward *et al.* 1990).

solution was filter-sterilized into sterile glass bottles in the laminar flow hood.

2.3.1.2 RPMI-1640: RPMI-1640 was prepared similarly to DMEM.

2.3.1.3 FBS: Sterile fetal bovine serum was heat inactivated according to manufacturer's instructions; it was divided into 40 mL aliquots into sterile tubes and frozen until use.

2.3.1.4 PBS: Phosphate-buffered saline was purchased as a 10X concentrated stock, diluted 1:10 into distilled deionized water, and filter-sterilized before use.

2.3.1.5 2-mercaptoethanol: A solution of 5 mM 2-mercaptoethanol was prepared in distilled deionized water and filter-sterilized before use.

2.3.2 Maintenance of Non-Adherent Cell Lines

The non-adherent cell lines THP1 and U937 were grown in RPMI-1640, supplemented with 10 % FBS. Cells were initially seeded at 10^5 cells/mL and subcultured into fresh media when the cell number reached 10^6 cells/mL. Addition of 0.1 mL 5 mM 2-mercaptoethanol per 10 mL medium prevented clustering of THP1 cells during culture. Cells were grown in a humidified incubator at 37°C and 5% CO_2.

2.3.3 Maintenance of Adherent Cell Lines

KNIH 3T3 cells were grown in DMEM until a nearly confluent monolayer formed. The medium was removed, the cells gently washed with 5 mL PBS, and then treated with 1 mL trypsin (0.05 % trypsin, 0.53 mM EDTA) for 3 minutes at 37°C. Growth medium (4 mL) was added to the detached cells and the cells were gently agitated to break apart clusters. An aliquot (1 mL) of this cell suspension was added to 10 mL fresh media in a new dish. Cells were then grown in a humidified incubator at 37°C and 5% CO_2.

2.3.4 Long Term Cell Storage

Cells were stored in liquid N_2 for extended periods. Cells were grown to 10^7 cells/ 10 mL, pelleted by centrifugation, and resuspended at 10^7 cells/mL in growth media containing 30 % FBS and 10% DMSO. Sterile freezing vials were filled with 1 mL of the cell suspension (10^7 cells/vial), tightly wrapped with adsorbent towels, placed in a box packed with styrofoam, and then the box placed in a -20°C freezer overnight. The next day, the cells were transferred to -70°C for 24 hours, and then to N_2(l) cryo-storage tanks.

Cells to be cultured after long term storage were removed from N_2(l), quickly thawed in a 37°C water bath, and transferred to 10 mL fresh growth medium (10% FBS). After 24

hours, the cells were pelleted by centrifugation (or for adherent cell line, the medium removed), and resuspended in 10 mL fresh growth medium (to remove excess FBS and DMSO present in the freezing solution). Cells were kept in culture for at least two weeks before use in experiments.

2.3.5 Determination of Cell Number

Cell number was determined by counting with a hemocytometer. Cells were suspended in growth media and diluted 1:1 with 0.4% trypan-blue staining solution. A small volume (<10 μL) of this solution was placed on the grid imbedded in the hemocytometer and a glass cover slip gently applied. The number of cells in each of the four large corner areas (16 squares in each area, bounded by a triple line on two sides, 1 mm^2 in area) was counted and the average determined. Only viable cells, which did not take up trypan blue, were counted; likewise, cells touching the right and bottom edges of each square were not included in that square's count. Each 1 mm^2 area has a volume of 10^{-4} mL; thus the total number of cells per 1 mL media was calculated by the formula

$$c = n*2*10^4$$

where n = average # cells/mm^2, c = total # viable cells/mL media, and "2" is the dilution factor (from the 1:1 dilution

of cell suspension with trypan blue solution).

2.3.6 Differentiation of Monocytic Cell Lines

The monocytic cell lines THP1 and U937 can be induced to differentiate to macrophage-like cells by treatment with PMA (phorbol ester, 12-O-tetradecanoylphorbol-13-acetate). A stock of PMA (1 mM) was prepared in acetone and divided into 10 μL (0.01 μmol) aliquots. Cultured monocytes were grown to a density of 10^6 cells/mL and then differentiated by the addition of 50 μL of 100 μM PMA (1 tube of 0.01 μmol brought to 100 μL in acetone, 500 nM final concentration with cells). Differentiated cells were cultured for 24, 48, or 72 hours, as indicated in specific experiments.

2.3.7 Incubation of Cells with Radiolabeled Inhibitors

Cells were grown to 10^6 cells/mL or differentiated for zero to 72 hours in 160 mm^2 culture dishes. The cells were preincubated 1 hour in serum-free media, followed by 3 hours incubation in 5 mL serum-free media containing 2 nmole (0.4 μM) radiolabeled inhibitor. After labeling was complete, cells were removed, pelleted, and washed 3 times in PBS (adherent cells, including differentiated cells, were removed by scraping with a rubber policeman). Cells were then either lysed by 3 cycles of freezing/thawing (see Section 2.1.12) or directly solubilized in sample buffer (see specific

experiments).

2.4 SYNTHESIS OF BSA-CL-Tyr-Ala-CHN_2 COMPLEX

2.4.1 Synthesis of Diazomethane

Diazomethane (CH_2N_2) was synthesized from N-nitroso-N-methyl-4-toluenesulfonamide (diazald) according to instructions provided by Aldrich Chemical Company. No glassware used in the synthesis contained ground glass joints and the synthesis was performed in a laboratory fume hood with the sash pulled down. The glassware was assembled as shown in Figure 2.5, with the cold trap containing dry ice and methanol. KOH (5 g) was dissolved in 8 mL water and added to 10 mL 95% ethanol in a 100 mL flask (reaction vessel). Diazald (5 g) was dissolved in 45 mL ethyl ether and carefully poured into a separatory funnel. When the contents of the reaction vessel reached 65°C, the diazald solution was added dropwise to the KOH solution over at least 30 minutes. The reaction vessel was kept between 65°and 70°C during the entire procedure. Etheral CH_2N_2 was collected (distillate). Once empty, the separatory funnel was rinsed with 20 ml ethyl ether and this solution was added dropwise to the KOH solution as before. The reaction was allowed to continue until the distillate was colorless. As reported, 16.7 mmoles diazomethane was produced by this method. This value was used

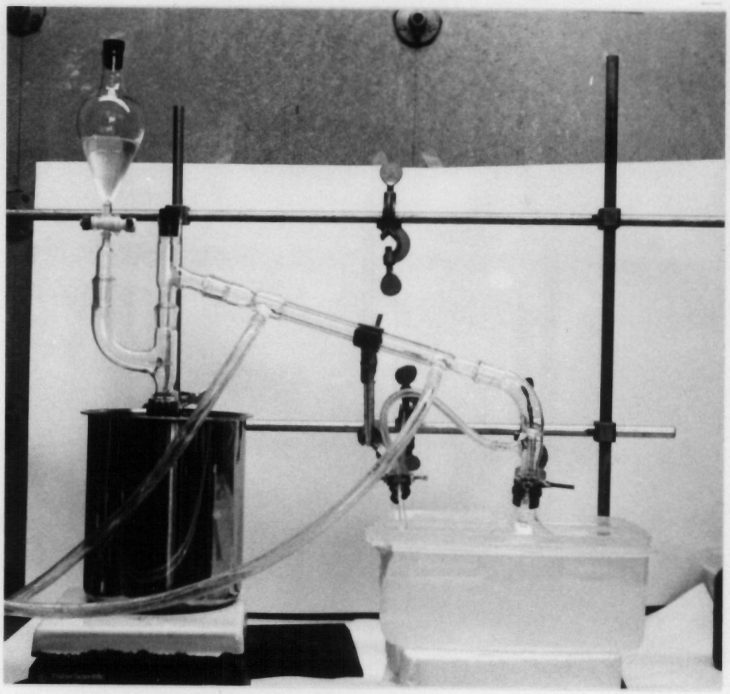

Figure 2.5 Glassware Assembly for Diazomethane Synthesis

The glassware for diazomethane synthesis was set up in a fume hood as shown. Diazald (5 g) in 45 mL ethyl ether was placed in the dropper flask; 5 g KOH in ethanol and water (see Section 2.4.1) was placed in the reaction flask. A water bath surrounding the reaction flask is kept between 65° and 70°C. The diazald solution was added dropwise to the reaction flask over 30 minutes; the distillate was collected in a flask cooled by a dry ice/acetone bath. Gaseous diazomethane was trapped by bubbling through 2 mL ether in the cold trap.

for calculation of CH_2N_2 concentration.

$$\text{Diazald} + \text{KOH} \xrightarrow[\text{ether, 65-70 °C}]{} CH_2N_2$$

2.4.2 Synthesis of the Peptide Acid Chloride

Fmoc-Tyr-Ala-OH was purchased from Bachem (Switzerland). The peptide (1 mmole) was dissolved in 5 mL THF (tetrahydrofuran) in a 25 mL flask. The flask was then covered with a rubber septum and a drying port (made from a 3 cc syringe filled with silica gel dessicant and plugged with tissue paper) was inserted. A syringe connected to an $N_2(g)$ line passing through a drying column was inserted into the septum and the flask purged with dry $N_2(g)$ for 10 minutes. N-methylmorpholine (0.8 mmoles) was added via a syringe , and the solution incubated at -20°C in a dry ice/ethanol bath. Isobutylchloroformate (0.8 mmoles) was added and the solution allowed to incubate 15 min at -20°C. This reaction was done in an air tight, low humidity (<10%) environment to prevent hydrolysis of the acid chloride.

$$\text{Fmoc-Tyr-Ala-OH} \xrightarrow[\text{isobutylchloroformate}]{\text{N-methylmorpholine}} \text{Fmoc-Tyr-Ala-COO-Cl}$$

2.4.3 Synthesis of Fmoc-Tyr-Ala-CHN_2

To the above solution at -20°C was added 6 mL etheral diazomethane, the solution was allowed to warm to 0°C, and the reaction continued for 15 minutes at 0°C. The Fmoc-Tyr-Ala-CHN_2 was retrieved from the reaction mixture by pouring over ice in a separatory funnel with 100 mL ethyl acetate and aqueous $NaHCO_3$. The organic layer was washed with aqueous NaCl (saturated) and dried with $MgSO_4$. The ethyl acetate was removed by rotary evaporation, and the residue dissolved in 85 % acetonitrile /15 % methanol.

$$\text{Fmoc-Tyr-Ala-COO-Cl} + CH_2N_2 \text{ --------> Fmoc-Tyr-Ala-}CHN_2$$

2.4.4 Purification of Fmoc-Tyr-Ala-CHN_2

The diazomethyl ketone was purified by HPLC. An aliquot (1 mL) of the peptide solution was loaded onto a Waters RCM 25x100 Bondapak C-18 column (pore size = 300 Å, particle size = 15-20 μm, "prep column") and eluted at 5 mL/min with an acetonitrile gradient from 20 to 100 % in 50 mM ammonium acetate, pH 6.8, over 80 minutes (Figure 2.6). Absorbance was measured at 260 nm. Fractions (5 mL) were collected from 35 minutes to 75 minutes. Each fraction was assessed for inhibition of papain by a stopped time assay and those fractions containing inhibitor re-chromatographed on a Waters μBondapak C-18 column (pore size = 125 Å, particle size = 10

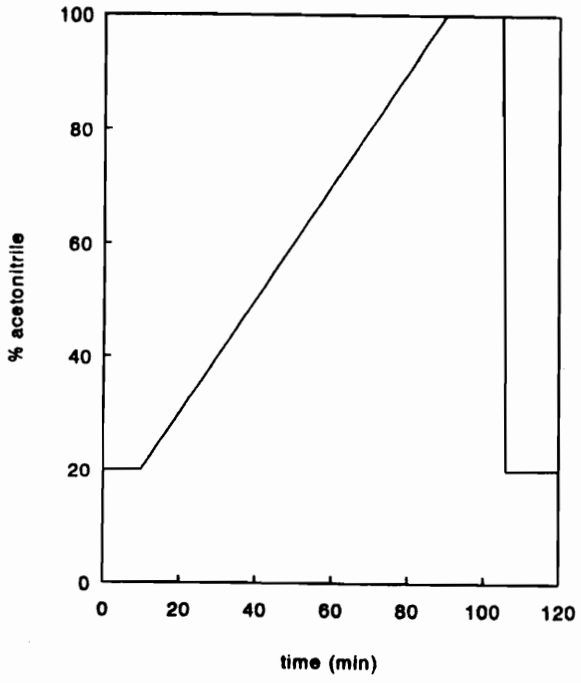

a. Prep column

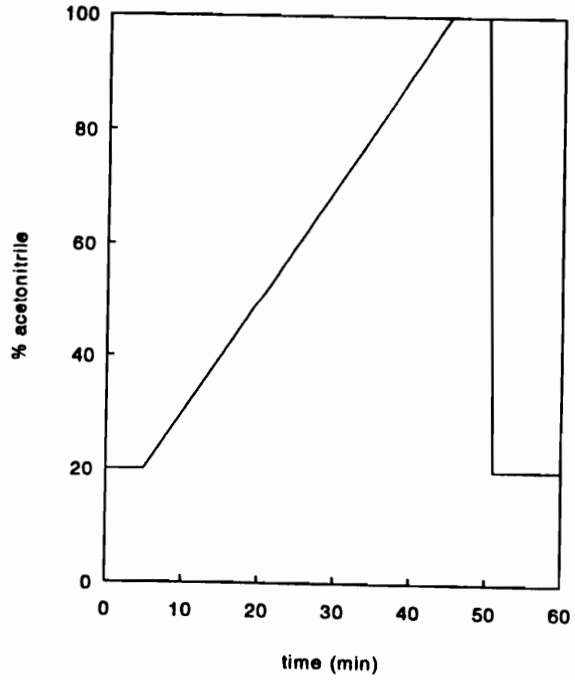

b. Analytical column

Figure 2.6 HPLC Gradient Profiles

μm, 3.9 x 300 mm, "analytical column") with gradient (20 - 100% acetonitrile in 50 mM ammonium acetate, pH 6.8, 1 mL/min) that was pumped over a 40 minute period. Again, absorbance at 260 nm was monitored. The concentration of inhibitor in each fraction was determined by papain titration (Section 2.2.9). Fractions with the greatest purity were lyophilized to remove HPLC solvents.

2.4.5 Mass Spectrometric Analysis of Fmoc-Tyr-Ala-CHN_2

Mass spectrometric analysis of the peptide inhibitor was performed by Dr. J. Shabanowitz of the Department of Chemistry Biological MS Laboratory at the University of Virginia, under the direction of Dr. D.F. Hunt. The inhibitor was injected into the instrument, ionized by electrospray technique, and subjected to both MS and tandem MS (MS/MS) analyses.

2.4.6 Deblocking Fmoc-Tyr-Ala-CHN_2

The peptide was dried, resuspended in DMF , and 8 mL piperidine / mmol peptide was added. The solution was incubated for 30 minutes at room temperature and then diluted into 2 mL ethyl acetate. The solution was applied to a silica gel column in ethyl acetate and washed with 3 column volumes of ethyl acetate to elute free Fmoc-OH. NH_2-Tyr-Ala-CHN_2 was eluted with 3 column volumes of 70 % chloroform/30% methanol. Purity was determined by HPLC and the solvent was removed by

rotary evaporation.

2.4.7 Cross-linking NH_2-Tyr-Ala-CHN_2 to BSA with Sulfo-SANPAH

Sulfosuccinimidyl 6-(4'azido-2'-nitrophenylamino) hexanoate (sulfo-SANPAH) is a water-soluble, irreversible, photoactivatable cross-linking agent. A 10 mg/mL solution was prepared in 70 % DMSO / 30% 0.1 M sodium borate (pH 8.4), in a light-shielded tube and used immediately. Initial cross-linking to the peptide inhibitor must be done in the dark to prevent photoactivation of the cross-linking agent.

The peptide inhibitor was dissolved in DMSO and then sodium borate (0.1 M) added to 30 % (v/v). To this solution was added 10 mmol sulfo-SANPAH per mmol NH_2-Tyr-Ala-CHN_2 present and incubated for 30 minutes in the dark. Next, glycine (10 mg/mL in water) was added to the same concentration as the sulfo-SANPAH to react with any free cross-linking agent and incubated in the dark for an additional 30 minutes. Finally, BSA (300 mg/mL in 50 % DMSO / 50% sodium borate buffer, pH 8.4) was added such that the molar ratio of protein to inhibitor was 1:10, as BSA contains many sites which can react with the cross-linking agent. This solution was transferred to a quartz cuvette and exposed to 10 bright light flashes at 1 cm. The bright light (λ= 320-350 nm) causes the phenylazide component of the crosslinker to react with nucleophilic groups in the protein.

2.4.8 Purification of the BSA-sulfo-SANPAH-Tyr-Ala-CHN_2 Complex

The solution from above (Section 2.4.7) was poured onto a Sephadex G-25 column in 0.1 M sodium borate, pH 8.4. Fractions (1 mL) were collected and assessed for protein content (Section 2.2.2) and inhibition of papain (Section 2.2.9). Protein containing fractions were pooled, concentrated using Amicon Centri-Prep 10 concentrators, and chromatographed over Sephadex G-25 as described above. Protein containing fractions were pooled, concentrated, and the protein and inhibitor concentrations determined. The complex was then washed 3 times in 0.1 M sodium borate by repeated concentration to remove non-specifically bound inhibitor (using Amicon Centri-prep 10 concentrators) and the protein and inhibitor concentrations were determined. The ratio of protein to inhibitor from each step was compared to determine if any inhibitor was being removed from the protein.

2.4.9 Carboxymethylation of BSA

Cysteine sulfhydryl groups in BSA were reacted with iodoacetic acid by a modification of the method of Waxdal et al. (1968; Fontana and Gross 1986). Briefly, BSA (400 mg) was dissolved in 20 mL of 0.5 M Tris-HCl (pH 8.3) in a 50 mL polypropylene tube and guanidine-HCl was slowly added to a final concentration 6M (final volume 40 mL). Air in the tube was replaced with $N_2(g)$; the tube was capped and incubated at

37° C for 30 min. Dithiothreitol (DTT: 1.8 mmoles, or 300 mmoles DTT/mol protein) was added to the solution, the air again replaced with N_2(g), and the solution incubated 4 h at 37° C. The tube was then covered with foil, cooled on ice, and iodoacetic acid added (2-fold molecular excess over free thiol (DTT) present, or 700 moles iodoacetic acid / mol protein). The pH was adjusted to pH 8. The solution was incubated on ice for 1 h after which 2-mercaptoethanol (500 X mol protein) was added. The solution was transferred to dialysis tubing and dialysed against 4 changes of 0.5 M Tris-HCl (pH 8.33). The solution was lyophilized, redissolved in 0.1 M sodium borate (pH 8.4), and then dialyzed against 0.1 M sodium borate (pH 8.4) for 24 hours.

2.4.10 Determination of R-SH in Carboxymethylcysteine BSA

The content of free cys-SH in the dialyzed protein was determined by the method of Thannhauser et al. (1984; Darbre 1986).

A stock solution of 0.5 mM DTNB (5,5'-dithiobis[2-nitrobenzoate], Ellman's reagent) was prepared by dissolving 0.1 g DTNB in 10 mL of 1 M Na_2SO_3, pH 7.5, at 38°C. Air passed through a silica gel drying column was bubbled through the solution for 4 hours during which the orange color disappeared leaving a pale yellow solution. Loss of absorbance at λ=412 nm signals the conversion of 2-nitro-5-thiobenzoate (NTB) to 2-

nitro-5-thiosulfobenzoate (NTSB) (Figure 2.7). The NTSB stock reagent was stored at -20° C. The assay solution was prepared by diluting the NTSB reagent 1:100 into 0.2 M Tris-HCl (pH 7.5), 0.1 M Na_2SO_3, 3 mM EDTA, 6 M guanidine-HCl, pH 9.5. A stock solution of 0.2 M Tris-HCl (pH 7.5), 3 mM EDTA, and 6M guanidine-HCl was prepared and stored at room temperature. Before each assay, Na_2SO_3 was added to the Tris-HCl/EDTA/guanidine-HCl solution to a final concentration of 0.1 M Na_2SO_3, the pH adjusted to 9.5, and the solution used to dilute the NTSB reagent. Various volumes (0.01 mL, 0.05 mL, 0.10 mL, and 0.20 mL) of protein solution were mixed with 3 mL NTSB assay reagent and incubated 25 minutes in the dark at room temperature. The absorbance at 412 nm was measured and the concentration of SH present was calculated using ϵ=13600 $M^{-1}cm^{-1}$.

2.4.11 Cross-linking BSA to NH_2-Tyr-Ala-CHN_2 Using Sulfo-SADP

Initial experiments using non-radioactive iodinated peptide revealed the ratio of inhibitor to cross-linking agent for effective cross-linking. Fmoc-Tyr-Ala-CHN_2 (4 μmoles) was deblocked, dried, and dissolved in 2-propanol. The deblocked peptide was iodinated as described, using non-radioactive NaI. NH_2-(I)Tyr-Ala-CHN_2 (1 μmole) was incubated with 1, 2, 5, or 10 μmole sulfo-SADP as described for the non-reducible analog, sulfo-SANPAH. After reaction with equimolar

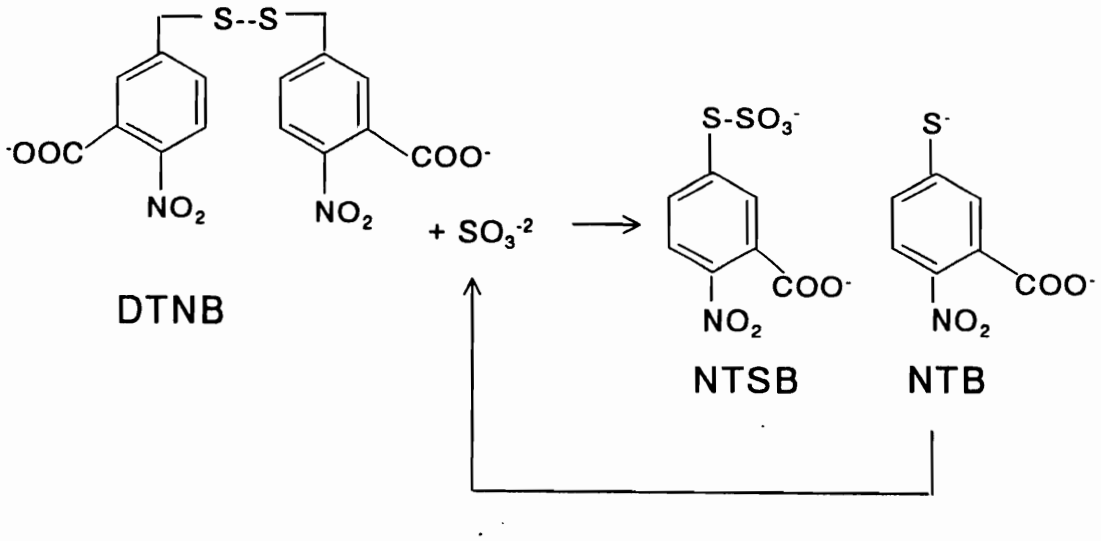

a. Reaction of DTNB to produce NTSB

$$R\text{-}S\text{-}S\text{-}R' + SO_3^{-2} \rightleftharpoons R\text{-}S\text{-}SO_3^{-} + R'\text{-}S^{-}$$

$$R'S^{-} + NTSB \rightleftharpoons R'S^{-} + NTB$$

b. Reaction of NTSB with R-S-S-R' and R-S^{-}

Figure 2.7 Determination of R-S-S-R and R-SH

a) DTNB reacts with SO_3^{-2} to produce NTSB and NTB. NTB reacts further with SO_3^{-2} to produce NTSB. b) Reaction of dithiols with SO_3^{-2} produces reduced thiols which react with NTSB to produce NTB, the production of which can be monitored at λ = 412 nm.

amounts of glycine and cross-linking agent, 0.1 μmole CM-BSA was added and the solution exposed to 10 bright light flashes at 1 cm. The complex was purified as described in Section 2.4.8. The concentration of protein and inhibitor were determined after the final wash as described in Sections 2.2.2 and 2.2.9.

CHAPTER 3 CHARACTERIZATION OF CELLULAR FORMS OF CATHEPSINS B, L, AND S

3.1 Introduction

The lysosomal cysteine proteinases cathepsins B, L, and S and their biosynthetic forms can be distinguished from each other by the use of active-site directed, irreversible, radiolabeled inhibitors such as Fmoc-(^{125}I)Tyr-Ala-CHN_2, followed by SDS-PAGE and autoradiography. In human cell lines, cathepsin B single-chain form has a molecular weight of 35 kDa; the light chain of the two-chain form (5 kDa) contains the active site cysteine that covalently interacts with the inhibitor. Human cathepsin L migrated as a band of 31 kDa (single chain) and 24 kDa (heavy chain of the two-chain form). Human cathepsin S has only a single chain form appearing at 28 kDa (Shi et al. 1992); bovine spleen cathepsin S is seen at 24 kDa (Xin et al. 1992). To distinguish cathepsin L (heavy chain of the two-chain form) from cathepsin S, differences in their isoelectric points are exploited: cathepsin L has a pI of 5.5 to 6.1 (Barrett and Kirschke 1981) while cathepsin S has a pI of 7.0 (Kirschke et al. 1989). Cathepsin B has a pI of 4.5 to 5.5 (Barrett and Kirschke 1981).

3.2 Identification of Cathepsins B, L, and S in Whole Cells

Two human cell lines were screened for their content of cathepsins B, L, and S. Cells were incubated with the irreversible inhibitor Fmoc-(^{125}I)Tyr-Ala-CHN_2, and cathepsins B, L, and S isolated by immunoprecipitation. Samples were then analyzed by SDS-PAGE and autoradiography.

3.2.1 U937

U937 is a human histocytic lymphoma cell line. Upon treatment with PMA (12-O-tetradecanoylphorbol-13-acetate), these cells differentiate into macrophage-like cells, initiating the production of cathepsin B (Ward et al. 1990). The presence of cathepsins B, L, and S was investigated in both non-differentiated cells and those treated with PMA for 24, 48, or 72 hours. Cells (10^6) were treated with 500 nM PMA for 24, 48, or 72 hours in RPMI containing 10% FBS. An equal number of cells was not treated (0 h) and served as a control. For the 48 and 72 h experiments, the medium was changed every 24 h. Following a 1 h incubation in serum-free media, the cells were incubated with 4 μM Fmoc-(^{125}I)Tyr-Ala-CHN_2 (2 nmole in 0.5 mL) for 3 h. Cells were harvested, washed twice in PBS, resuspended in 10 mM Tris-HCl pH 7.0, and subjected to three rounds of freezing and thawing. The lysate was treated remove any proteins that might bind non-specifically to IgG or PAS by incubating the samples with 10

μL rabbit anti-sheep IgG and 30 μL 10% PAS for 2 h on a rotary mixer. The PAS was pelleted by centrifugation and antibody against cathepsin B, L, or S (see Sections 2.2.12, 2.2.13, and 2.2.14) and 30 μL protein A or protein G Sepharose were added to the supernatant. The samples were incubated over night at room temperature on a rotary mixer. The samples were pelleted by centrifugation and the pellet washed twice in PBS, resuspended in 50 μL SDS-PAGE sample buffer (Table 2.1) and analyzed by SDS-PAGE (Bury system, Section 2.2.3.1) and autoradiography.

The immunoprecipitation of cathepsins B, L, and S from U937 cells is shown in Figure 3.1. No cathepsin B is present in undifferentiated cells (lane 1). Upon PMA treatment, however, cathepsin B synthesis is initiated as indicated by immunoprecipitation of cathepsin B at 33 kDa (lanes 2-4). This band corresponds to the single chain form of cathepsin B. A faint band at 31 kDa is present in anti-cathepsin L analyses in both nondifferentiated or differentiated cells (lanes 5-8). This indicates a low level of expression of cathepsin L in U937 cells. The amount expressed is not large compared to the amount of cathepsin B (lanes 1-4) and cathepsin S (lanes 9-12). Cathepsin S is present as 36 kDa, 28 kDa, and 26 kDa bands in differentiated cells. The 36 kDa band in lane 10 may represent an active pro-form of the enzyme that is capable of reacting with the inhibitor. The 28 kDa

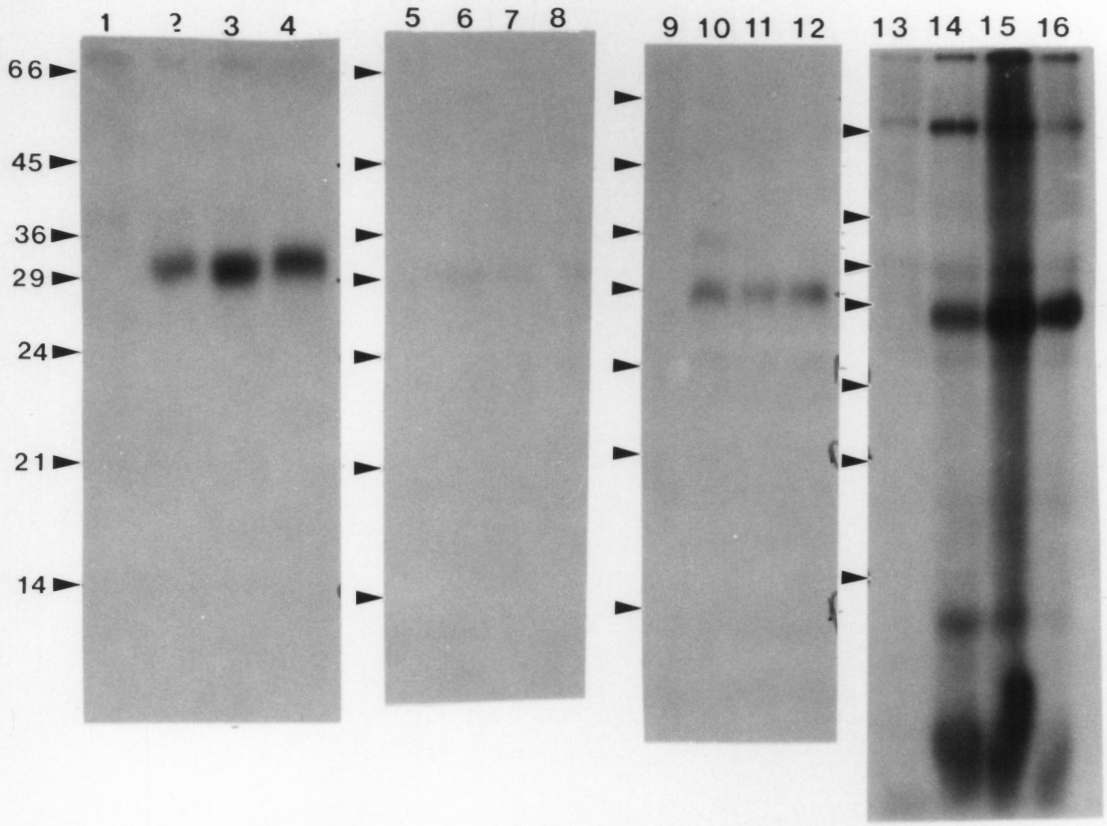

Figure 3.1 Cathepsins B, L, and S in U937 Cells

U937 cells (10^6) were treated with 500 nM PMA for 0 (no PMA added), 24, 48, or 72 h in 1 mL RPMI with 10% FCS. Cells were then incubated 1 h in 0.5 mL serum free RPMI, followed by 3 h in fresh RPMI with 4 μM Fmoc-(^{125}I)Tyr-Ala-CHN_2. Cells were harvested, washed twice in PBS, suspended in 10 mM Tris-HCl, pH 7.0, and lysed by three rounds of freezing and thawing. Cathepsins B, L, and S were immunoprecipitated as described in Sections 2.2.12-14, with the final pellets being suspended in 100 μL sample buffer. Each sample (10 μL) was analyzed by SDS-PAGE (Bury system), followed by autoradiography. Lanes 1-4: cathepsin B; lanes 5-8: cathepsin L; lanes 9-12: cathepsin S; lanes 13-16: whole cells. Lanes 1,5,9,13: 0 h PMA; lanes 2,6,10,14: 24 h PMA; lanes 3,7,11,15: 48 h PMA; lanes 4,8,12,16: 72 h PMA.

band corresponds to human cathepsin S as reported by Shi et al. (1992). The 26 kDa band may represent the heavy chain of a two-chain form of cathepsin S, although cathepsin S from tissue sources and human alveolar macrophages has not been reported to be further proteolytically processed after it has reached the single-chain form. Lanes 13-16 in Figure 3.1 are the SDS-PAGE and autoradiographic analyses of whole cells (no immunoprecipitation). The cell pellet, after washing twice in PBS, was suspended in 100 μL SDS-PAGE sample buffer and 10 μL, equivalent to 10^5 cells, were analyzed. Lane 13, nondifferentiated cells, shows no labeling with the inhibitor; thus, there are no detectable levels present of any enzyme which might react with the inhibitor. Differentiated cells (lanes 14-16) show 5 bands: 70 kDa (unknown), 36 kDa (pro-cathepsin S), 33-28 kDa (cathepsin B single-chain and cathepsin S), 26 kDa (single chain cathepsin S), and <14 kDa band (unknown).

3.2.2 THP1

THP1 is a human acute monocytic cell line (Tsuchiya et al. 1980). Like U937 cells, THP1 cells are differentiated to macrophage-like cells by treatment with PMA (Miller and Koeffler 1986). The presence of cathepsins B, L, and S in these cells, both before and after differentiation, was explored using Fmoc-(^{125}I)Tyr-Ala-CHN_2, followed by

immunoprecipitation of the enzymes.

Cells (10^6) in 1 mL RPMI media containing 10% FBS were treated with 500 nM PMA for 24, 48, or 72 h. Non-differentiated cells served as controls. Cells were incubated 1 h in serum-free RPMI, followed by 3 h in fresh serum-free media with 4 μM Fmoc-(^{125}I)Tyr-Ala-CHN_2 (2 nmole in 0.5 mL). Cells were harvested, washed, and lysed as before in 10 mM Tris-HCl, pH 7.0. The samples were incubated 2 h with non-specific rabbit anti-sheep IgG and 10% PAS to remove any proteins that may nonspecifically bind to either IgG or PAS. Following removal of the PAS/PGS, specific antibody (anti-cathepsin B, L, or S; see Sections 2.2.12 to 2.2.14) was added to the samples and the samples incubated overnight at room temperature on a rotary mixer. The PAS pellets were washed twice in PBS and solubilized in 100 μL sample buffer as before; 10 μL was analyzed by SDS-PAGE.

Figure 3.2 shows the results of immunoprecipitation of cathepsins B, L, and S from THP1 cells. Cathepsin B (33 kDa) is present in these cells in the non-differentiated state (lane 1); upon treatment with PMA, cathepsin B appears as a 31 kDa form, with increasing amounts from 24 to 72 h after differentiation (lanes 2-4). Immunoprecipitation of cathepsin L from all samples (lanes 5-8) shows labeled bands at 35 kDa, indicating the presence of cathepsin L in both differentiated and nondifferentiated cells. Intensity of labeling is

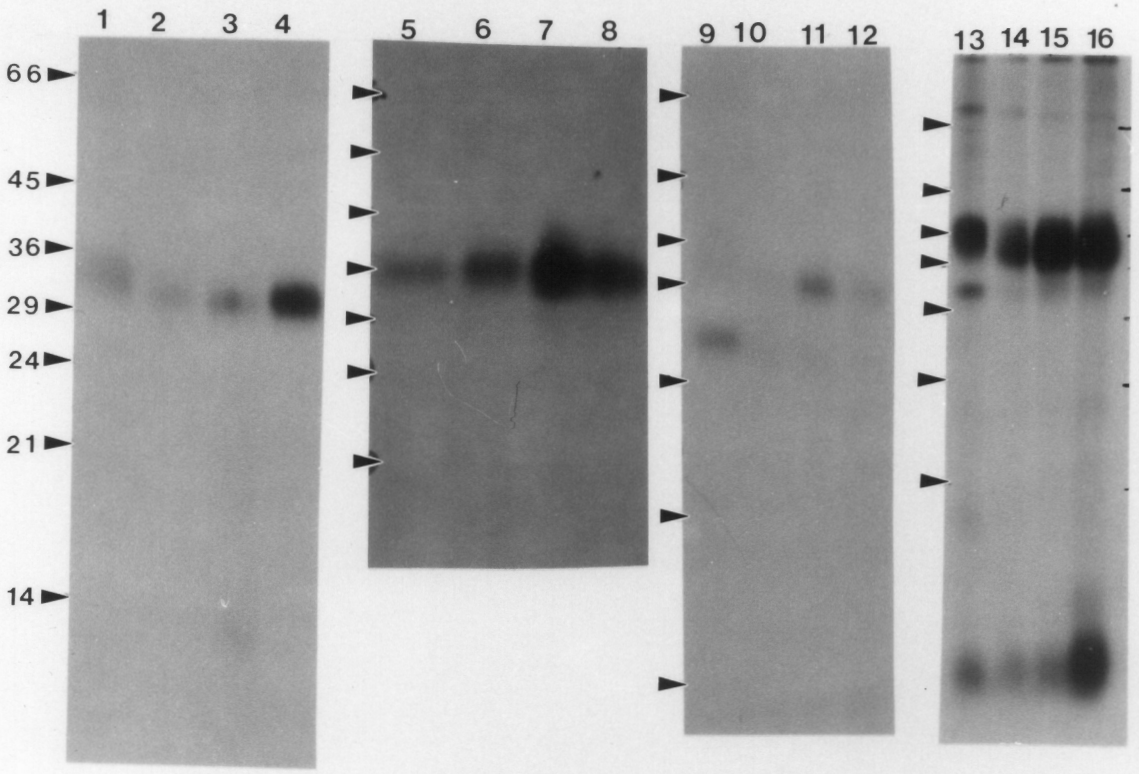

Figure 3.2 Cathepsins B, L, and S in THP1 Cells

THP1 cells (10^6) were treated with 500 nM PMA for 0 (no PMA added), 24, 48, or 72 h in 1 mL RPMI with 10% FCS. Cells were then incubated 1 h in 0.5 mL serum free RPMI, followed by 3 h in fresh RPMI with 4 μM Fmoc-(^{125}I)Tyr-Ala-CHN_2. Cells were harvested, washed twice in PBS, suspended in 10 mM Tris, pH 7.0, and lysed by three rounds of freezing and thawing. Cathepsins B, L, and S were immunoprecipitated as described in Sections 2.2.12-14, with the final pellets being suspended in 100 μL sample buffer. 10 μL of each sample was analyzed by SDS-PAGE (Bury system), followed by autoradiography. Lanes 1-4: cathepsin B; lanes 5-8: cathepsin L; lanes 9-12: cathepsin S; lanes 13-16: whole cells. Lanes 1,5,9,13: 0 h PMA; lanes 2,6,10,14: 24 h PMA; lanes 3,7,11,15: 48 h PMA; lanes 4,8,12,16: 72 h PMA.

increased from 0 to 72 h of PMA treatment, indicating that more cathepsin L is synthesized after differentiation. Two-chain cathepsin L was not detected in THP1 cells. Cathepsin S is also present in both differentiated and nondifferentiated cells (lanes 9-12), although in a lower molecular weight form (26 kDa, lane 9) in untreated cells than in PMA treated cells (29 kDa, lanes 10-12). The labeling of the 29 kDa form intensifies over time of differentiation; the 26 kDa form is also present in the differentiated cells, although not as much as in the nondifferentiated cells (26 kDa band, lanes 10-12 compared to lane 9). As in U937 cells, a high molecular weight form (35 kDa) is also faintly seen in undifferentiated cells only. It is likely that the 26 and 28 kDa bands represent a single- and two-chain form of the enzyme. The 26 kDa form labels very strongly in undifferentiated whole cells (lanes 13, no immunoprecipitations performed); its intensity is weakened over time of differentiation (lanes 14-16).

3.3 Determination of Isoelectric Points of Cathepsins B, L, and S

Bovine cathepsin B (Sigma Chemical company), sheep liver cathepsin L, and bovine spleen cathepsin S were analyzed by 2-dimensional electrophoresis (IEF/SDS-PAGE) to determine their isoelectric points. Each enzyme (cathepsin B: 10 μL, 5 μg; cathepsin L: 10 μL, 0.11 μg,; cathepsin S: 200 μL, 10 μg) was

incubated for 30 minutes with 20 μL 400 mM sodium acetate buffer , 4 mM EDTA, 4 mM DTT (pH 5.5) and 0.67 nmol Z-(^{125}I)Tyr-Ala-CHN_2. IEF sample buffer (40 μL) was added and 10 μL was loaded onto IEF tube gels (Section 2.2.4) and subjected to 2-dimensional electrophoresis as described in Section 2.2.4. Figure 3.3 shows the results of such analyses. Cathepsin B is present at 24 kDa/pI 5.9. The molecular weight is much lower than that seen in cells (Section 3.2), reflecting differences between cathepsin B isoforms in commercially available preparations and cathepsin B present in whole cells. Sheep liver cathepsin L (Figure 3.3.b) has multiple pI forms near the cathodic (pH 3) end. A laddering effect is seen involving 4 spots: 30 kDa/pI 3.0, 30 kDa/pI 4.0, 25 kDa/pI 3.0, and 25 kDa/pI 4.0. Additional spots are seen at 24 kDa/pI 4.6, 21 kDa/pI 4.6; and 21 kDa/pI 6, 17 kDa/pI 6. Bovine spleen cathepsin S (Figure 3.3.c) appears to have a pI of 5.9 and two molecular weight forms of 25 and 23 kDa. The 2 kDa difference could be due to differently glycosylated forms. Note that cathepsins B and S cannot be differentiated from each other using 2-dimensional electrophoresis, as both enzymes from the sources used appear to have the same pI and molecular weight.

3.4 2-Dimensional Analysis of Differentiated THP1 Cathepsin L

Immunoprecipitated cathepsin L from THP1 cells has

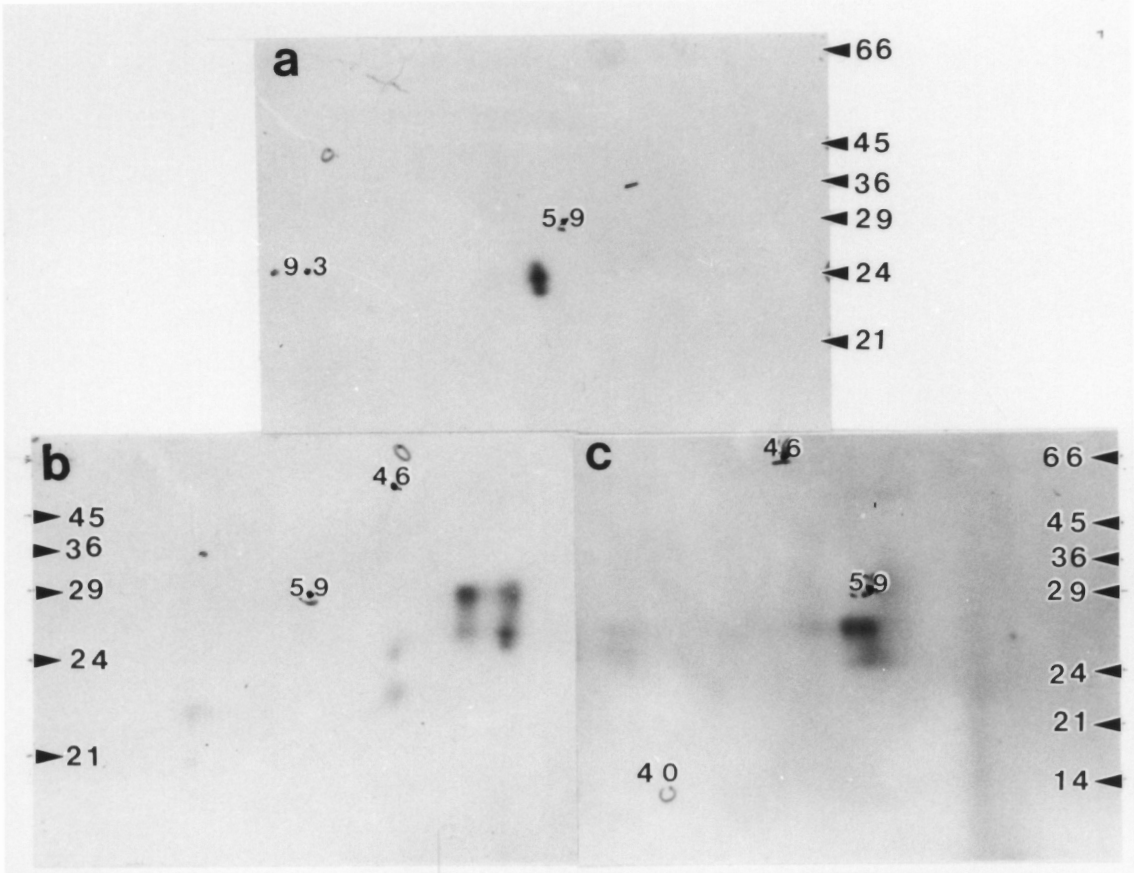

Figure 3.3 IEF/SDS-PAGE of Cathepsins B, L, and S

Bovine cathepsin B (Sigma Chemical Company), sheep liver cathepsin L, and bovine spleen cathepsin S were analyzed by 2-dimensional electrophoresis (IEF/SDS-PAGE) to determine their isoelectric points. Each enzyme (cathepsin B: 10 μL, 5 μg; cathepsin L: 10 μL, 0.11 μg,; cathepsin S: 200 μL, 10 μg) was incubated for 30 minutes with 20 μL 400 mM sodium acetate buffer (pH 5.5, 4 mM EDTA, 4 mM DTT) and 0.67 nmol Z-(^{125}I)Tyr-Ala-CHN_2. IEF sample (40 μL) buffer was added and 10 μL was loaded onto IEF tube gels (Section 2.2.4); molecular weight/IEF standards (5 μL) were loaded on top of the sample, followed by sample overlay buffer (Table 2.5). The samples were subjected to a vertical electric field for 7 h at 500 V, with the anode on top (0.1 M phosphoric acid) and the cathode on the bottom (0.2 M NaOH). After 7 h, the gel was forced from the tube by water pressure, incubated 30 minutes in hot SDS-PAGE sample buffer E, and then laid across the top of the SDS-PAGE stacking gel. After electrophoresis, the slab gel was stained with Coomassie brilliant blue G-250, destained, dried, and subjected to autoradiography. a.) cathepsin B b.) cathepsin L c.) cathepsin S.

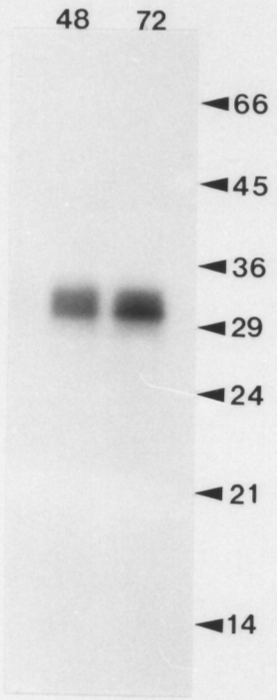

Figure 3.4 Multiple Forms of Cathepsin L

THP1 cells were incubated 3 h with Fmoc-(^{125}I)Tyr-Ala-CHN_2 following 48 or 72 h PMA treatment. Cells were washed and cathepsin L was immunoprecipitated as described above. The final cathepsin L pellet was solublized in SDS-PAGE sample buffer and analyzed by SDS-PAGE (Bury system) and autoradiography. Three difficult-to-distinguish bands are apparent.

appeared as 3 difficult-to-distinguish forms of 31-35 kDa following SDS-PAGE (Figure 3.4) on 20 cm gels. IEF/SDS-PAGE (2-dimensional) analysis of immunoprecipitated cathepsin L from differentiated THP1 cells was investigated to determine whether the forms could be better separated as seen for sheep liver cathepsin L (Figure 3.3.b). Cells (10^7) were treated with 500 nM PMA for 24, 48, or 72 in RPMI with 10% FBS. The cells were incubated 1 h in serum-free media, followed by a 3 h incubation in fresh serum free media containing 0.4 μM Fmoc-(^{125}I)Tyr-Ala-CHN_2. Cells were harvested, washed twice in PBS, and solubilized in 100 μL IEF sample buffer (Table 2.5). Figure 3.5 shows a pattern similar to that seen in Figure 3.3.b; there is no real difference between samples treated with PMA for 24, 48 or 72 h. All three samples show two streaks of pI 3.0 and 3.7, with molecular weights of 35 - 24 kDa. The M_r/pI forms of 24/4.6, 21/4.6, 21/6, and 17/6 are not seen in cathepsin L from THP1 cells.

3.5 Glycosidase Treatment of Immunoprecipitated Cathepsin L

The multiple pI forms of cathepsin L seen above (Figures 3.3.b and 3.5) may be due to differently glycosylated isoforms of the protein. To test this hypothesis, 3 glycosidases were used to treat immunoprecipitated cathepsin L: endoglycosidase H (to remove mannose 6-phosphate containing carbohydrates), neuraminidase (to remove sialic acid residues), and PNGase F

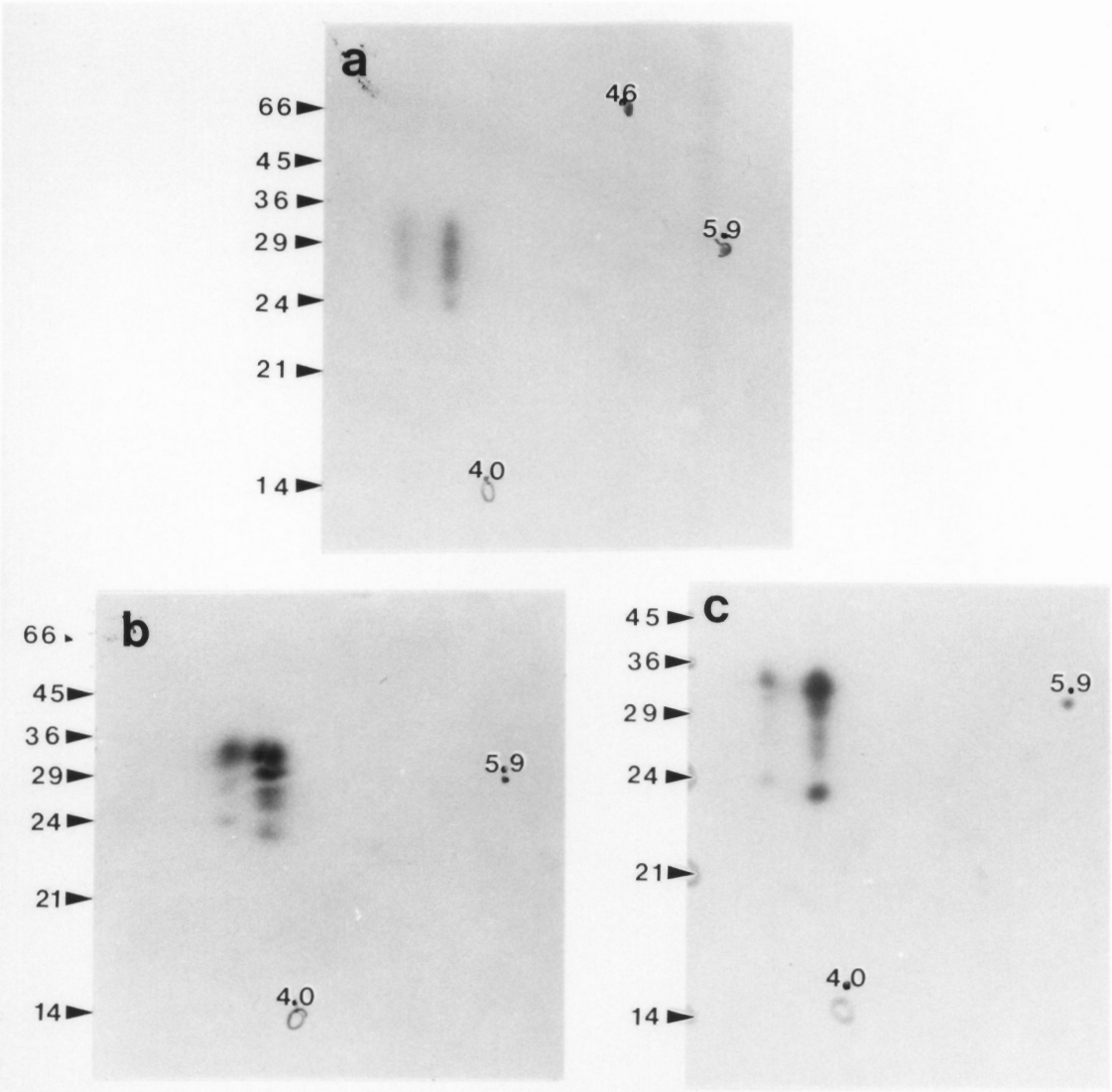

Figure 3.5 IEF/SDS-PAGE of Immunoprecipitated Cathepsin L from Differentiated THP1 cells

THP1 (10^{7}) cells were differentiated by PMA treatment for a.) 24, b.) 48, or c.) 72 hours. The cells were then incubated in serum-free RPMI-1640 for 1 h, followed by 3 h in RPMI-1640 plus 4 μM Fmoc-(^{125}I)Tyr-Ala-CHN_2. Cells were harvested, washed, lysed by freezing and thawing, and cathepsin L immunoprecipitated. The final immunoprecipitate was suspended in 100 μL IEF sample buffer. Protein from 10^{6} cells was analyzed by IEF/SDS-PAGE and autoradiography.

(to remove all N-linked carbohydrates). Endoglycosidase H and neuraminidase were purchased from Boehringer-Mannheim (Indianapolis, IN) and PNGase F (N-glycadase) from Genzyme (Cambridge, MA).

3.5.1 Glycosidase Controls

The glycosidases were tested for their activity against two test proteins; fetuin and RNase B. Test protein (100 μg of 5 mg/mL in 0.05 M NaCl) was diluted in 70 μL 50 mM sodium acetate , pH 5.5, 5 mM $CaCl_2$ and 20 μL 50 μM E-64; 10 μL neuraminidase (100 mUnits) were added and the samples incubated overnight at room temperature. Likewise, 100 μg test protein was diluted in 80 μL 100 mM sodium acetate, pH 5.5, and 20 μL of 50 μM E-64; 20 mUnits endoglycosidase H were added and the samples incubated overnight at room temperature. To test PNGase F, the test protein (100 μg) was diluted in 50 μL IEF-sample buffer, 50 μL 1:4 dilution gel buffer B (Table 2.1), and 25 μL of 50 μM E-64; 1 unit of enzyme was added and the samples incubated 24 hours at 37°C. Samples were analyzed by SDS-PAGE (Bury system; Figure 3.6). Neuraminidase treatment of fetuin caused a shift from 66 kDa to 60 kDa (Figure 3.6.a, lane 1 versus 3), but did not affect RNase B (lane 4 versus 6). Endoglycosidase H had little effect on fetuin (Figure 3.6.a, lane 2 versus 3), but caused a large change in RNase B mobility (20 kDa to 18 kDa, lane 5 versus

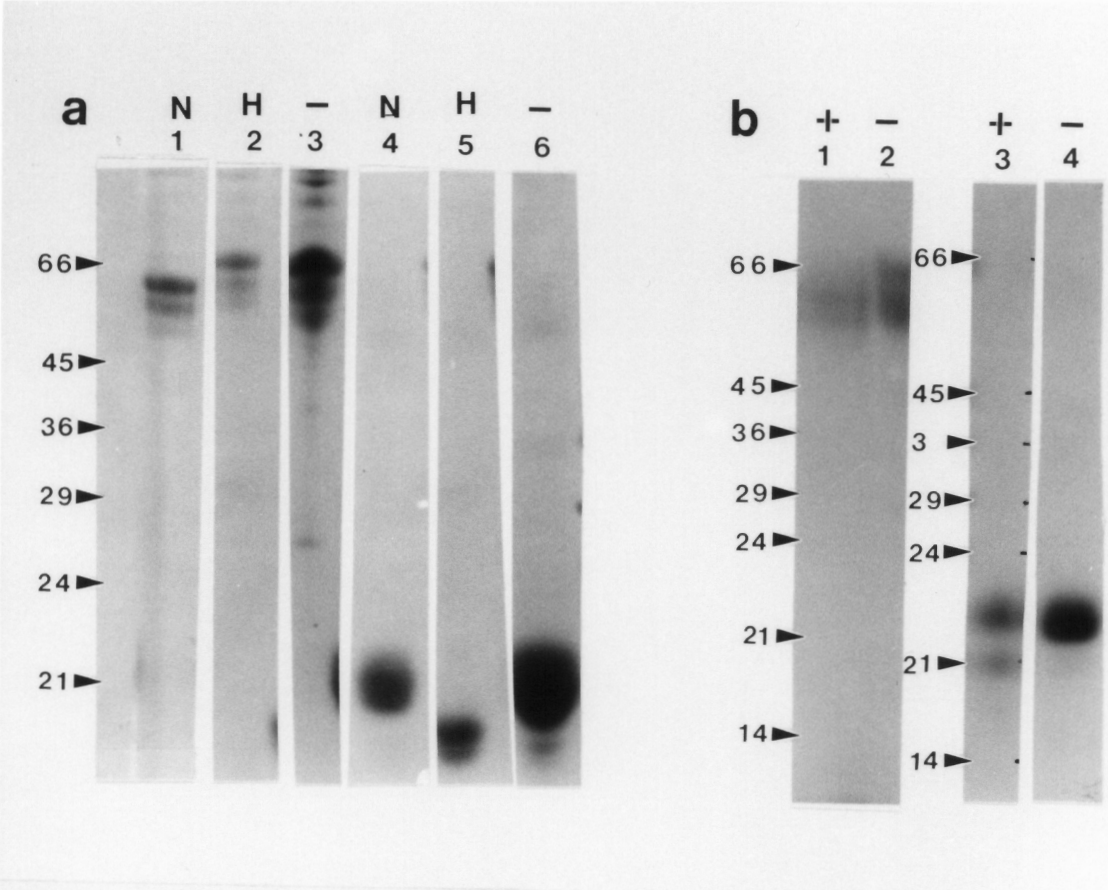

Figure 3.6 Glycosidase Tests

Fetuin or RNAse (100 μg of 5 mg/ml in 0.05 M NaCl) was diluted in 70 μL 50 mM sodium acetate buffer, pH 5.5, 5 mM $CaCl_2$ and 20 μL 50 μM E-64; 10 μL neuraminidase (100 mUnits) was added and the samples incubated overnight at room temperature. Likewise, 100 μg test protein was diluted in 80 μL 100 mM sodium acetate, pH 5.5, and 20 μL of 50 μM E-64; 20 mUnits endoglycosidase H was added and the samples incubated overnight at room temperature. To test PNGase F, the test protein (100 μg) was diluted in 50 μL IEF-sample buffer, 50 μL 1:4 dilution gel buffer B (Table 2.1), and 25 μL of 50 μM E-64; 1 unit of enzyme was added and the samples incubated 24 hours at 37°C. Samples were analyzed by SDS-PAGE (Bury system). a.) lanes 1 and 4: neuraminidase; lanes 2 and 5 : endoglycosidase H; lanes 3 and 6: no glycosidase added; lanes 1,2,and 3 ; fetuin ; lanes 4,5, and 6 : RNAse B . b.) lanes 1 and 3: PNGase F; lanes 2 and 4: no glycosidase; lanes 1 and 2: fetuin; lanes 3 and 4: RNAse B.

6). PNGase F altered fetuin from 66 kDa (Figure 3.6.b, lane 2) to 60 kDa (lane 1), but had no effect on RNase B (lane 3 versus 4). Thus, the glycosidases are active under the conditions described above. These same conditions will be used for the analyses of immunoprecipitated cathepsin L.

3.5.2 Endoglycosidase H

THP1 cells ($2x10^6$) were incubated 3 h with Fmoc-(^{125}I)Tyr-Ala-CHN_2 following 48 h PMA treatment. Cells were washed and cathepsin L was immunoprecipitated as described above. Sodium acetate (20 μL of 100 mM, pH 5.5), 50 μM E-64 (2 μL), and endoglycosidase H (20 mUnits, 5 μL) was added to the final cathepsin L pellet; control samples were prepared and analyzed in parallel, in which the immunoprecipitate was suspended in the sodium acetate buffer (plus E-64), but without endoglycosidase H. The samples were incubated overnight at room temperature on a rotary mixer and then analyzed by IEF-PAGE.

There is no difference in mobility the sample treated with endoglycosidase H and the untreated sample (Figure 3.7). Labeling is not very strong and the spots are difficult to detect; even so, the laddering effect is apparent in endoglycosidase treated cells (Figure 3.7.b). The two isoforms (pI 3 and 3.5) are detected in both treated and untreated samples. Therefore, the different forms of cathepsin L seen

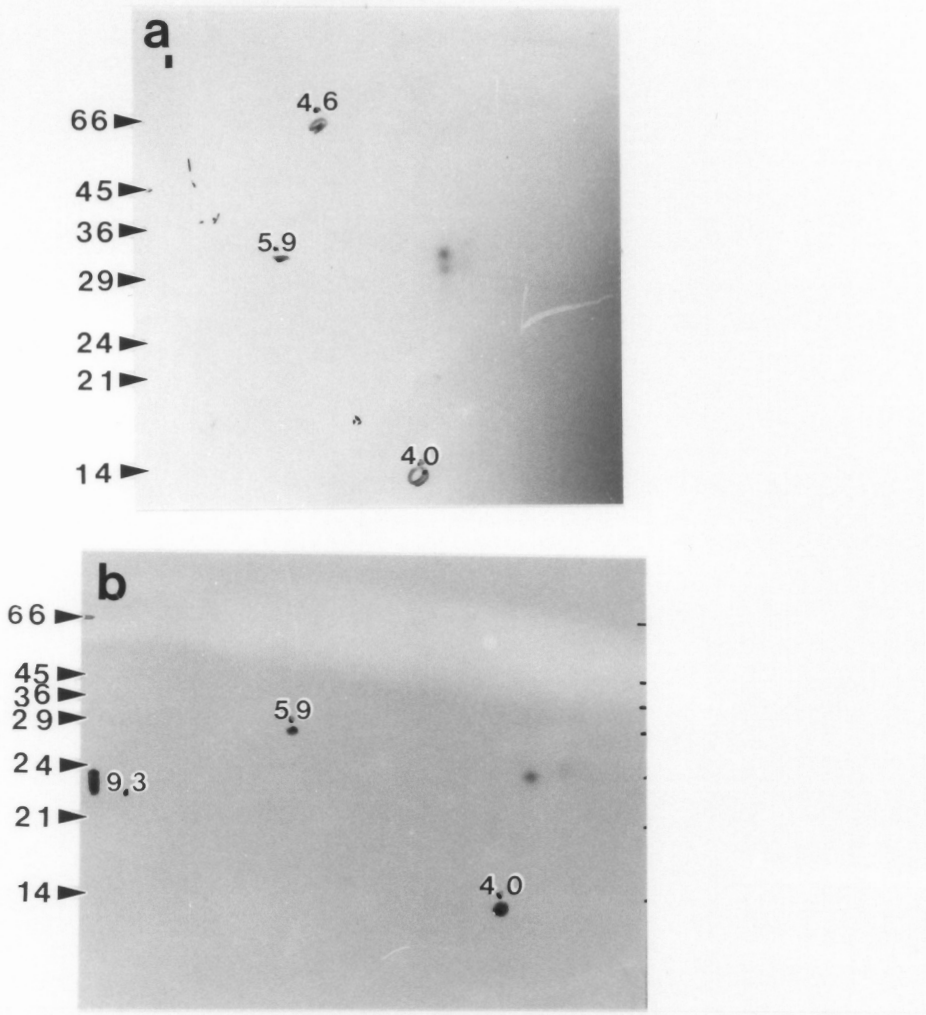

Figure 3.7 Endoglycosidase H Treatment of Immunoprecipitated Cathepsin L

THP1 cells ($2x10^6$) were incubated 3 h with Fmoc-(^{125}I)Tyr-Ala-CHN_2 following 48 h PMA treatment. Cells were washed and cathepsin L was immunoprecipitated as described above. To the final cathepsin L pellet was added 20 μL 100 mM sodium acetate, pH 5.5, 2 μL 50 μM E-64, and 5 μL endoglycosidase H (20 mUnits); control samples were prepared and analyzed along side in which the immunoprecipitate was suspended in the sodium acetate buffer (plus E-64), but without endoglycosidase H. The samples were incubated overnight at room temperature on a rotary mixer and then analyzed by IEF-PAGE. a) no endoglycosidase H treatment; b) with endoglycosidase H treatment.

in Figures 3.3.b and 3.5 are not due to high mannose oligosaccharides on the protein.

3.5.3 Neuraminidase

THP1 cells ($2x10^6$) were incubated 3 h with Fmoc-(^{125}I)Tyr-Ala-CHN_2 following 0, 24, 48, or 72 h PMA treatment. Cells were washed and cathepsin L was immunoprecipitated as described above. Sodium acetate (20 μL of 50 mM, pH 5.5, 5 mM $CaCl_2$), 50 μM E-64 (2 μL), and neuraminidase (50 mUnits; 5 μL) was added to the final cathepsin L pellet and the sample incubated overnight at room temperature on a rotary mixer. As above, a control samples were incubated without neuraminidase. Figure 3.8.a shows that neuraminidase treatment had no effect on the molecular forms present seen after a 1-D analysis. Note also the increase in labeling, and thus cathepsin L synthesis, from nondifferentiated cells to those treated for 72 h with PMA. Figure 3.8.b and 3.8.c show that in 2-dimensions there is also no difference in the two pI cathepsin L forms after treatment of THP1 cells with PMA for 72 h. The laddering effect is diminished but still present in the neuraminidase-treated sample (Figure 3.8.c) resulting in the appearance of only the low molecular weight forms (24 and 23 kDa). The pI of each form, however, is not affected. Although reported to contain no proteases by the manufacturer (determined by checking for the degradation of casein; Twinning 1984), an active enzyme

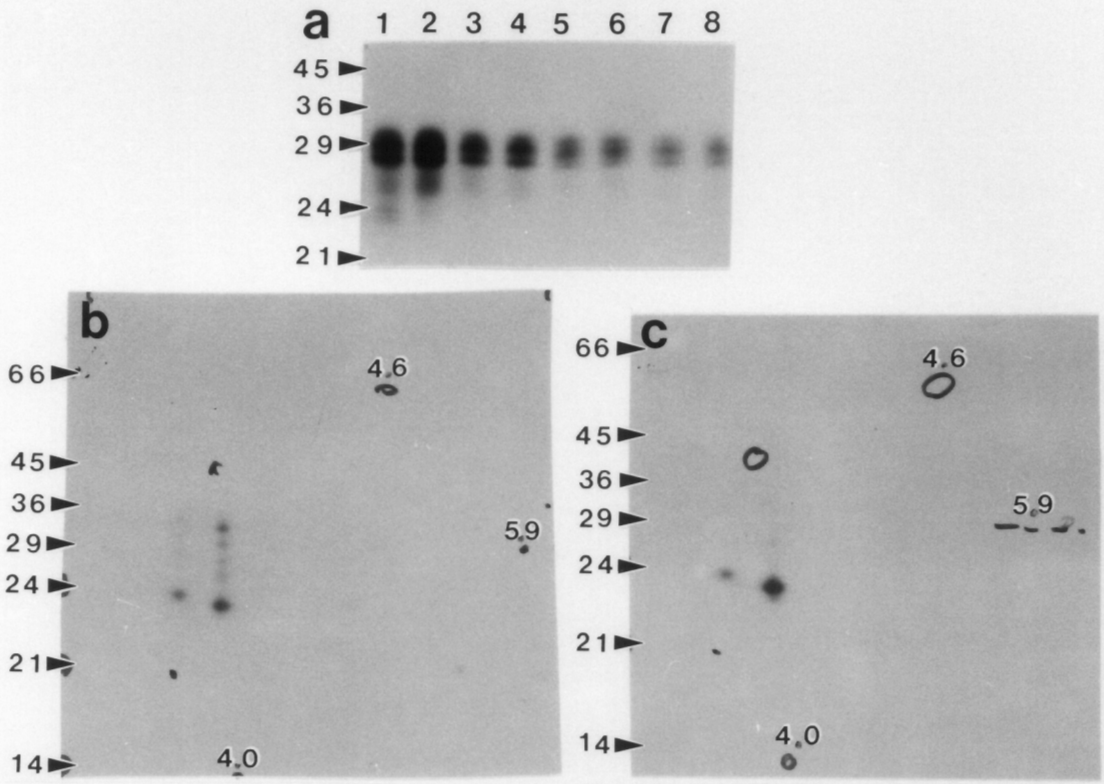

Figure 3.8 Neuraminidase Treatment of Immunoprecipitated Cathepsin L

THP1 cells ($2x10^6$) were incubated 3 h with Fmoc-(^{125}I)Tyr-Ala-CHN_2 following 0, 24, 48, or 72 h PMA treatment. Cells were washed and cathepsin L was immunoprecipitated as described above. To the final cathepsin L pellet was added 20 μL 50 mM sodium acetate buffer, pH 5.5, 5 mM $CaCl_2$, 2 μL 50 μM E-64, and 5 μL neuraminidase (50 mUnits) and the sample incubated overnight at room temperature on a rotary mixer. As above, a control sample for each PMA time-treatment was prepared along side without added neuraminidase (increased sodium acetate buffer amount by 20 μL). a.)1-Dimensional analysis of samples: lane 1: 72 h PMA, no neuraminidase treatment; lane 2: 72 h PMA, with neuraminidase treatment; lane 3: 48 h PMA, no neuraminidase treatment; lane 4: 48 h PMA, with neuraminidase treatment; lane 5: 24 h PMA, no neuraminidase treatment; lane 6: 24 h PMA, with neuraminidase treatment; lane 7: 0 h PMA, no neuraminidase treatment; lane 8: 0 h PMA, with neuraminidase treatment. b.) 2-Dimensional analysis of 72 h PMA treated THP1 cathepsin L, no neuraminidase treatment; c.) 2-Dimensional analysis of 72 h PMA treated THP1 cathepsin L, with neuraminidase treatment.

may be present in the glycosidase preparation that has converted the higher molecular weight forms to the lower. The different isoforms of cathepsin L are not due to sialic acid residues present on the oligosaccharide chains.

3.5.4 PNGase F

THP1 cells ($2x10^6$) were incubated 3 h with Fmoc-(^{125}I)Tyr-Ala-CHN_2 following 72 h PMA treatment. Cells were washed and cathepsin L was immunoprecipitated as described above. IEF sample buffer (10 μL), gel buffer B (10 μL of a 1:4 dilution; Table 2.1), 50 μM E-64 (3 μL), and PNGase F (1 unit, 4 μL) were added to the final cathepsin L pellet. Controls without added PNGase F were also prepared. The samples were incubated overnight at room temperature on a rotary mixer and protein from 10^6 cells analyzed by IEF/SDS-PAGE. Figure 3.9 shows, again, no difference between PNGase-F treated cathepsin L and cathepsin L not treated with the glycosidase.

3.6 Discussion

Experiments described in this section have identified cathepsins B and S in U937 cells only after treatment with PMA, which causes the cells to differentiate to macrophage-like cells. THP1 cells express cathepsins B, L, and S both before and after treatment with PMA, with increased synthesis

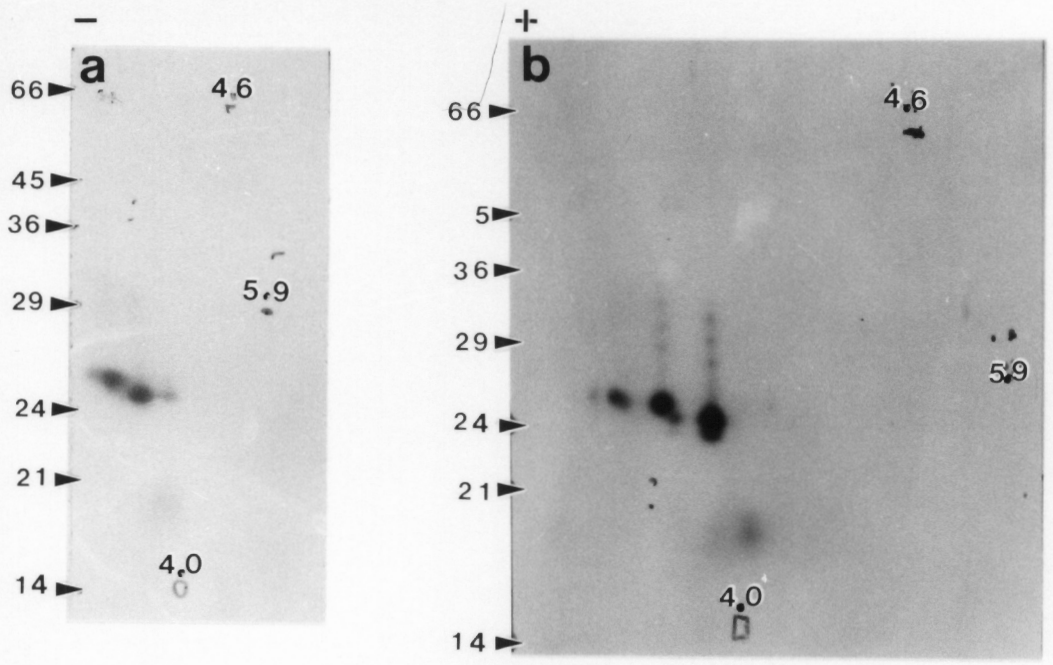

Figure 3.9 PNGase F Treatment of Immunoprecipitated Cathepsin L

THP1 cells ($2x10^6$) were incubated 3 h with Fmoc-(^{125}I)Tyr-Ala-CHN_2 following 72 h PMA treatment. Cells were washed and cathepsin L was immunoprecipitated as described above. To the final cathepsin L pellet was added 10 μL IEF sample buffer, 10 μL 1:4 gel buffer B (Table 2.1), 3 μL 50 μM E-64, and 4 μL (1 unit) PNGase F. Controls without added PNGase F were also prepared. The samples were incubated overnight at room temperature on a rotary mixer and protein from 10^6 cells analyzed by IEF/SDS-PAGE. a.) no PNGase F treatment. b.) with PNGase F treatment.

of all three enzymes after differentiation. The presence of two and three labeled proteins in the anti-cathepsin S immunoprecipitation experiments is seen in both cell lines before (THP1) and after (THP1 and U937) differentiation. The 26 kDa form corresponds to the reported molecular weight for bovine spleen cathepsin S (Xin et al. 1992). However, Shi et al. (1992) report a single-chain 28 kDa form from cathepsin S cDNA derived from human alveolar macrophages and expressed in COS cells. The 35 kDa form may correspond to a partially active pro-form that is able to bind the inhibitor. The 28 kDa form may represent a single chain form of the enzyme and the 26 kDa form a two-chain form. A more detailed discussion appears in Section 5.1. Metabolic labeling studies will help determine whether these proteins are biosynthetic forms of cathepsin S.

When analyzed by 2-dimensional electrophoresis (IEF/SDS-PAGE), cathepsin L shows at least 4 forms of low pI (near 3), with additional forms producing a laddering effect between 33 kDa (single chain form) and 23 kDa (heavy chain of the two chain form). The differences in the forms were hypothesized to be the result of differently glycosylated proteins. The low pI was also hypothesized to be the result of negatively charged carbohydrate units present on the oligosaccharide chain, such as mannose 6-phosphate or sialic acid. Treatment of immunoprecipitated cathepsin L from THP1 cells with

endoglycosidase H, neuraminidase, or PNGase F had no effect on the pI forms present. The same pattern is seen both in glycosidase-treated samples and in untreated samples. Thus, the carbohydrate chains or their constituent sugars are not responsible for the different isoforms of cathepsin L seen following 2-dimensional electrophoresis. Other modifications must be responsible, including perhaps sulfation, phosphorylation, and myristolyation. Cathepsin L is not glycosylated, as treatment with PNGase F did not affect the mobility of cathepsin L analyzed by SDS-PAGE.

CHAPTER 4 SYNTHESIS OF BSA-TYR-ALA-CHN_2 CONJUGATES

4.1 Introduction

As described in Section 1.4.4, active forms of the cysteine proteinases cathepsins B, L, and S and their biosynthetic forms can be distinguished from each other by the use of active-site directed, irreversible peptide inhibitors such as Fmoc-Tyr-Ala-CHN_2. Normally able to permeate cellular membranes, these compounds must be modified, so that they are internalized by endocytosis if they are to be useful for the study of the delivery of lysosomal proteinases to vesicles containing recently endocytosed proteins. To achieve this goal, the peptide inhibitor Fmoc-Tyr-Ala-CHN_2 was covalently attached to BSA via photoactivatable chemical cross-linking agents. This chapter details the synthesis and characterization of such complexes.

4.2 FMOC-TYR-ALA-CHN_2 Synthesis

Fmoc-Tyr-Ala-CHN_2 was made from Fmoc-Tyr-Ala-OH and diazomethane as described in Sections 2.4.1 to 2.4.3, with a yield of 3.5 %, based on the amount of Fmoc-Tyr-Ala-OH used. Yield was low due to loss of product in the organic extraction; improvements in yield can be achieved by omitting the extraction steps and proceeding directly to HPLC purification procedures.

4.2.1 Preparative HPLC Purification of Fmoc-Tyr-Ala-CHN_2

As described in Section 2.4.4, Fmoc-Tyr-Ala-CHN_2 was purified on a Waters RCM 25 X 100 Bondapak C-18 "Prep" column using a 20-100% acetonitrile gradient in 50 mM ammmonium acetate, pH 6.8. Ammonium acetate was used as the buffering system as 1) low pH buffers commonly used in HPLC, such as TFA, will destroy the diazomethyl derivative on the peptide, and 2) the components are easily removed and, thus, will not corrode the HPLC tubing. Fractions (5 mL) were collected from 35 to 75 minutes into the gradient (Figure 4.1).

4.2.2 Determination of Inhibitor in HPLC Fractions

Each fraction was assessed for inhibition of papain by incubating 25 μL of 0.025 mg/mL papain (approximately 0.6 μM in the incubation solution) in 50 μL 400 mM sodium acetate, pH 5.5, 4 mM DTT (see Table 2.7) with 25 μL of each fraction for 30 minutes at 37°C with water or 10 μM E-64 as controls. Samples were diluted to 5 mL with 0.01% Brij and 50 μL of each assayed as described in Section 2.2.6. Fluorescence was plotted against fraction number (Figure 4.2); fractions in which fluorescence was very low (i.e., papain was inhibited and the concentration of inhibitor was $\geq$ 0.6 μM) were lyophilized in 1.25 mL aliquots. A tube of each fraction was resuspended in 1.25 mL 85 % acetonitrile / 15% methanol for further analyses.

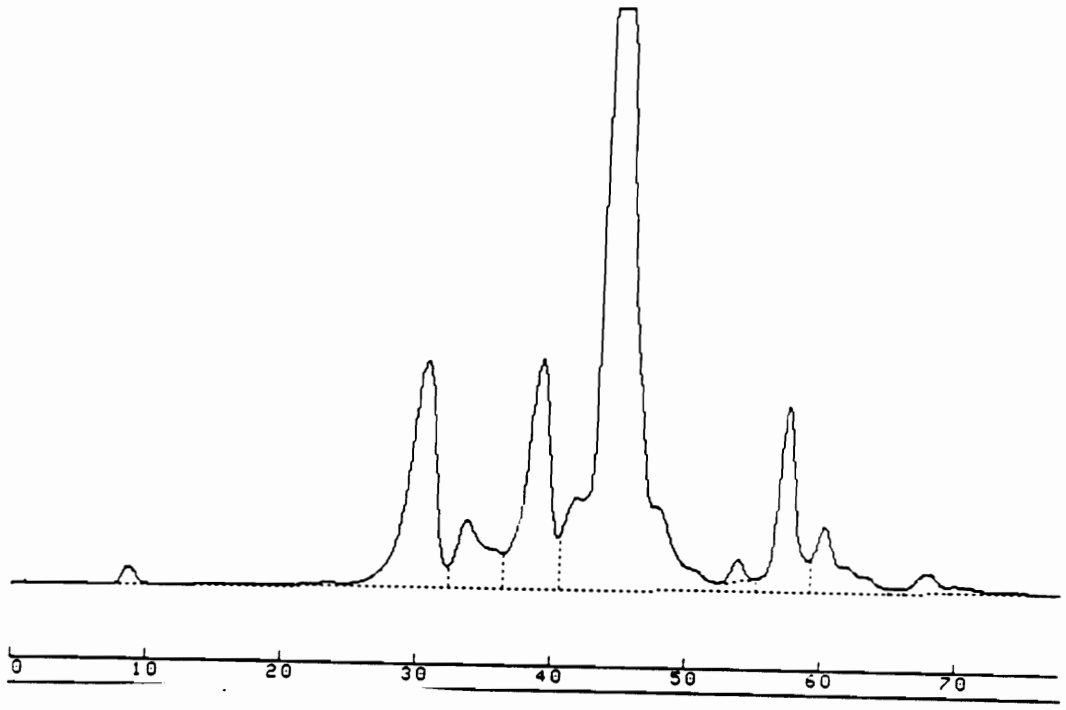

Figure 4.1 Chromatogram of Fmoc-Tyr-Ala-CHN_2 from Prep Column

Fmoc-Tyr-Ala-CHN_2 synthesis solution (1 mL) was injected onto a Waters RCM 25 x 100 Bondapak C-18 column and eluted at 5 mL/min with a 20-100% gradient of acetonitrile in 50 mM ammonium acetate, pH 6.8 (see Figure 2.6). Fractions (5 mL) were collected from 35-75 minutes. Absorbance at 260 nm was monitored. The chromatogram shown was produced with the attenuation set at 10 (2.56 absorbance units full scale).

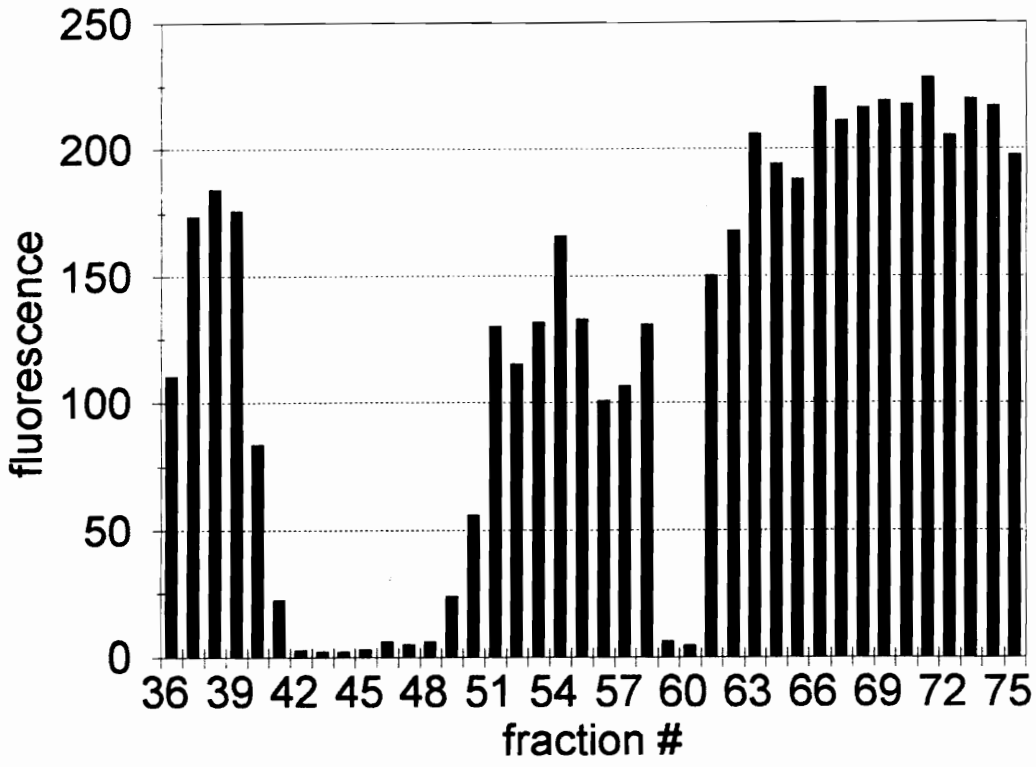

Figure 4.2 Inhibition of Papain by Prep HPLC Fractions

Fractions 36-75 were assessed for inhibition of papain as described in Section 4.2.2. An aliquot of each fraction (25 μL) was incubated with 25 μL of 25 μg/mL papain in 50 μL 400 mM sodium acetate, pH 5.5, 4 mM DTT, for 30 min at 37°C. Each sample was diluted to 5 mL with 0.01% Brij and then 50 μL assayed as described in Section 2.2.6. Fluorescence units were plotted against fraction number. Fractions 41-49 and 59-60 inhibited papain. Fractions 41-49 correspond to the major peak in the chromatogram in Figure 4.1; fractions 59-60 correspond to a small peak. Fractions 41-49 were retained for further analyses.

4.2.3 Analytical HPLC Analyses of Inhibitory Fractions

A portion of each fraction which inhibited papain (10 μL) was further analyzed on a 20 cm C-18 HPLC column, as described in Section 2.4.4. Preparative HPLC column fractions gave multiple peaks when assessed for purity (Figure 4.3). The area under each peak was recorded, as was the elution time for each peak (Table 4.1).

4.2.4 Determination of Inhibitor Concentration in Each Prep Column Fraction

Prep column fractions were diluted 1:5, 1:10, 1:100, 1:500, and 1:1000 in 85% acetonitrile / 15% methanol and the concentration of inhibitor in each determined as described in Section 2.2.9 (Table 4.1).

4.2.5 Determination of Purest Prep Column Peaks

Figure 4.4 was derived from the data listed in Table 4.1, in which the area of each peak present and the concentration of inhibitor was plotted for each peak in each prep column fraction. As seen for fractions 43 and 44, the peak at 19.5 min corresponds strongly with the amount of inhibitor present. Based on this, the 19.5 min peak was taken to correspond to Fmoc-Tyr-Ala-CHN_2. All tubes of fractions 43 and 44 were resuspended and pooled in 85 % acetonitrile / 15% methanol and the concentration of the pool determined to be 194 μM (6.0

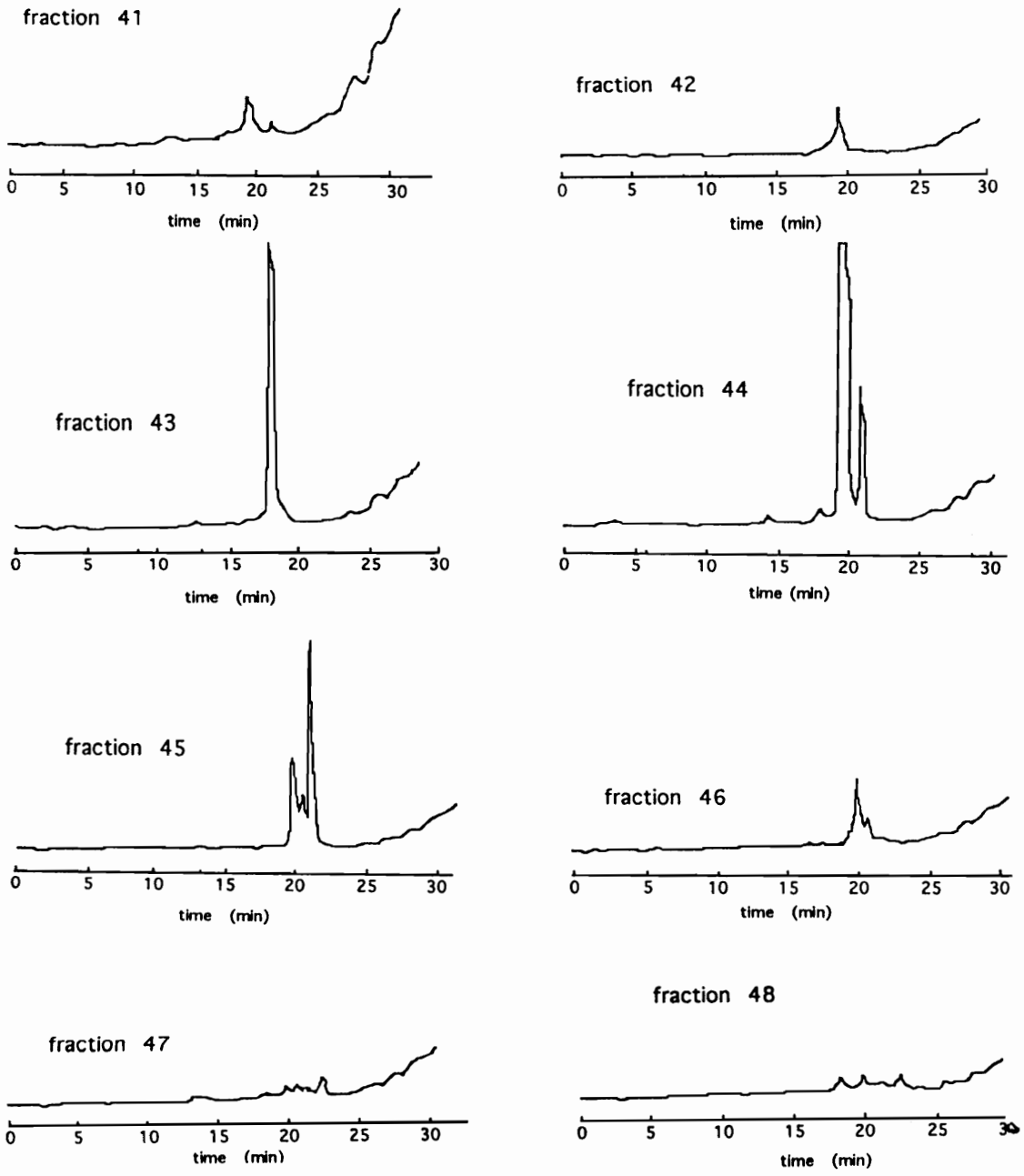

Figure 4.3 Analytical HPLC Chromatograms of Prep Column Fractions

A portion of fractions 41-48 (10 μL) were injected onto an analytical HPLC column (waters μBondapak C-18 column; see Section 2.4.4). Each chromatogram is shown at attenuation of 5. The peak at 19.5 min increased from fractions 41-44; in fraction 44, a neighboring peak appears (20.8 min), which later becomes the major peak in fractions 45-46. Fractions 47 and 48 contain very little of either peak.

Table 4.1 Analytical HPLC Analysis of Prep HPLC Fractions

fract.#	[I], μM	19.0 min	19.5 min	20.2 min	20.8min
41	1.03	257000	0	0	40000
42	5.7	0	240000	0	0
43	258	0	1360000	0	0
44	574	0	2820000	0	408000
45	54	0	293000	18400	574000
46	1.38	0	47800	236000	96800
47	0.89	0	53700	57500	53000
48	0.95	0	79700	0	63700

Each Prep HPLC fraction (10 μL) was analyzed on analytical HPLC, the area under each peak recorded, and the concentration of inhibitor assessed by papain titration (Section 2.2.9). As seen, the Prep fractions were not pure. Fractions 43 and 44 were pooled for further studies, as these two had the greatest correlation between peak area (peak at 19.5 min) and concentration of inhibitor.

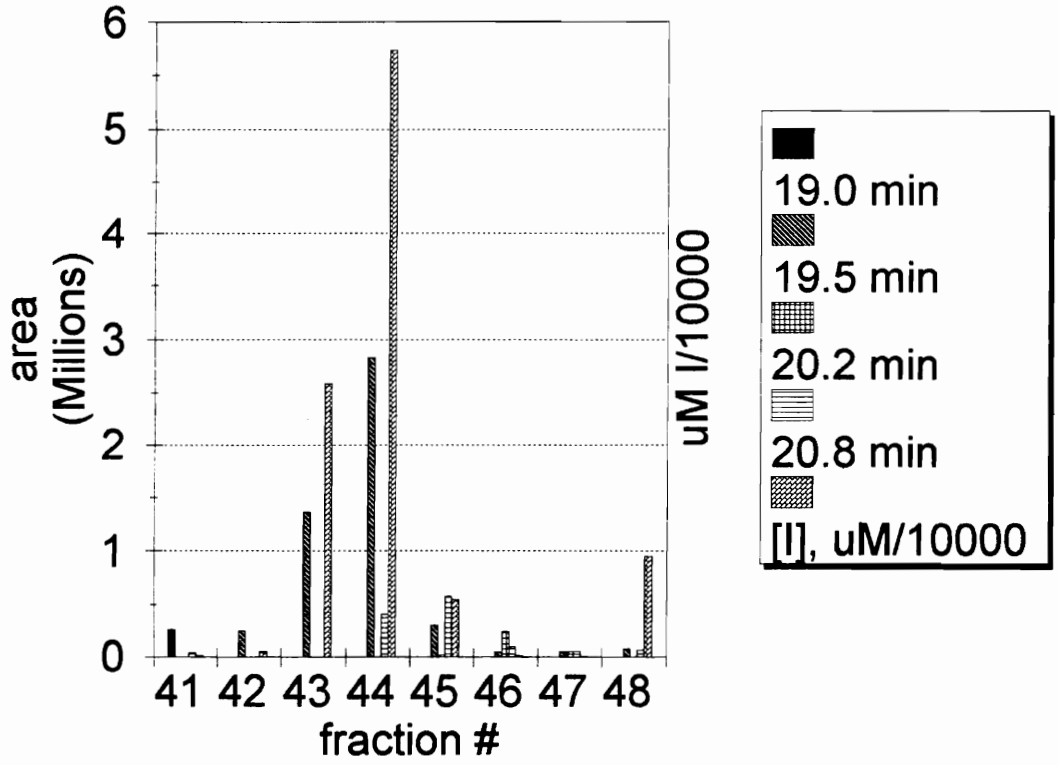

Figure 4.4 Analytical HPLC Analysis of Prep Column Fractions

Data from Table 4.11 was combined graphically. The concentration of inhibitor is greatest in fraction 44, as is the area under the 19.5 min peak. Fraction 43 and 44 were pooled and analyzed further.

μmoles).

4.3 Characterization of Fmoc-Tyr-Ala-CHN_2

4.3.1 Mass Spectrometric Analysis of Fmoc-Tyr-Ala-CHN_2

Mass spectrometric (MS) analysis was performed by Dr. Jeff Shabanowitz, Department of Chemistry, Biological Mass Spectrometry Lab, University of Virginia. The freeze-dried peptide was directly injected into the instrument and subjected to MS analysis utilizing electrospray ionization. Figure 4.5 shows the spectrograph generated, with the peak M+1 = 499.4 corresponding to Fmoc-Tyr-Ala-CHN_2. The M+1= 471.4 is the peptide having lost N_2. Peaks M+1 = 515.7 and 585.8 are contaminants in the preparation. Each peak was subjected to electrospray ionization and MS analysis (MS/MS) to generate fragments to help determine each peak's identity; major ions were individually selected for a second MS analysis. The secondary MS analysis of M= 499.4 peak (Figure 4.6) generated peaks of M = 179, 250, 294, and 472. These peaks correspond to the peptide fragments (A) Fmoc ($-CO_2$), (B) NH_2-Tyr-Ala-CO-CH_3, (C)OCO-NH-Tyr-Ala-CH_2, and (D) Fmoc-YA-CH^{-1}, respectively (Figure 4.7). Fragmentation of the M = 472 peak generated a similar pattern (Figure 4.8), with peaks A, B, C, and D, as above. Secondary MS analysis of M = 585.8 and 515.7 generated fragments of M = 145, 330, and 515 (Figure 4.9).

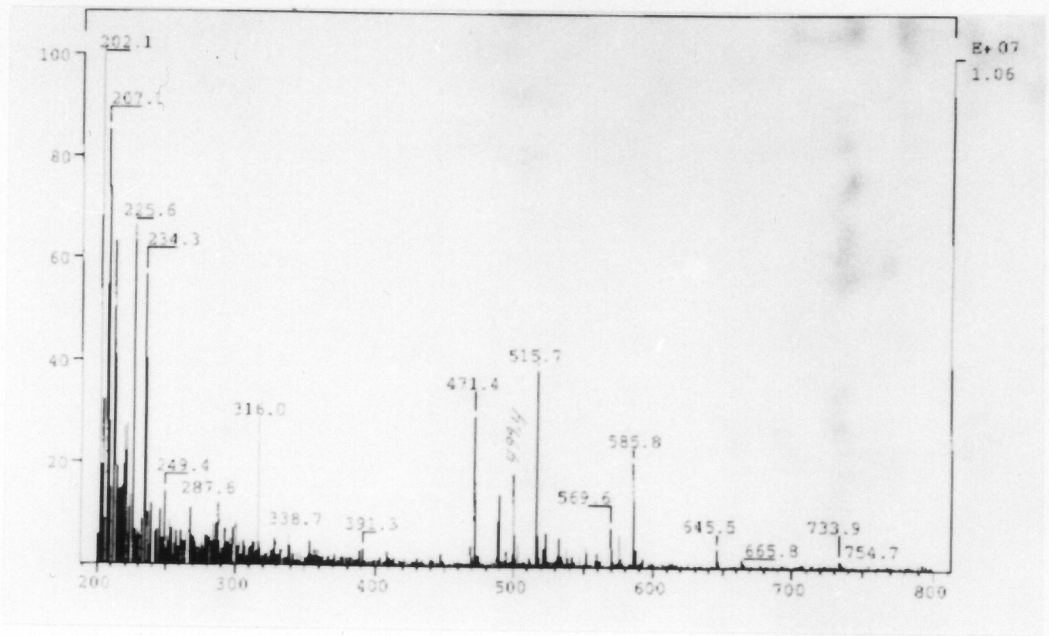

Figure 4.5 MS of Fmoc-Tyr-Ala-CHN_2

Freeze-dried inhibitor was analyzed by MS utilizing electrospray ionization. Calculated mass of the inhibitor is 498; a peak is present at M+1 = 499. Each major peak (M+1 = 585, 515, 499, and 472) was analyzed by an additional round of MS (MS-MS) to help further identify the molecules by their fractionation patterns.

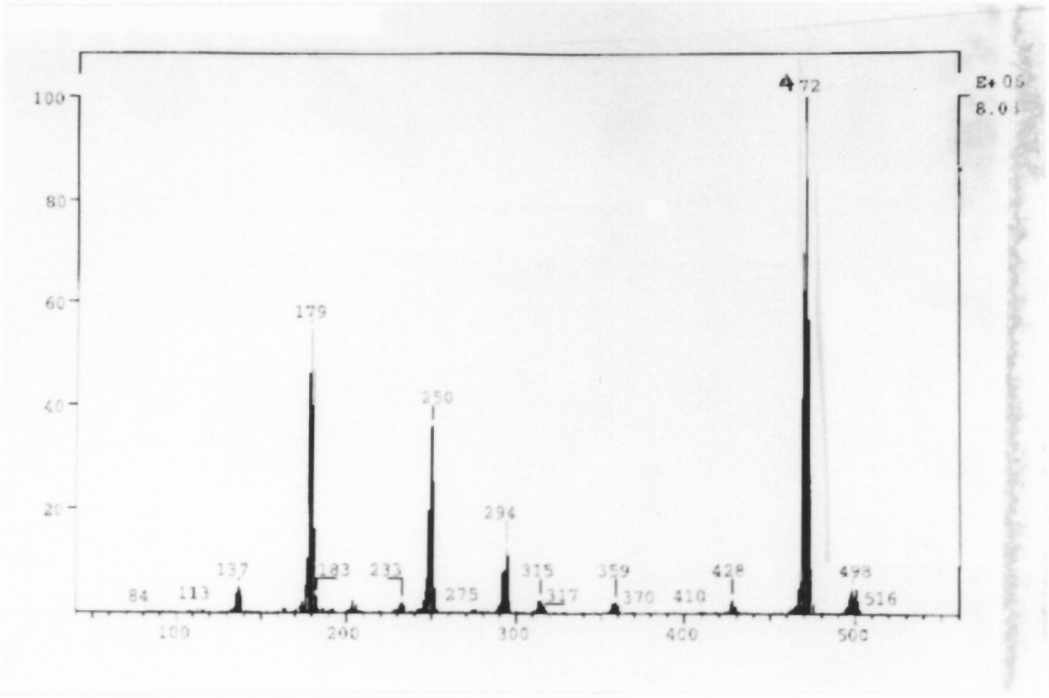

Figure 4.6 MS-MS of Peak M = 499.4

Peak M = 499.4 was subjected to additional MS analysis, resulting in fragments M = 472, 294, 250, and 179. Figure 4.7 shows that this pattern corresponds to masses of fragments of Fmoc-Tyr-Ala-CHN_2.

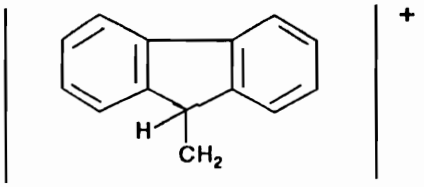

M = 179

$C_{14}H_{11}$

a. peak M = 179

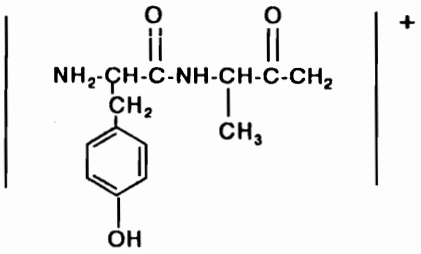

M = 249

$C_{13}H_{17}N_2O_3$

b. peak M = 249

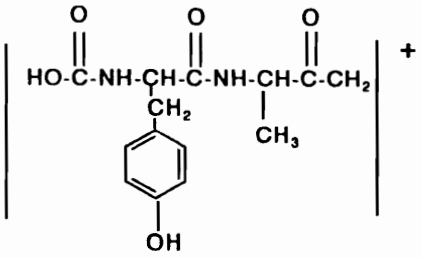

M = 294

$C_{14}H_{17}N_2O_5$

c. peak M = 294

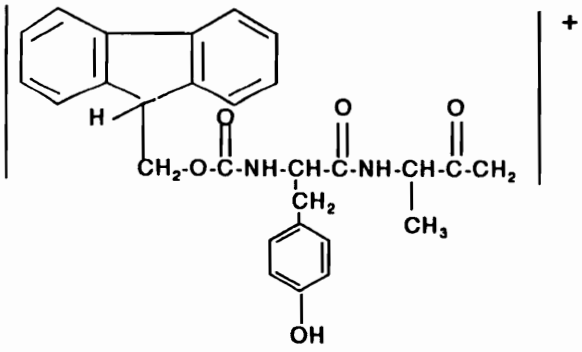

M = 472

$C_{28}H_{27}N_2O_5$

d. peak M = 472

Figure 4.7 Structures of Fmoc-Tyr-Ala-CHN_2 Fragments

Shown are possible fragments of Fmoc-Tyr-Ala-CHN_2 and their masses. Each of these mass peaks are seen in the MS-MS analysis of the M+1 = 499.4 peak.

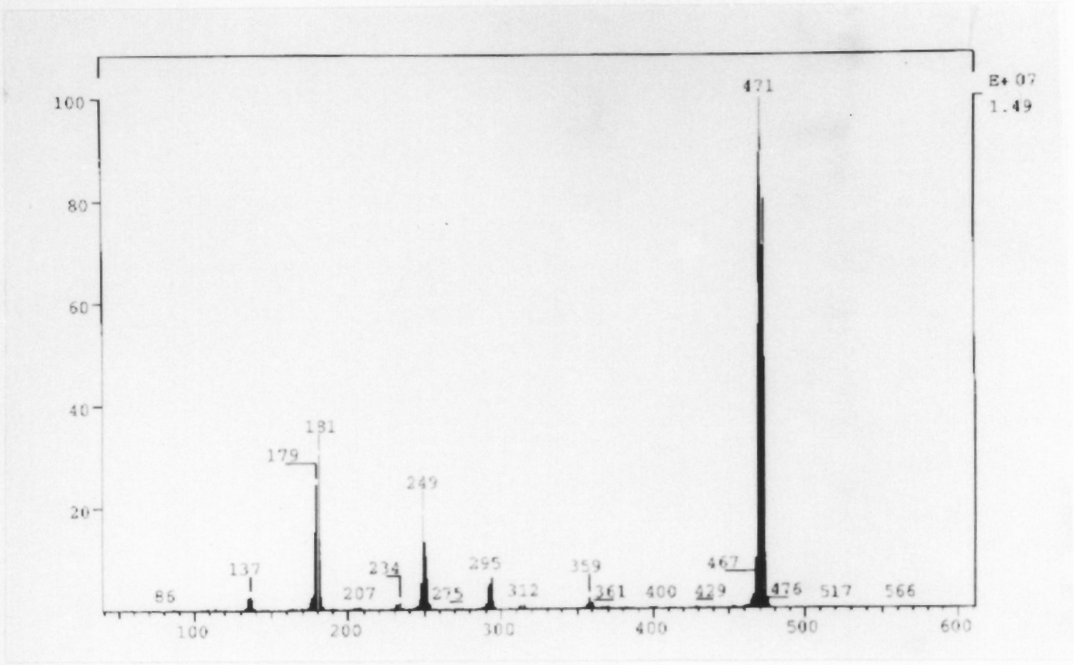

Figure 4.8 MS-MS analysis of Peak M = 471

The M = 471 molecule was subjected to additional MS analysis. This molecule fragments to give molecules of M = 295, 250, and 179. This is in agreement with the assignment of structures with peaks in Figure 4.7.

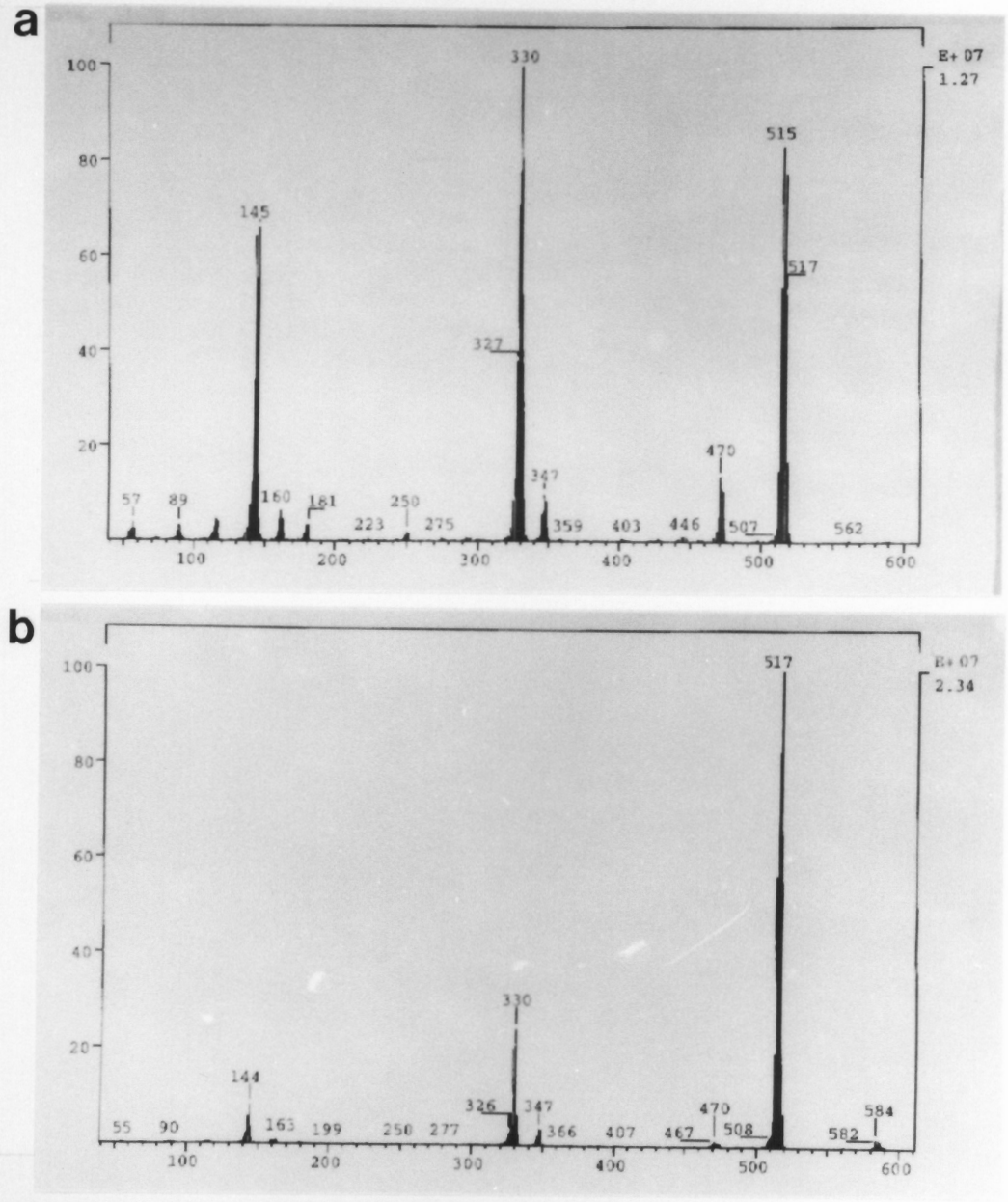

Figure 4.9 MS-MS of Peaks M = 585 and 515

MS-MS analysis of peaks M= a.)585 and b.) 515 results in fragments of M = 515, 330, and 145. Each peak differed by a constant mass: 185. This fragmentation pattern does not resemble that of Fmoc-Tyr-Ala-CHN_2 or any of its fragments. The M = 585 peak was probably due to a contaminant present from Preparative-HPLC fraction 44 (see Figures 4.3 and 4.4, fraction 44).

This fragmentation pattern does not resemble that predicted for Fmoc-Tyr-Ala-CHN_2 or a related compound. Thus, it was concluded that the molecule of M = 585 was unrelated to Fmoc-Tyr-Ala-CHN_2 and is probably derived from contaminants in the HPLC fractions (see Section 4.2.3), solvents used in the peptide synthesis, or from chemicals leached from the polypropylene tubes in which the Fmoc-Tyr-Ala-CHN_2 was stored.

4.3.2 Labeling of Cellular Cathepsins B, L, and S with Fmoc-(^{125}I)Tyr-Ala-CHN_2

Fmoc-Tyr-Ala-CHN_2 was radiolabeled as described in Section 2.2.16. Inhibitor (10 μM) was incubated with 10^7 KNIH 3T3 cells for 3 hours. The cells were harvested, washed, solubilized, and analyzed by SDS-PAGE as described in Sections 2.3.7 and 2.2.3.1. Cell pellets were dissolved in 100 μL sample buffer E and 10 μL loaded per well (10^6 cells per well). In parallel, Z-(^{125}I)Tyr-Ala-CHN_2 (4 μM) was also incubated with 10^7 cells. Fmoc-(^{125}I)Tyr-Ala-CHN_2 enters cells and reacts with cellular forms of cathepsins B, L, and S, just as the Z-inhibitor does, with the exception of the loss of the 16 kDa band seen in cells incubated with the Z-inhibitor (Figure 4.10).

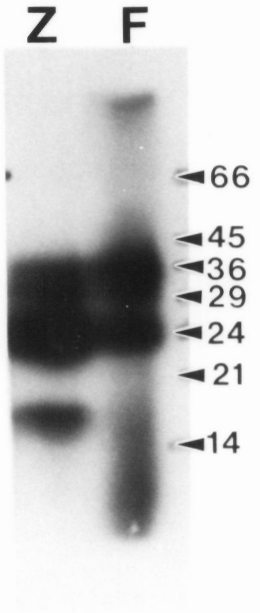

Figure 4.10 Labeling of KNIH 3T3 Cells with Z-(^{125}I)Tyr-Ala-CHN_2 and Fmoc-(^{125}I)Tyr-Ala-CHN_2

Cells (10^7, KNIH 3T3) were incubated with 4 μM Z-(^{125}I)Tyr-Ala-CHN_2 and Fmoc-(^{125}I)Tyr-Ala-CHN_2 and analyzed by SDS-PAGE (Bury system) as described in Sections 2.3.7 and 2.2.3.1. Autoradiography shows three main bands for cells treated with the Z-inhibitor (lane 1: 35 kDa - cathepsin B single chain, 24 kDa - cathepsin L heavy chain of two-chain form , 16 kDa - unknown). The Fmoc-inhibitor treated cells show two main bands after autoradiography (lane 2: 36 kDa - cathepsin B single chain, 24 kDa - cathepsin L heavy chain of two chain form). Some labeling is seen near the bottom of the autoradiograph, most likely corresponding to unbound inhibitor.

4.4 Synthesis and Characterization of BSA-sulfo-SANPAH-Tyr-Ala-CHN_2

4.4.1 Crosslinking Fmoc-Tyr-Ala-CHN_2 to BSA using Sulfo-SANPAH

NH_2-Tyr-Ala-CHN_2 was crosslinked to BSA using the photoactivatable reagent sulfo-SANPAH [sulfosuccinimidyl 6-(4'-azido-2'-nitrophenylamino) hexanoate]. The succinyl moiety in the reagent reacts with amide groups, while the photoactivatable phenyl azide rearranges and reacts nonspecifically with nucleophilic groups such as amino groups in proteins. As described in Section 2.4, the protein-inhibitor complex was synthesized by first removing the Fmoc-group from 4 μmoles of the peptide inhibitor (see Figure 4.11), followed by reaction of the deblocked peptide with 12 μmole sulfo-SANPAH in the dark, and then reaction of the crosslinker-inhibitor complex with BSA (0.4 μmoles) upon exposure to bright light. The reaction product from the first step in cross-linking procedure, the inhibitor bound to the cross-linking agent, was not characterized as the photo-activatable group on the cross-linking reagent would react quickly and non-specifically with other inhibitor molecules in the solution before any analyses could be performed. The complex was purified as previously described (Section 2.4.8). Table 4.2 compares the amount of inhibitor present as

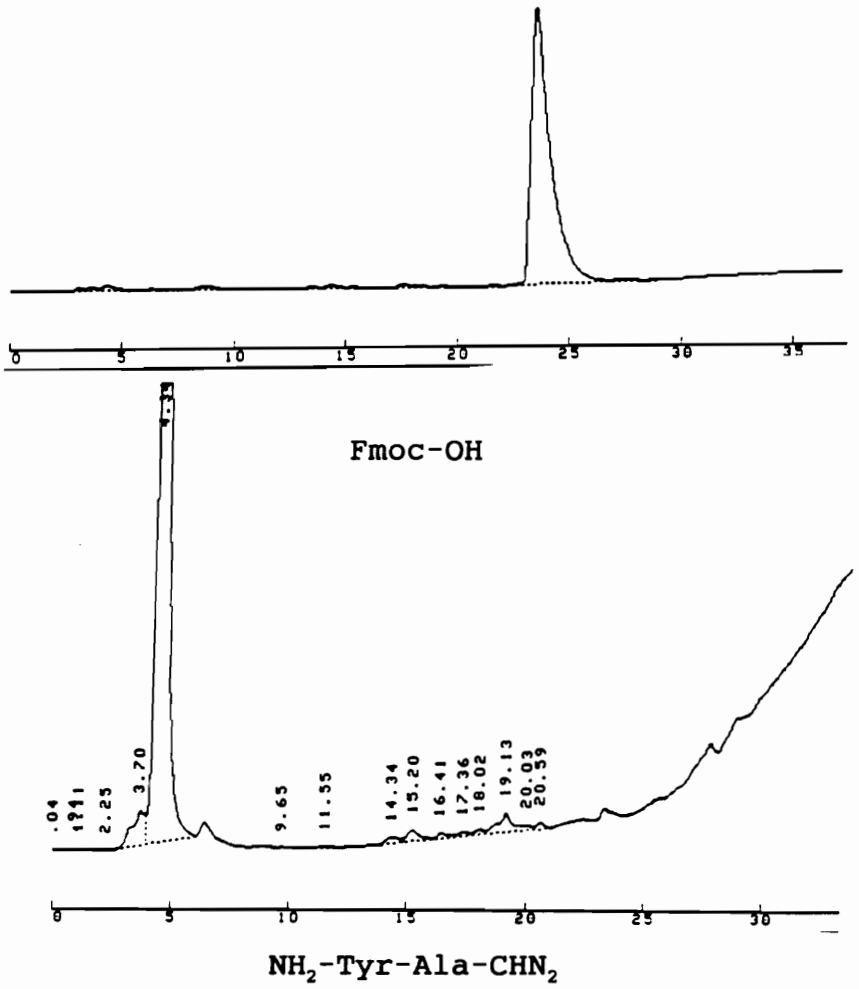

Figure 4.11 HPLC Chromatograph of NH_2-Tyr-Ala-CHN_2 and Fmoc-OH

Fmoc-Tyr-Ala-CHN_2 (4 μmoles in 1 mL DMF) was treated with 32 μL piperidine (8 mL/mmole peptide) for 1 hour at room temperature. The solution was diluted with 2 mL ethyl acetate and poured over silica gel in ethyl acetate. The gel was washed with 50 mL ethyl acetate, eluting free Fmoc-OH, and then 50 mL 70% chloroform / 30% methanol to elute the deblocked peptide. Chromatograph A shows the analytical HPLC chromatograph of the ethyl acetate wash (free Fmoc-OH; see Section 2.4.4 for HPLC methods); chromatograph B shows the analysis of the chloroform / methanol wash (NH_2-Tyr-Ala-CHN_2). Note that the Fmoc-peptide (peak 19.5 minutes, see Figure 4.3) was no longer present, indicating complete removal of the Fmoc- group.

Table 4.2 Ratio of BSA to Inhibitor after Cross-linking with Sulfo-SANPAH

	μmoles BSA	μmoles I	ratio BSA:I
pre-wash	0.090	0.060	1.5 : 1
wash 1	0.086	0.064	1.3 : 1
wash 2	0.086	0.067	1.3 : 1
wash 3 (final)	0.074	0.059	1.3 : 1

BSA was cross-linked to NH_2-Tyr-Ala-CHN_2 and purified as described in Sections 2.4.7 and 2.4.8. The sample was washed 3 times in a Centri-prep 10 spin cartridge to remove any non-specifically bound inhibitor from the protein. After each wash, the concentrate was assessed for protein and inhibitor content. The ratio of each was compared after each wash as shown. No further washes were performed, as the ratio of protein to inhibitor did not change, while some product was being lost.

determined by papain titration (Section 2.2.9) with the amount of protein during and after purification. The ratio of inhibitor to protein in the final product is 1.3:1; ideally the complex would have a ratio of 10:1 (inhibitor : protein; yield = 13%). The final concentration of BSA-sulfo-SANPAH-Tyr-Ala-CHN_2 (based on inhibitory properties) is 30 μM.

4.4.2 Kinetic Characterization of Inhibition of Cathepsins B, L, S, and Papain by Fmoc-Tyr-Ala-CHN_2 and BSA-sulfo-SANPAH-Tyr-Ala-CHN_2

The kinetic parameters of the reaction of Z-Tyr-Ala-CHN_2 with cathepsin L was determined previously (Crawford et al. 1988). Similar kinetic studies were performed on Z-Tyr-Ala-CHN_2, Fmoc-Tyr-Ala-CHN_2, and BSA-sulfo-SANPAH-Tyr-Ala-CHN_2, as described in Section 2.2.11. Table 4.3 lists the results. For BSA-sulfo-SANPAH-Tyr-Ala-CHN_2, the amount of inhibitor present, not the amount of protein, was used for calculations. BSA-sulfo-SANPAH-Tyr-Ala-CHN_2 is slightly more inhibitory than Fmoc-Tyr-Ala-CHN_2 to cathepsin B, and 8 times more inhibitory than Z-Tyr-Ala-CHN_2. With Cathepsin L, BSA-sulfo-SANPAH-Tyr-Ala-CHN_2 is as inhibitory as Fmoc-Tyr-Ala-CHN_2 and Z-Tyr-Ala-CHN_2, given the variation in the Fmoc-Tyr-Ala-CHN_2 data. With cathepsin S, BSA-sulfo-SANPAH-Tyr-Ala-CHN_2 is equally inhibitory as Fmoc-Tyr-Ala-CHN_2; both are 2 to 4 times more inhibitory than Z-Tyr-Ala-CHN_2. Versus papain, Fmoc-Tyr-

Table 4.3 Inhibition of Cysteine Proteinases with Z-Tyr-Ala-CHN_2, Fmoc-Tyr-Ala-CHN_2, and BSA-sulfo-SANPAH-Tyr-Ala-CHN_2

Z = Z-Tyr-Ala-CHN_2
F = Fmoc-Tyr-Ala-CHN_2
C = BSA-sulfo-SANPAH-Tyr-Ala-CHN_2
n = number of determinations

enzyme	[I]	n	k_{obs} (sec^{-1})	k_{2app} ($M^{-1}sec^{-1}$)
cathepsin B	Z (1 μM)	1	0.00116	1160
	F (100 nM)	3	0.00062 ± 0.00022	4600 ±2100
	(500 nM)	3	0.00177 ± 0.00078	
	C (500 nM)	2	0.00400 ±0.00010	8000 ± 200
cathepsin L	Z (100 nM)	1	0.00220	22000
	F (100 nM)	3	0.00268 ± 0.00072	39000
	F (50 nM)	3	0.00231 ± 0.00104	± 20000
	C (100 nM)	2	0.00208 ± 0.00001	21000 ± 900
cathepsin S	Z (1 μM)	1	0.00166	1600
	F (100 nM)	1	0.00057	4600 ± 1100
	F (500 nM)	1	0.00179	
	C (100 nM)	1	0.00526	
	C (500 nM)	1	0.00223	4800 ± 400
papain	F (50 nM)	2	0.00158 ± 0.00001	32000 ±1700
	C (5 nM)	2	0.00236 ± 0.00026	615000
	C (2.5 nM)	2	0.00184 ± 0.00016	± 136000

Ala-CHN_2 acts as it does against cathepsin L; however, BSA-sulfo-SANPAH-Tyr-Ala-CHN_2 is 20 times more effective than Fmoc-Tyr-Ala-CHN_2. This is probably because the Fmoc- group is not able to fit well into the S_3 site of papain, while the cross-linker spacer between the BSA and Tyr-Ala-CHN_2 lies across the S_3 site.

4.4.3 Radiolabeling the BSA-sulfo-SANPAH-Tyr-Ala-CHN_2 Complex

The protein-inhibitor complex was iodinated as described in Section 2.2.16. Briefly, 10 nmoles complex (335 μL of 30 μM) was iodinated with 1 mCi $Na^{125}I$ using Iodobeads. The solution was diluted to 500 μL with 50% Acetonitrile / 50% 50 mM sodium phosphate (pH 7.0) and aliquoted into tubes containing 32 μM protein (0.65 nmole protein) and 20 μM inhibitor (0.4 nmole).

4.4.4 Irreversible Labeling of Papain with ^{125}I-Labeled BSA-sulfo-SANPAH-Tyr-Ala-CHN_2

Papain (5 μM or 0.5 μM) was incubated with 0.4 μM ^{125}I-labeled BSA-sulfo-SANPAH-Tyr-Ala-CHN_2 and the complex analyzed by SDS-PAGE (Section 2.2.3.2) to determine whether the cross-linking of the inhibitor to BSA was successful. Papain (25 μL of 0.25 mg/mL or 0.025 mg/mL) was incubated 30 min in 50 μL 400 mM sodium phosphate, pH 5.5, 4 mM DTT and 25 μL ^{125}I-labeled BSA-sulfo-SANPAH-Tyr-Ala-CHN_2 (0.4 μM). The solution

was then diluted to 0.5 mL with 10 mM Tris-HCl, pH 7.5, 1 mM EDTA. Papain was immunoprecipitated as described in Section 2.2.13. The final pellet was suspended in 100 μL SDS-PAGE sample buffer (with 2-mercaptoethanol), while the final supernatant was acid precipitated (Section 2.2.15). Each sample (10 μL) was loaded and run on a 7.5 % acrylamide gel with a 3.5% acrylamide stacking gel (Laemmli system), and then autoradiography was performed (Figure 4.12). As seen in lanes 2 and 4, a laddering effect was produced, representing the interaction of the ^{125}I-labeled BSA-sulfo-SANPAH-Tyr-Ala-CHN_2 with one (97 kDa), and two (116 kDa) molecules of papain. The crosslinking was successful as seen by the laddering effect present in lanes with papain, while no laddering is seen in the lane (lane 5) with no papain added.

4.4.5 Incubation of ^{125}I-Labeled BSA-sulfo-SANPAH-Tyr-Ala-CHN_2 with KNIH 3T3 Cells

The inhibitor complex was incubated with KNIH 3T3 cells to determine whether cellular forms of cathepsins B, L, and S react with the complex. As described in Section 2.3.7, cells were preincubated in serum-free medium for 1 h, followed by 3 h in serum free media containing 0.08 μM ^{125}I-labeled BSA-sulfo-SANPAH-Tyr-Ala-CHN_2. Cells were harvested, washed in PBS, and suspended in SDS-PAGE sample buffer and analysed by the Laemmli PAGE system (7.5% acrylamide separating gel, 3.5%

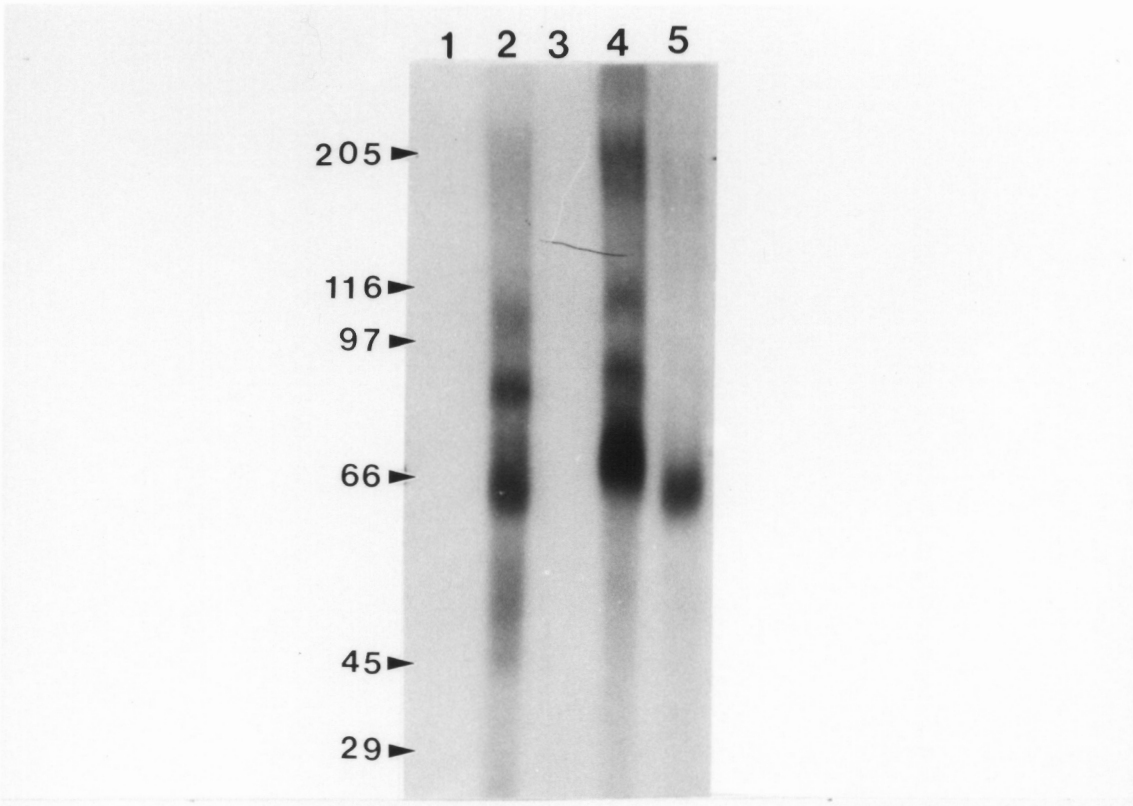

Figure 4.12 Covalent Interaction of Papain with ^{125}I-Labeled BSA-sulfo-SANPAH-Tyr-Ala-CHN_2

Papain (5.0 μM or 0.5 μM) was incubated with 0.4 μM ^{125}I-labeled BSA-sulfo-SANPAH-Tyr-Ala-CHN_2 for 30 minutes and the papain-inhibitor complex immunoprecipitated with rabbit anti papaya as described in Section 4.9. The samples were analyzed by SDS-PAGE (Laemmli system, 7.5 % acrylamide separating gel, 3.5% acrylamide stacking gel) and autoradiography.

Lane 1: 5 μM papain / 0 μM ^{125}I-labeled BSA-sulfo-SANPAH-Tyr-Ala-CHN_2; Lane 2: 5 μM papain /0.4 μM ^{125}I-labeled BSA-sulfo-SANPAH-Tyr-Ala-CHN_2; Lane 3: 0.5 μM papain / 0 μM ^{125}I-labeled BSA-sulfo-SANPAH-Tyr-Ala-CHN_2; Lane 4: 0.5 μM papain / 0.4 μM ^{125}I-labeled BSA-sulfo-SANPAH-Tyr-Ala-CHN_2; Lane 5: 0 μM papain / 0.4 μM ^{125}I-labeled BSA-sulfo-SANPAH-Tyr-Ala-CHN_2.

As seen in lanes 2 and 4, a ladder was present with bands at 66 kDa , 95 kDa, and 120 kDa, corresponding to ^{125}I-labeled BSA-sulfo-SANPAH-Tyr-Ala-CHN_2 with no papain bound, ^{125}I-labeled BSA-sulfo-SANPAH-Tyr-Ala-CHN_2 with 1 molecule papain, and ^{125}I-labeled BSA-sulfo-SANPAH-Tyr-Ala-CHN_2 with 2 molecules papain. Papain interacted covalently with the Tyr-Ala-CHN_2 tethered to BSA by sulfo-SANPAH. Thus, the crosslinking was successful.

acrylamide stacking gel). As Figure 4.13 shows, the laddering effect was not as apparent as in Figure 4.12; however, a band was seen at 120 kDa, corresponding to 2 molecules of enzyme bound to the protein-inhibitor complex. The strong band at 66 kDa was from the inhibitor complex itself. Thus, the inhibitor is able to enter cells and react irreversibly with cellular forms of lysosomal cysteine proteinases.

4.5 SYNTHESIS OF BSA-sulfo-SADP-Tyr-Ala-CHN_2

Different biosynthetic forms of cellular cathepsins B, L, and S can be distinguished by incubating cells with small membrane permeable inhibitors such as Fmoc-(^{125}I)Tyr-Ala-CHN_2 and Z-(^{125}I)Tyr-Ala-CHN_2 and analyzing the labeled proteins by SDS-PAGE and autoradiography. Radiolabeled protein bands of 25 kDa can be easily distinguished from 30 kDa and 35 kDa bands. However, when the inhibitors are cross-linked to BSA, the molecular weights of the enzyme-cross-linked inhibitor complex will rise to approximately 91 kDa, 96 kDa, and 101 kDa, that are not so easily differentiated. However, were the BSA removed via cleavage of the cross-linker, different enzyme forms could be distinguished. Thus, a reducible form of the BSA inhibitor complex was needed, such that once the enzyme interacts with the complex, the BSA can be removed by reducing agents. The crosslinking agent used for this purpose was sulfo-SADP [sulfosuccinimidyl(4-azidophenyldithio)

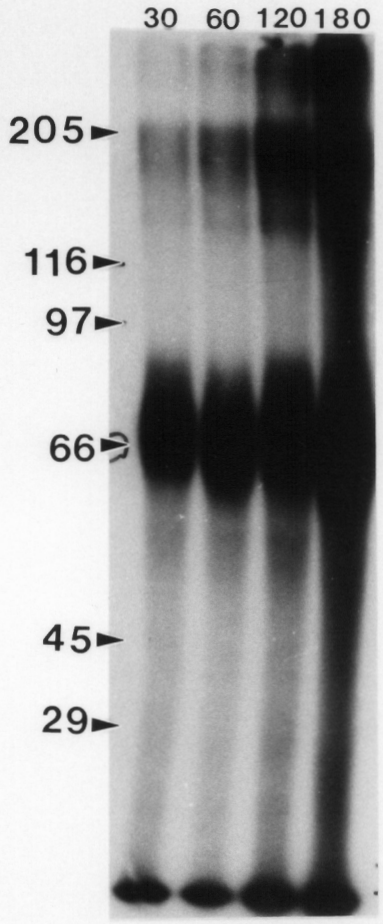

Figure 4.13 Incubation of KNIH 3T3 Cells with ^{125}-I-Labeled BSA-sulfo-SANPAH-Tyr-Ala-CHN_2

Radio-iodinated BSA-sulfo-SANPAH-Tyr-Ala-CHN_2 was incubated with $5X10^6$ KNIH 3T3 cells for 30 minutes, 1 hour, 2 hours, or 3 hours. The cells were washed and analyzed by SDS-PAGE (Laemmli system) as described in Section 4.10. A laddering effect was demonstrated with bands at 66 kDa (no cysteine proteinase bound), and 120 kDa (2 molecules cysteine proteinase bound). The inhibitor complex was internalized by cells and reacted with various numbers of cellular cysteine proteinases.

proprionate]. Figure 4.14 compares the structures of both cross-linking agents.

Kinetic studies were performed with the nonreducible SANPAH complex. Such studies are not possible with the reducible analog because the enzymes require DTT (or any reducing agent) to be present in the assay and incubation solutions. If the reducible analog were used, it could not be determined whether the enzymes had interacted with the inhibitors tethered to BSA.

4.5.1 Carboxymethylation of BSA

BSA contains 35 cysteine residues, 34 of which are involved in disulfide bonds. These sulfhydryl groups could reduce the cross-linking agent SADP. Thus, the cysteine sulfhydryls in BSA were carboxymethylated as described in Section 2.4.9.1. The presence of free R-SH was assessed as described in Section 2.4.9.2. There were no free R-SH present after the modification of BSA to carboxymethylcysteine BSA (CM-BSA) (Figure 4.15). All free R-SH added during the modification procedure were removed by dialysis. Native BSA and reduced BSA were also used as positive controls. BSA was reduced by incubation of 1.5 μmoles BSA and 0.8 mmoles 2-mercaptoethanol in 0.2 M Tris-HCl (pH8.3), 3 mM EDTA, and 6 M guanidine-HCl for 6 hours. The sample was dialyzed for 12 hours against the 2 changes of same buffer. An average of 7

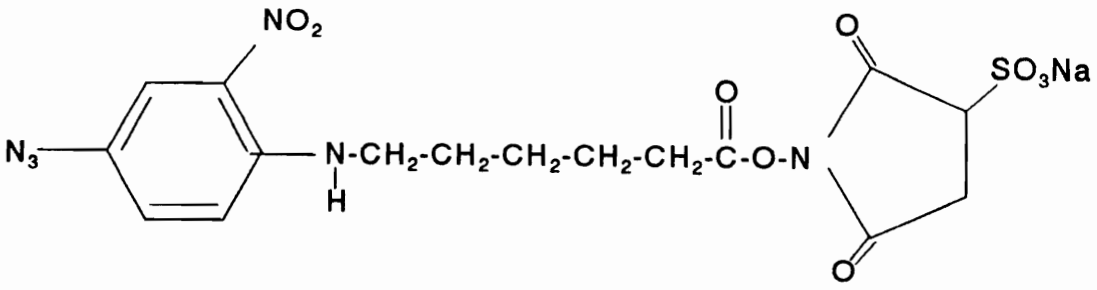

Sulfo-SANPAH

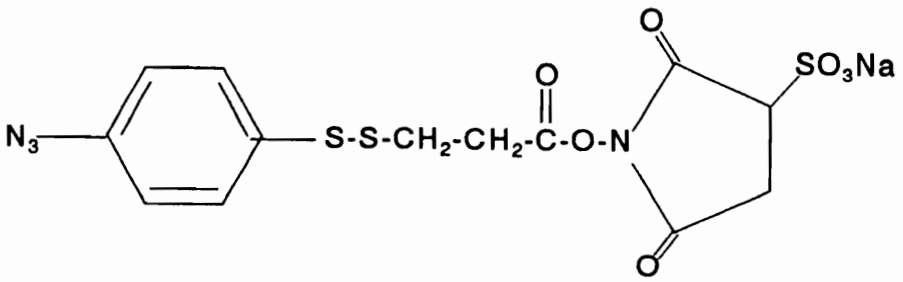

Sulfo-SADP

Figure 4.14 Crosslinking Agents

SADP contains a reducible linkage (R-S-S-R') whereas sulfo-SANPAH does not.

µL 1:1000 β-ME	A 412 -bkg	µM R-SH
0	0.000	0
7	0.238	17.5
14	0.321	23.65
21	0.433	31.8
28	0.744	54.7
35	0.886	65.1

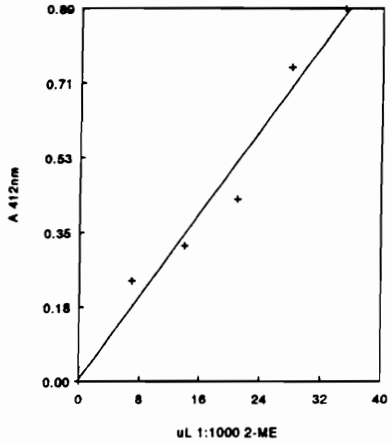

a. R-SH Standard curve

sample	nmoles BSA	A 412 nm -bkg	µM R-SH	nmoles RSH	ratio BSA:SH
CM-BSA	1.5	0.010	0.70	2.3	1 : 1.5
	7.5	0.011	0.81	2.6	3 : 1
	15	0.012	0.88	2.8	5.3 : 1
	30	0.014	0.88	2.8	11 : 1
native BSA	1.5	0.064	4.7	15	1 : 10
	7.5	0.201	15	48	1 : 6.4
	15	0.466	34	109	1 : 7.3
	30	0.739	54	173	1 : 5.7
reduced BSA	1	0.075	5.5	18	1 : 18
	5	0.218	16	51	1 : 10
	10	0.386	28	91	1 : 9.1
	20	0.661	49	156	1 : 7.8

b. BSA tests

Figure 4.15 Carboxymethylation of BSA Cysteine Residues

BSA was treated with iodoacetic acid as described in Section 4.5.1 to modify irreversibly cysteine sulfhydryls in the protein. Following dialysis, the protein was assessed for its content of R-SS-R' and R-SH using Ellman's reagent (ϵ=13.6 $mM^{-1}cm^{-1}$, Section 2.4.9.2). As compared to native and reduced BSA, CM-BSA had no R-SS-R' or R-SH that were able to react with the assay dye reagent.

nmoles R-SH were detected for every 1 nmole native BSA (Figure 4.15). Likewise, 11 nmoles R-SH were detected for every 1 nmole reduced BSA. Less then 1 nmole R-SH was apparent per nmole CM-BSA. Why only 11 moles R-SH were detected per mole BSA is not clear; the BSA may still have been folded such that the assay reagent could not interact with R-S-S-R', even though the BSA was in 6 M guanidine-HCl.

4.5.2 Crosslinking of Carboxymethylcysteine BSA to NH_2-(I)Tyr-Ala-CHN_2

CM-BSA-sulfo-SADP-(I)Tyr-Ala-CHN_2 was synthesized as described in Section 2.4.11. Deblocked NH_2-Tyr-Ala-CHN_2 (4 μmoles) was prepared as described in Section 2.4.6 and then iodinated (Section 2.2.16). The inhibitor (4 X 1 μmole) was then reacted with sulfo-SADP (1, 2, 5, or 10 μmoles) in the dark for 30 minutes, followed by reaction with glycine (equimolar to the amount of sulfo-SADP present) to react with excess sulfo-SADP. CM-BSA (0.1 μmole per tube) was then added and the solutions exposed to 10 bright light flashes at 1 cm. The solutions were purified as before (Section 2.4.8). The protein and inhibitor concentrations were assessed as in Sections 2.2.2 and 2.2.9; the ratio of inhibitor to protein was, on average, 0.7 : 1 (Table 4.4), with the most efficient coupling occurring when the inhibitor and cross-linking agent were present in a 1:1 ratio.

Table 4.4 Ratio of Protein to Inhibitor in CM-BSA-SADP-(I)Tyr-Ala-CHN_2

sample	designed ratio I : CL	nmole I	ratio I: BSA
1	1 : 1	0.54	1.3 : 1
2	1 : 2	0.39	0.47 : 1
3	1 : 5	0.44	0.40 : 1
4	1 : 10	0.53	0.64 : 1

NH_2-(I)Tyr-Ala-CHN_2 (1 μmole) was reacted with 1, 2, 5, or 10 μmole sulfo-SADP ("CL") and 0.1 μmole CM-BSA as described in Section 2.4.10. The complex was purified over two Sephadex G-25 columns and washed as before. The ratio of inhibitor to BSA was 0.7 : 1 (± 0.4). Cross-linking did occur with a 7 % efficiency.

4.5.3 Cross-Linking Carboxymethylcysteine-BSA to NH_2-(^{125}I)Tyr-Ala-CHN_2

Deblocked inhibitor (160 nmoles) was radiolabeled with 5 mCi $Na^{125}I$ as described in Section 2.2.16. The radiolabeled inhibitor was cross-linked to CM-BSA (5 nmoles) using sulfo-SADP (640 nmole). Following purification, only 2.8 pmole inhibitor was present on 1.5 nmole CM-BSA, with a total of 13.8 μCi ^{125}I. The sample was incubated with papain in the presence of 4 mM DTT for 30 min at 37 °C and analyzed by SDS-PAGE and autoradiography; a band corresponding to papain (25 kDa) was detected. When analyzed by non-reductive SDS-PAGE (Laemmli system), the "complex" alone was expected to be detected as a radiolabeled band at 66 kDa; this was not seen (data not shown). A large complex was detected near the top of the separating gel and in the bottom of the wells in the stacking gel, implying that the CM-BSA was being cross-linked to additional protein molecules as well as to the radiolabeled inhibitor, forming massive complexes that could not penetrate the 3.5 % acrylamide stacking gel. The cross-linking was unsuccessful, as demonstrated by the low yield (0.06%, calculated from the ratio of inhibitor cross-linked to protein of 1:500, not 32:1 as expected) and lack of a 66 kDa band following non-reducing SDS-PAGE analysis. Why the cross-linking failed is not clear; the ratio of inhibitor to cross-linker (1:4) and the ratio of cross-linker to protein

(128:1) may have caused the protein to link to neighboring protein molecules.

4.6 Discussion

The work described in this chapter was aimed towards 1) the synthesis of Fmoc-Tyr-Ala-CHN_2 and the characterization of its inhibitory properties against cysteine proteinases both *in vitro* and *in vivo*, and 2) the synthesis of a protein-cysteine proteinases inhibitor complex.

Fmoc-Tyr-Ala-CHN_2 was synthesized from Fmoc-Tyr-Ala-OH via a mixed anhydride reaction. Yield, after initial purification steps, was 3.5 %. Omitting the wash steps and proceeding directly to HPLC purification would greatly increase yield.

Identity of the compound isolated as Fmoc-Tyr-Ala-CHN_2 was confirmed by MS-MS analysis. A contaminant is present in the preparation, as evident by the M+1 = 585.8 and 515 peaks (Figure 4.9) and the small contaminating peak at 20.8 min seen in the analytical HPLC chromatograph of the prep-column fraction #44 (Figure 4.3). It is not known if the contaminant in fraction 44 corresponds to the molecule of mass 585. Based on MS fragmentation patterns, this compound does not seem related to Fmoc-Tyr-Ala-CHN_2. It is a minor component of the total mixture as seen by analytical HPLC.

The ability of Fmoc-Tyr-Ala-CHN_2 to inhibit cathepsins B,

L, and S *in vitro* was assessed by continuous rate assays; the Fmoc-blocked peptidyl inhibitor behaves similarly to the Z-blocked inhibitor (Table 4.3). Cellular forms of cathepsins B, L, and S react with radio-iodinated Fmoc-Tyr-Ala-CHN_2 as seen in Figure 4.10.

Tyr-Ala-CHN_2 was cross-linked to BSA using the hetero-bifunctional cross-linking agent sulfo-SANPAH, giving a final concentration of 30 μM inhibitor. The non-reducible analog was used for studies characterizing the inhibition of the complex against cysteine proteinases. No real difference in inhibitory properties are seen between Z-Tyr-Ala-CHN_2, Fmoc-Tyr-Ala-CHN_2, and BSA-sulfo-SANPAH-Tyr-Ala-CHN_2 for cathepsins B, L, and S (Table 4.3). With papain, however, the protein-inhibitor complex is a much better inhibitor than the Fmoc-inhibitor as demonstrated by the k_{2app} of the protein/inhibitor complex of 615,000 ± 136,000, 20 times greater than that for the Fmoc-inhibitor. As mentioned, this is likely due to the enzymes ability to better accommodate the cross-linker and attached protein over and beyond the S_3 subsite than Fmoc-Tyr-Ala-CHN_2.

The BSA-sulfo-SANPAH-Tyr-Ala-CHN_2 complex was radio-iodinated and then assessed for its ability to interact with cysteine proteinases both *in vitro* and *in vivo*. Incubation with papain, followed by immunoprecipitation of papain bound to inhibitor, demonstrated covalent binding of 1, and 2

molecules of proteinase (Figure 4.12). Incubation with whole cells demonstrated in vivo binding of 2 molecules of enzyme. Thus, the complex is able to enter cells and interact irreversibly with cellular cysteine proteinases.

A reducible protein-inhibitor complex is needed to distinguish cellular forms of the cysteine proteinases reacted with the complex after incubation in cells. A reducible protein-inhibitor complex was synthesized utilizing sulfo-SADP as the cross-linking agent. Sulfo-SADP is a photoactivatable, heterobifunctional cross-linking reagent that interacts with N-termini of peptides and nucleophilic groups of proteins using the same chemistry as sulfo-SANPAH. The primary difference between the two reagents is that sulfo-SADP contains a disulfide bond in the chain connecting the reactive groups (Figure 4.14). Since BSA contains 35 cysteine residues, 34 of which are involved in internal disulfide bonds, the protein was denatured and the cysteines modified by treatment with iodoacetic acid. No free R-SH were detected after modification, as compared to 7 or 11 moles per mole native or reduced BSA, respectively. Varying amounts of sulfo-SADP were reacted with NH_2-Tyr-Ala-CHN_2 to attempt to increase cross-link yields. A 1:1 ratio of inhibitor to cross-linker gave the best results with respect to ratio of inhibitor bound to CM-BSA. The yield of the cross-linking reaction was 13%.

Cross-linking radiolabeled NH_2-(^{125}I)Tyr-Ala-CHN_2 to CM-

BSA using sulfo-SADP was not successful. The ratio of cross-linker to protein (128:1) was too high, such that multiple molecules of CM-BSA were being linked together. The ratio of inhibitor to cross-linker was 1:4; although glycine (a 10-fold molar excess to the cross-linker) was added to react with any cross-linker that had not reacted with the inhibitor, the cross-linker was apparently still able to link CM-BSA to CM-BSA. Future work with this sulfo-SADP may be pursued such that the inhibitor, cross-linker, and protein are present in a 10:10:1 ratio. Other cross-linking strategies should also be investigated that do not rely on the photo-activatable cross-linking agents. Thiol groups can be chemically introduced into proteins and these groups then reacted with a thiol group chemically added to the N-terminus of the inhibitor.

In summary, Fmoc-Tyr-Ala-CHN_2 is as efficient an inhibitor as is Z-Tyr-Ala-CHN_2 and is able to enter cells and completely inactivate cellular cathepsins B, L, and S. A BSA-inhibitor complex is also an efficient inhibitor of cathepsins B, L, and S, and papain; it has been demonstrated to react irreversibly with the enzymes, attaching 1 or 2 molecules of enzyme per molecule of protein-inhibitor complex. This prototype complex shows that such compounds can be used to identify cellular cysteine proteinases that are first encountered by endocytosed molecules.

CHAPTER 5 GENERAL DISCUSSION

The goals of this project were 1.) to identify and characterize active forms of cathepsins B, L, and S in the monocytic cell lines THP1 and U937, both before and after differentiation; and 2.) to synthesize and characterize a protein-cysteine proteinase inhibitor complex. Chapter 3 described the results of experiments designed to meet the first goal, while Chapter 4 described the synthesis and characterization of a non-reducible protein inhibitor complex.

5.1 Cellular Forms of Cathepsins B, L, and S

Cellular forms of cathepsins B, L, and S were identified by incubation of THP1 and U937 cells with the membrane permeable inhibitor Fmoc-(^{125}I)Tyr-Ala-CHN_2. The inhibitor is shown to be capable of reacting completely with active forms of cathepsins B, L, and S in cells. Both of the cell lines used are human monocytic cell lines, with THP1 cells further down the lineage to macrophages than U937 cells, and can be induced to differentiate to macrophage-like cells by treatment with the phorbol ester PMA.

THP1 cells express three cysteine proteinases able to be identified with Fmoc-(^{125}I)Tyr-Ala-CHN_2 (cathepsins B, L, and S, Figure 3.2). All three proteinases are present in both differentiated and undifferentiated cells. Cathepsin B is

present in undifferentiated cells as a 34 kDa form; the appearance of a 30 kDa form (single chain) increased over time of differentiation. Two-chain cathepsin B is present as is evident from the very low molecular weight spot present in lanes 13-16 (Figure 3.2). This represents the light chain of the two chain enzyme, which binds the labeled inhibitor, as the active-site cysteine is present in the light chain. Cathepsin L synthesis is increased over time in differentiated cells resulting in increased steady state levels. Only the single chain form (35 kDa) of the enzyme is present even after 72 h PMA treatment. Cathepsin S is present in undifferentiated cells as a 26 kDa form; upon differentiation, a 28 kDa form appears, with the loss of the 26 kDa form. The 26 kDa form seems to be lost by either inactivation or excretion; new enzyme is then synthesized, as demonstrated by the transient appearance of the 28 kDa band and later appearance of the 26 kDa form. Thus, after differentiation, the steady state levels of cathepsins B and L increase in THP1 cells, while the steady state level of cathepsin S drops and then returns to the previous level.

U937 cells express cathepsin B (Figure 3.1) only after differentiation. Cathepsin L is also present in differentiated U937 cells, but only in minute quantities. The inhibitor used reacts much more quickly with cathepsin L than B; the lack of intense labeling of cathepsin L shows that it

is present in very limiting amounts. Cathepsin S is also present in differentiated U937 cells. A 35 kDa form is seen in the 24 h treated cells; this is processed down to 28 and 26 kDa forms over time.

The 35 kDa form may represent an active pro-form of cathepsin S. From sequence data (Shi et al. 1992) the molecular weight of the pro-enzyme is predicted to be 35.5 kDa; this is in agreement with the 35 kDa band seen. Active pro-forms of cathepsins B and L have not been demonstrated; they do not interact with the radiolabeled inhibitor, presumably because the pro-peptide blocks access to the enzyme active site. This is, therefore, the first evidence for an active pro-form of a cysteine proteinase. The 35 kDa form is apparent in differentiated U937 cells; it also appears faintly in undifferentiated THP1 cells.

The presence of an active pr-form of cathepsin S in vivo is significant with respect to the processing of other latent pro-proteinases to their active forms. Auto-activation of pro-cathepsins B (Mach et al. 1994) and L (Mason and Massey 1994) by a uni-molecular reaction has been demonstrated at physiologically relevant pH (4.5-5.5). The presence of active pro-cathepsin S in vivo implies that pro-cathepsin S may be autoactivated, first to an active pro-form and then to an active single chain form. Either of these forms may be responsible for the inter-molecular proteolytic activation and

processing of pro-cathepsin B and pro-cathepsin L. Active pro-cathepsin S in cells, however, may not be totally beneficial. Although the cellular location of the active pro-form demonstrated in these studies is not known, it would not be advantageous for the isoform to be active in the ER or Golgi body. An active proteinases could degrade the enzymes present in these organelles that are responsible for the post-translational modification and transport of lysosomal enzymes and proteins to be excreted. Most logically, therefore, active pro-cathepsin S would be present in the pre-lysosomal compartment and perhaps endosomes, but not within the ER or the Golgi body.

The presence of the two lower molecular weight forms of cathepsin S (28 and 26 kDa) in both cell lines suggests that cathepsin S exists in both a single and two-chain form. This is the first evidence for such processing of cathepsin S. To investigate whether a possible cleavage site similar to the cleavage site in cathepsin L exists, the sequences of mouse cathepsin L (Troen et al. 1987), human cathepsin L (Gal and Gottesman 1988), human cathepsin S (Shi et al. 1992), and bovine cathepsin S (Wiederanders et al. 1991) were compared (Figure 5.1). The S_1 site of the processing enzyme for mouse and human cathepsin L can accommodate aspartic acid and asparagine; P_3 to P_1 of human cathepsin L are similar to P_3 to P_1 of mouse cathepsin L (Asp-Ser/Leu-Asn). In bovine

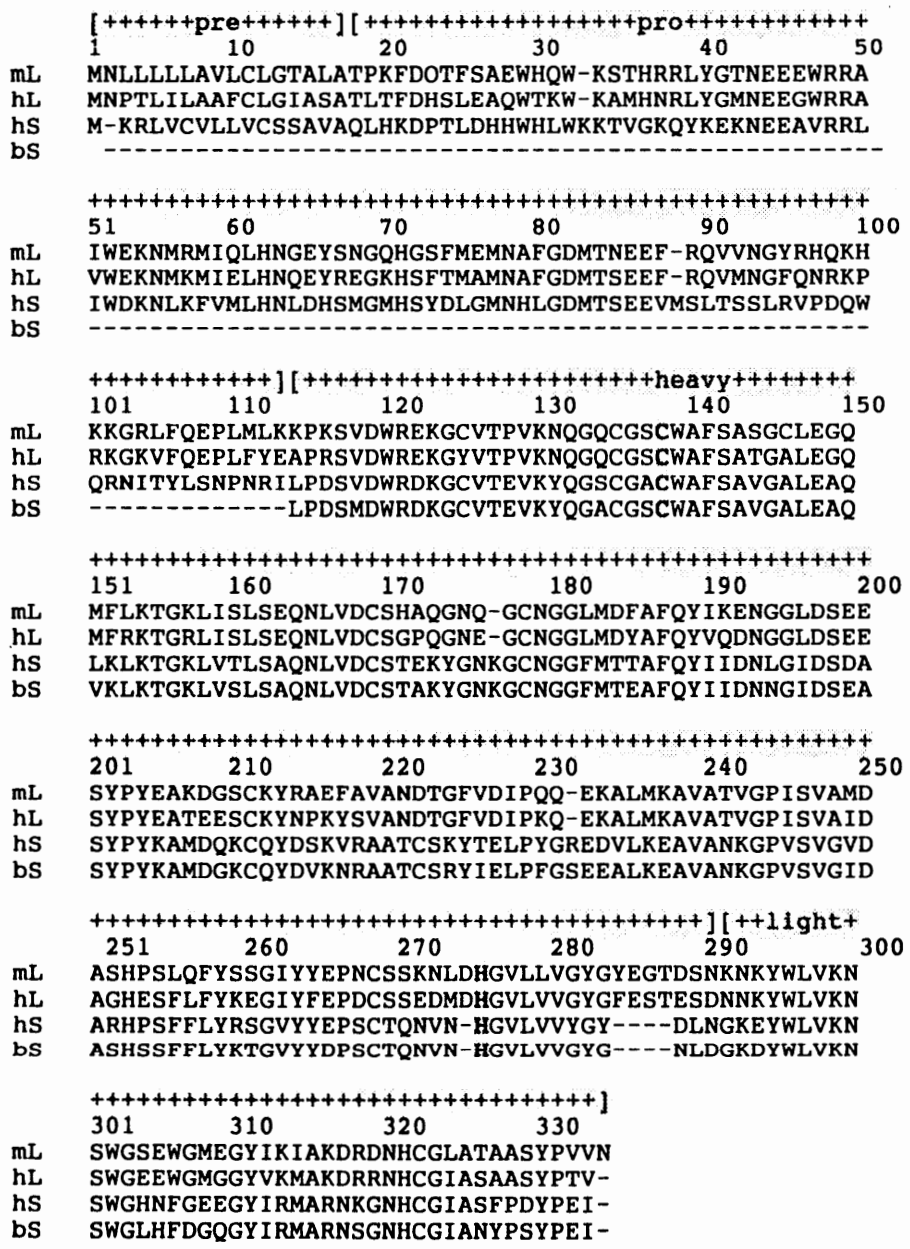

Figure 5.1 Sequence Comparison of Cathepsin L and Cathepsin S

N = glycosylation site
m = mouse L = cathepsin L
h = human S = cathepsin S
b = bovine **C,H** = active site Cys and His

cathepsin S, P_3 is Asn, not the negatively Asp or Glu residues, as in human and mouse cathepsin L and human cathepsin S. These differences between human and mouse cathepsin L and human cathepsin S versus bovine cathepsin S could explain why bovine cathepsin S is not cleaved to a two chain form while the others are, assuming that the same proteinase or a proteinase with a very similar substrate specificity is responsible for the cleavage. This may not be the case, however, given that cathepsin L is present only in the single chain form in THP1 cells (Figure 3.2, lanes 5-8) while cathepsin S is present in a possible two-chain form. Metabolic labeling with ^{35}S-methionine followed by immunoprecipitation of cathepsin S would aid in identifying all biosynthetic forms of cathepsin S present in these cell lines, including the 35 kDa, 28 kDa, and 26 kDa form.

Results from this thesis indicate that THP1 cells are a good model for human macrophages. Reilly et al. (1989) investigated the forms of cathepsin L found in human alveolar macrophages isolated from human subjects by transbronchioscopic lavage. These cells, under culture conditions, initially contain both the 43 kDa and 25 kDa forms of cathepsin L; after 24 h in culture, the pro-form is processed to the 34 kDa (single-chain) form. Human macrophages also express cathepsins B and S (Shi et al. 1992). Low expression of cathepsin L by U937 cells indicate

that these cells are not a good model for studying proteolytic events by human macrophages.

Evidence from the present study suggests that different cysteine proteinases are present in cells at different stages during macrophage maturation. Undifferentiated U937 cells contain no cysteine proteinases capable of labeling with Fmoc-(^{125}I)Tyr-Ala-CHN_2; upon differentiation, the most prevalent enzyme is cathepsin B, followed by cathepsin S. Very little cathepsin L is present. In cells at a later stage (THP1 cells, undifferentiated), all three of these enzymes are present; after differentiation, steady state levels of cathepsins B and L increase while active cathepsin S is inactivated or excreted and replaced by newly synthesized enzyme. Cathepsin L is the most prevalent, followed by cathepsin B and then cathepsin S. Thus, cathepsin B is the initial proteinase synthesized by cells at different stages along the maturation pathway to macrophages, followed by cathepsin S. Cathepsin L becomes the predominant cysteine proteinase in cells at later stages, with cathepsin S levels falling off before cathepsin B levels.

Upon PMA treatment, U937 cells exhibit increased phagocytic activity and expression of the cell surface marker p150/95 (Ward et al. 1990), differentiating the cells form promonocytes to monocyte-like cells. Cathepsin B mRNA levels increase after PMA treatment, while cathepsin G (a serine

proteinase) and elastase mRNA levels decrease. Undifferentiated THP1 cells have both Fc and C3b surface receptors (Tsuchiya et al. 1980), but no surface or cytoplasmic immunoglobulins, implying the monocytic nature of these cells. Upon PMA treatment, THP1 cells become more macrophage-like with respect to cell surface markers. The cell morphology of undifferentiated and differentiated U937 and THP1 cells supports the evidence presented in this study, with respect to content of cathepsins B, L, and S, that undifferentiated U937 cells represent a very early stage along the maturation pathway to macrophages, followed by differentiated U937 cells, then undifferentiated THP1 cells, and finally differentiated THP1 cells being most similar to mature macrophages. This supports the finding that differentiated THP1 cells are a good model for human macrophages.

Cathepsins B and L have been described as general "house-keeping" lysosomal proteinases, present in cells at all times, while cathepsin S synthesis was thought to be more tightly regulated. Evidence presented in this study suggests the opposite: cathepsin S is present constitutively in differentiated U937 cells and both undifferentiated and differentiated THP1 cells, while cathepsin B and cathepsin L synthesis is more tightly regulated. Cathepsin S is present in steady levels both before and after differentiation, while

cathepsins B and L are present in low to moderate levels before differentiation and in high levels after differentiation. This suggests that cathepsin S may be involved in normal lysosomal proteolytic events while cathepsins B and L are expressed and activated only in situations where high proteolytic activity is necessary, as in mature macrophages involved in the degradation of native and foreign proteins.

IEF/SDS-PAGE analysis of both sheep liver cathepsin L and cathepsin L immunoprecipitated from cells showed multiple forms of the enzyme of pI 3 and 3.5, with molecular weights ranging from 35 to 24 kDa (Figures 3.3.c and 3.5). This pI is much lower than the reported value of 5.5 for native cathepsin L isolated from tissues (Barrett and Kirschke 1981). Likewise, cathepsin B and cathepsin S are found to have pIs near 5.9; the pI for cathepsin B agrees closely with that reported (4.5 to 5.5, Barrett and Kirschke 1981). Cathepsin S, however, is reported to have a pI of 7.0 (Kirschke et al. 1989). The differences in pI values reported and those determined in this study may reflect differences in the techniques used to determine the pI of each enzyme. The pI of native cathepsin S was determined using Serva Precotes pH 3-10; pH was determined by migration of marker proteins. The gel was then cut into small pieces and activity of cathepsin S in each fraction was measured by activity against the

substrate Z-Phe-Arg-NHMec. In the present study, the proteins were denatured in urea, mercaptoethanol, and NP-40 before isoelectric focussing. Initial studies were performed on whole cells; the denaturing agents and detergents were added to solubilize the cells. The same sample buffer was used for subsequent analyses of pure and immunoprecipitated cathepsins B, L, and S to maintain identical analytical conditions. Future work may involve similar 2-dimensional analyses of immunoprecipitated cathepsins B, L, and S from whole cells solubilized in sample buffer lacking urea, 2-mercaptoethanol, and NP-40.

Multiple forms of cathepsin L are also evident after SDS-PAGE (Figure 3.4). To determine whether the different isoforms were due to glycosylation, Fmoc-(^{125}I)Tyr-Ala-CHN_2 labeled cathepsin L was isolated from cells by immunoprecipitation and treated with endoglycosidase H (to remove high mannose oligosaccharides), neuraminidase (to remove sialic acid), or PNGase F (to completely remove the oligosaccharide chains from the polypeptide), hypothesizing that removal of the carbohydrate molecules would convert the protein to a single pI form.

Figure 3.7 shows the results of endoglycosidase treatment. The two different pI forms are seen in both control and treated samples. Thus, the multiple pI forms are not due to high mannose oligosaccharides, or the presence of

mannose 6-phosphate on the oligosaccharide chain.

Treatment of immunoprecipitated cathepsin L with neuraminidase does not effect the pI of the forms present, although the laddering effect is lost. The intensity of labeling of the lower molecular weight forms is increased with the loss of the higher molecular weight forms. This shift in the distribution from higher to lower molecular weight forms may be the result of contaminating proteinases in the neuraminidase preparation. The manufacturers report that no proteolytic activity is present against casein as a substrate; degradation of casein is not a sensitive measure of proteolytic activity. If there is a contaminating proteinase, it is most likely an aspartic proteinase, given the low pH (5.5) of the incubation buffer; the presence of E-64 in the incubation buffer rules out the possibility that the contaminating proteinase is a cysteine proteinase. Nonetheless, there was no effect on the different pI forms of cathepsin L.

Treatment of cathepsin L with PNGase F (Figure 3.9) also had no effect on the different pI forms seen. Three pI forms appear in both treated and untreated samples; the presence of three pI forms has been demonstrated in other sample preparations, with and without glycosidase treatments (not shown). The three pI forms are difficult to distinguish in Figure 3.9.a. Only a small pI separation is seen, as compared

to the sample shown in Figure 3.9.b. This is due to the presence of a small air bubble that formed in the tube during the IEF stage of the analysis. The separation achieved was, however, sufficient to see the three pI forms of cathepsin L near the pH 3 end of the gel.

Thus, the different pI forms of cathepsin L displayed after IEF/SDS-PAGE are not due to differently glycosylated forms. The active forms of cathepsin L detected do not seem to be glycosylated. This is expected if active cathepsin L is present in prelysosomal compartments and lysosomes. Once delivered to prelysosomal compartments from the trans-Golgi network via the MPR pathway, the mannose 6-phosphate delivery signal may be removed to prevent recycling of active proteinases back to the trans-Golgi network. Lysosomal glycosidases are also likely to be delivered to prelysosomal compartments and lysosomes in the same vesicles as immature, glycosylated cathepsin L. The lowered pH of the prelysosomal compartments and lysosomes may activate the glycosidases and thus promote the removal of mannose 6-phosphate containing oligosaccharides. Therefore, the active (single- and two-chain) forms of cathepsin L may not be glycosylated, as suggested in the present study. Another post translational modification of the protein must be responsible, such as protein phosphorylation, sulfation, or myristolyation.

5.2 Synthesis of a Protein-Cysteine Proteinase Inhibitor Complex

The cysteine proteinase inhibitor Fmoc-Tyr-Ala-CHN_2 was covalently crosslinked to a carrier protein, BSA, to generate a membrane-impermeable analog of the inhibitor capable of being internalized by cells via endocytosis. The synthesis of this complex involved diazomethylation of Fmoc-Tyr-Ala-OH, purification of the peptidyl diazomethane inhibitor, removal of the N-terminal blocking group, and finally cross-linking to BSA. Fmoc-Tyr-Ala-OH was selected over Z-Tyr-Ala-OH as the N-terminal protecting group must be removed for cross-linking to BSA. The Z-group is removable by acid treatment, a process which would destroy an added diazomethyl group. Fmoc, on the other hand, can be fully removed by treatment with piperidine, an alkaline reagent that does not destroy the diazomethyl moiety.

Mass spectrometric analysis was performed on the sample and confirmed the presence of the inhibitor Fmoc-Tyr-Ala-CHN_2 by both the presence of a peak at mass M+1 = 499.4 and the masses of fragments generated by secondary MS analysis. A contaminant was present of mass M+1 = 585.8; this is probably the molecule seen as a small peak in analytical HPLC analyses of the prep column fractions that was present in fraction 44 (Figure 4.3). The contaminant is not related to Fmoc-Tyr-Ala-CHN_2 as their fragmentation patterns are not similar. The M+1

= 585.8 loses a single fragment of mass 68 and two fragments of mass 185. Fmoc-Tyr-Ala-CHN_2, however, loses fragments of masses 28, 204, 248, and 319. Thus, related fragments are not lost. The contaminant, therefore, is not likely to be a reaction side product, but a contaminant present in the reagents or HPLC solvents used during purification. MS analysis is a qualitative technique, not quantitative. The appearance of a stronger signal for the M+1 = 585.8 molecule than for the M+1 = 498 does not imply that a greater amount of the contaminant is present in the sample than Fmoc-Tyr-Ala-CHN_2.

The peptide inhibitor was then assessed for its ability to inhibit cathepsins B, L, and S both in vitro (Table 4.3) and in vivo (Figure 4.10). The ability of Z-(^{125}I)Tyr-Ala-CHN_2 to enter cells by diffusion through membranes has been demonstrated previously (Mason et al. 1989a). As seen in Figure 4.10, Fmoc-(^{125}I)Tyr-Ala-CHN_2 labels cellular forms of cathepsins B and L as efficiently as Z-(^{125}I)Tyr-Ala-CHN_2. Z-(^{125}I)Tyr-Ala-CHN_2 also labels an additional protein of 16 kDa that does not interact with Fmoc-(^{125}I)Tyr-Ala-CHN_2. Thus, Fmoc-(^{125}I)Tyr-Ala-CHN_2 can be used to identify cellular forms of cathepsins B and L in vivo. The contaminant present in the inhibitor preparation does not appear to interfere with the efficacy of the inhibitor.

The ability of Fmoc-Tyr-Ala-CHN_2 to inhibit cathepsins

B, L, and S and papain *in vitro* was also assessed (Table 4.3). Fmoc-Tyr-Ala-CHN_2 was found to inhibit cathepsins B, L, and S twice as fast as the Z-blocked inhibitor. Together with the *in vivo* characterization described above, Fmoc-Tyr-Ala-CHN_2 is a useful reagent for inhibiting cysteine proteinases both *in vivo* and *in vitro*. The results imply that the Fmoc- group does not interfere with, and may contribute to, the binding of the inhibitor to the enzyme.

Small membrane permeable forms of cysteine proteinase inhibitors, such as Fmoc-Tyr-Ala-CHN_2, may have therapeutic value. For example, cathepsins L and S can degrade elastin, the protein in lung tissue that gives the organ its elastic properties, with cathepsin S being active at neutral pH (Xin *et al*. 1992; Reilly *et al*. 1991). These enzymes are released my alveolar macrophages in response to agents such as cigarette smoke. Degradation of elastin is evident in cigarette smokers and other patients suffering from emphysema. Administration of specific peptidyl diazomethane inhibitors, such as Z-Leu-Leu-Tyr-CHN_2, to emphysema patients by an aerosol inhalation may irreversibly block activity of cathepsins L and S involved in elastin degradation.

Similarly, macrophages excrete high levels of cysteine proteinases in autoimmune diseases such as rheumatoid arthritis. Pro-cathepsin L can be activated and proteolytically processed to mature forms in the presence of

poly-anionic molecules (Mason and Massey 1992) and surfaces present in dextran sulfate and the proteoglycans of cartilage. Administration of inhibitors of cathepsin L may prevent degradation of the proteoglycan matrix and thus prevent the degradation of cartilage seen in rheumatoid arthritis.

The peptidyl diazomethane inhibitors may also be helpful in preventing tissue rejection following organ transplantation, by inactivating the lysosomal proteinases involved in the attack and degradation of the foreign tissue by the immune system. Delivery of the inhibitors must not be systemic but to the specific organ to prevent side effects from the inhibition of lysosomal cysteine proteinases in other healthy tissues. Unless specific enzymes are inactiaved by use of inhibitors that react with only one of the cysteine proteinases, side effects of the administration of these compounds would occur. The patient may become immuno-compromised if all macrophage lysosomal cysteine proteinases are inhibited, as the immune cell would have a major percentage of its hydrolytic arsenal inactivated. Systemic side effects could occur over long periods of inhibitor administration, with symptoms resembling I-cell disease,, in which proteins delivered to lysosomes would not be degraded. If the inhibitor is targeted to a specific cell type by covalent attachment to a carrier protein recognized by a specific cell-surface molecule, systemic side effects may not

occur.

The peptidyl diazomethane inhibitors can also be used to inhibit the lysosomal proteinases oversecreted by tumor cells involved in metastasis. Cancerous cells secrete proteinases to degrade basement membranes and other tissue barriers, allowing a free cancerous cells to migrate to a new site and form a new secondary tumor. The inhibitors can be targeted to cancerous cells by attaching the inhibitor to a molecule that is recognized only by the tumor cell. The inhibitor can be linked, for example, to an antibody against a tumor-specific surface antigen. The inhibitor would then be present on the outer surface of cancerous cells, inactivating any extracellular cysteine proteinases present.

The hetero-bifunctional cross-linking agent sulfo-SANPAH was selected to covalently attach the peptidyl diazomethane inhibitor to BSA on the basis of its non-specific reactivity with proteins. It is also a non-reducible agent, creating a non-reducible complex that can be used to study the kinetics of inhibition of a BSA-inhibitor complex with cysteine proteinases in vitro. Sulfo-SANPAH contains a succinyl group at one end which reacts with free N-termini of peptides (in this case, the free N-terminus of Tyr-Ala-CHN_2) and a photoactivatable phenyl azide at the other end to react non-specifically with nucleophilic groups in proteins, such as amide groups in the peptide bond. The first cross-linking

step (attachment of the free N-terminus of the inhibitor to the cross-linking agent through reaction with the succinyl group) must be performed in the dark. Upon exposure to light (λ= 320-350 nm), the azide moiety reacts with a photon of light causing nitrogen gas (N_2) to escape, leaving a phenyl nitrene which rapidly rearranges to form a 7-membered ring system containing a strained diene (Figure 5.2). The free electron pair in the amide nitrogen in a peptide bond then reacts with the central carbon in the diene; the adjacent nitrogen molecule in the ring structure abstracts the proton from the amide, resulting in the final cross-linked product.

The BSA-sulfo-SANPAH-Tyr-Ala-CHN_2 complex was assessed for its inhibitory properties against cathepsins B, L, and S and papain as before. The complex is slightly more inhibitory than either the Fmoc- or Z- inhibitor versus cathepsins B, L, and S. Against papain, the BSA-inhibitor complex is 20 times more inhibitory than the Fmoc- inhibitor. This is probably because the Fmoc-group cannot fit very well into the S_3 sub-site in the enzyme, while the cross-linker spacer between the BSA and inhibitor lays across the S_3 site.

The BSA-inhibitor complex was radiolabeled as before and then incubated with papain <u>in vitro</u> to determine if the cross-linked complex would indeed react with multiple molecules of the enzyme. As seen in Figure 4.12, lanes 2 and 4, a laddering effect is seen, with bands corresponding to BSA-

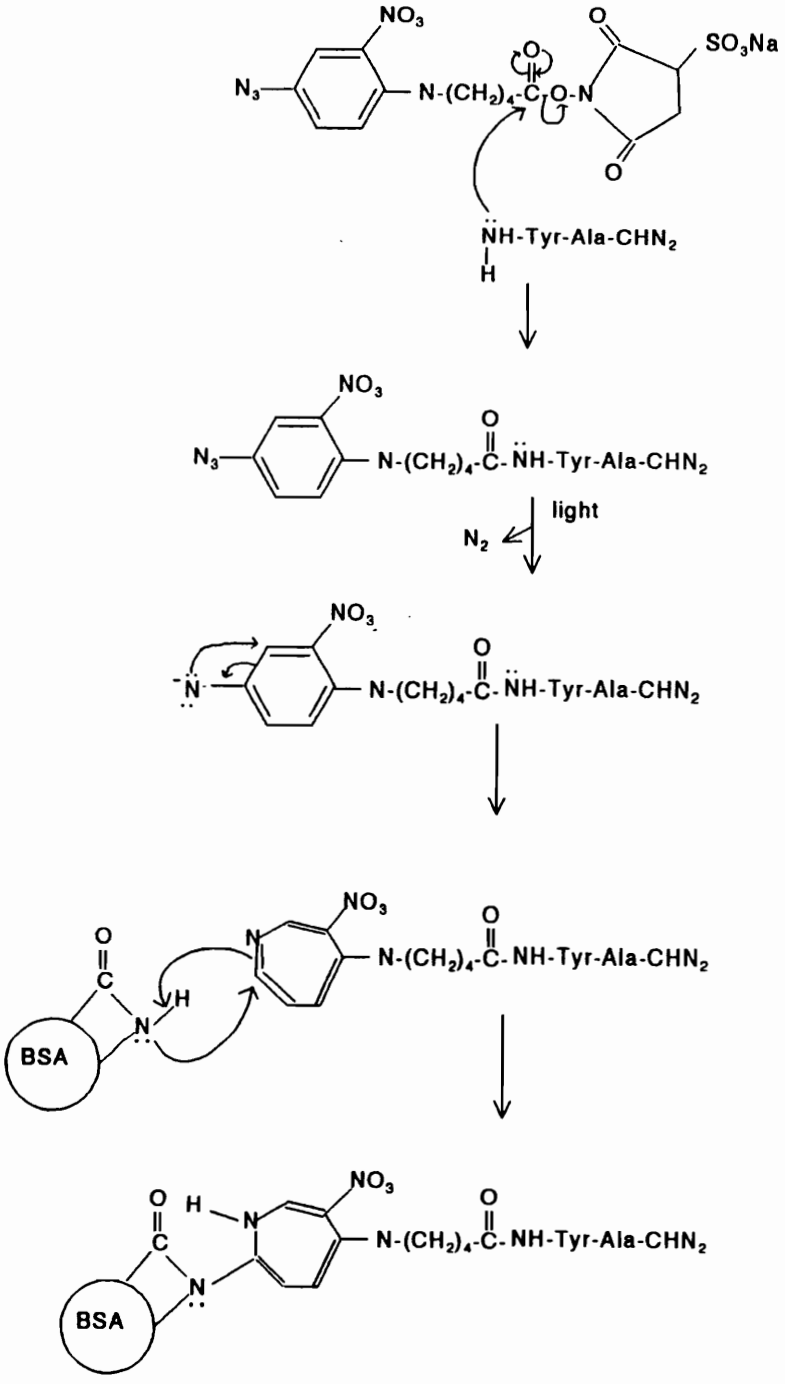

Figure 5.2 Cross-linking Tyr-Ala-CHN_2 to BSA Using sulfo-SANPAH

sulfo-SANPAH-Tyr-Ala-CHN_2 bound to 0, 1, and 2 molecules of papain. This demonstrates that such protein-inhibitor complexes can interact with cysteine proteinases in a specific and covalent manner that can be detected by biochemical methods such as SDS-PAGE and autoradiography.

To see if the complex would accomplish the same in vivo, KNIH 3T3 cells were incubated with 0.08 μM ^{125}I-labeled BSA-sulfo-SANPAH-Tyr-Ala-CHN_2. As seen in Figure 4.13, bands corresponding to 0 and 2 molecules of cysteine proteinase (mean molecular weight = 30 kDa) bound to the BSA-inhibitor complex are apparent. Thus, the complex can interact with cysteine proteinases within cells. The complex is internalized probably by the scavenger receptors gp 18 and gp 30 (Schnitzer et al. 1992 and 1993), which have been shown to bind and internalize modified BSA.

As is apparent from cell incubations with ^{125}I-labeled BSA-sulfo-SANPAH-Tyr-Ala-CHN_2, specific cysteine proteinases and their biosynthetic forms are not distinguishable when an non-reducible cross-linker is used. A reducible cross-linker can be used, such that the inhibitor is delivered to cellular compartments by endocytosis of the protein-inhibitor complex, where it can interact with any cysteine proteinases present. After harvesting and washing the cells, incubation on SDS-PAGE sample buffer containing β-mercaptoethanol would reduce the cross-linker, freeing the radiolabeled inhibitor and bound

enzyme from the carrier protein. The enzyme-inhibitor complex would appear on gels and autoradiographs at the same molecular weight as Fmoc-inhibitor-enzyme complexes described in Chapter 3. To this end, the reducible cross-linker sulfo-SADP was used to cross-link BSA to (I)Tyr-Ala-CHN_2. Because BSA contains 35 cysteine residues, 34 of which are involved in disulfide bonds, BSA was denatured and the cysteines modified with iodoacetic acid to produce carboxymethylcysteine BSA. No free sulfhydryl groups were detected in modified BSA, as compared to the presence of 7 or 11 sulfhydryl groups in native and reduced BSA, respectively. So few R-SH were detected as the BSA in the sample refolded after removal of reducing agents after dialysis, rendering the disulfide bonds inaccessible to the assay reagent. The BSA-S-S-inhibitor complex was initially synthesized with non-radioactive iodine to work out exact procedures necessary, as well as the ratio of inhibitor to protein that gave the most efficient coupling. When cross-linking was attempted with the radio-iodinated inhibitor NH_2-(^{125}I)Tyr-Ala-CHN_2, only 0.001% of the inhibitor was attached to the carrier protein, and less than 0.3 % of the radioactivity associated with the protein. The ratio of protein to inhibitor in the reaction was not optimal, neither was the ratio of cross-linker to protein. This lead to the poor cross-linking efficiency.

5.3 Additional Directions to Explore

Attempts at cross-linking radio-iodinated inhibitor to carboxymethylcysteine BSA were not successful for reasons mentioned above. Additional work is necessary in this area to develop a reducible, radiolabeled protein inhibitor complex that can be used in cell incubation studies. The use of different cross-linking strategies and reagents should be explored to achieve more efficient coupling of the inhibitor to the carrier protein.

Future work with related compounds can provide insight into the role of cysteine proteinases in the early proteolytic processing of various ligands, depending on the carrier protein used. For example, denatured BSA is rapidly internalized by cells via the scavenger receptors gp 18, gp 30 and gp 60 (Schnitzer et al. 1992; Schnitzer and Bravo, 1993). If the inhibitor is cross-linked to denatured BSA, the complex can be used to determine whether cathepsin B, L, or S is present in endosomes involved in general protein internalization. If the carrier protein is the Fc portion of IgG, the role of these enzymes in antigen processing and presentation can be investigated. Likewise, attachment to EGF may help identify which, if any, of the lysosomal cysteine proteinases are involved in the proteolytic processing of EGF to its bioactive forms. Attachment to transferrin could determine whether these enzymes are present in endosomes where

ligand uncoupling occurs. Using a different inhibitor, such as Leu-Leu-(^{125}I)Tyr-CHN_2, could help identify the role of cathepsin H in the above processes.

The use of such protein-inhibitor complexes can identify if a specific proteinase is present in endosomes, or if a specific proteinase is involved in auto-immune or disease-related proteolysis. Once the specific proteinase is identified, the complex can be used to specifically inhibit that enzyme, preventing protein degradation associated with the specific disease state.

5.4 Conclusions

The work described in this dissertation accomplished two goals: the identification and characterization of active cathepsins B, L, and S in human monocytic cell lines and initial development and characterization of protein-cysteine proteinase inhibitor complexes for the study of the delivery of lysosomal enzymes to endosomes.

With regard to the first goal, both THP1 and U937 cells contain active cysteine proteinases whose synthesis is increased by differentiation to macrophage-like cells by treatment with phorbol esters. THP1 cells contain cathepsins B, L, and S both before and after differentiation, with the synthesis of each enzyme increased after PMA treatment. U937 cells contain no detectable levels of cathepsins B, L, or S

before differentiation. Upon PMA treatment, however, cathepsin B is synthesized in great amounts, with cathepsin S being produced is lesser amounts. Cathepsin L is detected after differentiation, although in very limiting amounts.

In both cell lines, cathepsin S appears in 3 forms of 35, 29, and 26 kDa. This suggests an active pro-form (35 kDa), a single (29 kDa), and a two-chain (26 kDa) form of the enzymes. This is the first evidence for an active pro-form of a cysteine proteinase as well as a two-chain form of cathepsin S.

As presented in this study, THP1 cells are a good model for mature human macrophages with respect to cathepsin L synthesis and processing. U937 cells appear to be at an early stage of maturation of monocytes to macrophages; they express no cathepsins B, L, or S until differentiated by PMA treatment. Even after differentiation, U937 cells express limiting amounts of cathepsin S, and even less cathepsin L. Cathepsin B is present in much greater amounts. Thus, U937 cells do not seem to fully differentiate to macrophage-like cells. THP1 cells, on the other hand, are further along the maturation pathway, as they contain cathepsins B, L, and S both before and after differentiation, with the levels of cathepsins B and L increasing and inactivation or excretion followed by new synthesis and processing of cathepsin S. After differentiation, THP1 expression of cathepsins B, L, and

S appears to be the same as in lung macrophages.

The peptidyl diazomethane inhibitor, Fmoc-Tyr-Ala-CHN_2 was synthesized and characterized with respect to its ability to inhibit cathepsins B, L, and S both in vitro and in vivo. This molecule can be synthesized from Fmoc-Tyr-Ala-OH as is prepared by solid phase peptide synthesis utilizing Fmoc-chemistry. The deblocked peptidyl inhibitor was successfully crosslinked to BSA using the hetero-bifunctional, non-reducible cross-linking agent sulfo-SANPAH. This reagent was characterized with respect to its inhibitory properties of cathepsins B, L, and S and papain both in vivo and in vitro, demonstrating that such protein-inhibitor complexes can interact with cysteine proteinases.

CHAPTER 6 REFERENCES CITED

Atkinson, P.H., and Lee, J.T. (1984). Co-translational excision of α-glucose and α-mannose in nacent vesicular stomatitis virus G protein. J. Cell Biol. 98:2245-2249.

Barrett, A.J., Kembhaui, A.A., Brown, M.A., Kirschke, H., Knight, G.C., Tamai, M., and Hanada, K. (1982). E-64 and its analogs as inhibitors of cysteine proteinases including cathepsins B, H, and L. Biochem. J. 201:189-198.

Barrett, A.J. and Kirschke, H. (1981). Cathepsin B, cathepsin H, and cathepsin L. Meth. Enzymol. 80:535-561.

Beck, K.A., Chang, M., Brodsky, F.M. and Keen, J.H. (1992). Clathrin assembly protein AP-2 induces aggregation of membrane vesicles: a possible role for AP-2 in endosome formation. J. Cell Biol. 119:787-796.

Beltzer, J.P. and Speiss, M. (1991). In vitro binding of the asialoglycoprotein receptor to the β-adaptin of plasma membrane coated vesicles. EMBO J. 10:3735-3742.

Blum, J.S. and Cresswell, P. (1988). Role for intracellular proteases in the processing and transport of class II HLA antigens. Proc. Natl. Acad. Sci. USA 85:3975-3979.

Bucci, C., Parton, R.G., Mather, I.H., Stunnenberg, H., Simons, K., Hoflack, B. and Zerial, M. (1992). The small GTPase rab5 functions as a regulatory factor in the early endocytotic pathway. Cell 70:715-728.

Bury, A.F. (1981). Analysis of protein and peptide mixtures: evaluation of three sodium dodecyl sulfate - polyacrylamide gel electrophoresis buffer systems. J. Chromatography 213:419-500.

Canfield, W.M., Johnson, K.F., Ye, R.D., Gregory, W., and Kornfeld, S. (1991). Localization of the signal for rapid internalization of the bovine cation-independent mannose 6-phosphate/insulin-like growth factor II receptor to amino acids 24-29 of the cytoplasmi tail. J. Biol. Chem. 266:5682-5688.

Carlsson, S.R. and Fukuda, M. (1992). The lysosomal membrane glycoprotein lamp-1 is transported to lysosomes by two alternative pathways. Arch. Biochem. Biophys. 296:630-639.

Carter, L.L., Redelmeier, T.E., Wollenweber, L.A., and Schmid, S.L. (1993). Multiple GTP-binding proteins participate in clathrin-coated vesicle-mediated endocytosis. J. Cell Biol. 120:37-45.

Casciola-Rosen, L.A.F. and Hubbard, A.L. (1991). Hydrolases in intracellular compartments of rat liver cells: evidence for selective activation and/or delivery. J. Biol. Chem. 266:4341-4347.

Casciola-Rosen, L.A.F., Renfew, C.A., and Hubbard, A.L.(1992). Leumenal labeling of rat hepatocyte endocytic compartments: distribution of several acid hydrolases and membrane receptors. J. Biol. Chem. 267:11856-11864.

Chan, S.J., SanSegundo, B.S., McCormick, M.B. and Steiner, D.F. (1986). Nucleotide and predicted amino acid sequences of cloned human and mouse preprocathepsin B cDNAs. Proc. Natl. Acad. Sci. USA 83:7721-7725.

Chau, H.V.J., Waheed, A., Pohlmann, R., Hille, A., and von Figura, K. (1990). Mannose 6-phosphate receptor dependent secretion of lysosomal enzymes. EMBO J. 9:3507-3513.

Chen, W-J., Goldstein, J.L., and Brown, M.S. (1990). NPXY, a sequence often found in cytoplasmic tails, is required for coated pit-mediated internalization of low density lipoprotein receptor. J. Biol. Chem. 265:3116-3123.

Collawn, J.F., Stangel, M., Kuhn, L.A., Esekogwu, V., Jing, S., Trowbridge, I.S., and Tainer, J.A. (1990). Transferrin receptor internalization sequence YXRF implicates a tight turn as the structural recognition motif for endocytosis. Cell 63:1061-1072.

Conner, G.E., Blobel, G., and Erikson, A.H. (1987). Biogenesis of lysosomal proteinases: polypeptide chain. in **Lysosomes: their role in protein breakdown.** (eds H. Glaumenn and F.J. Ballard), pp. 151-161. Academic Press, London.

Crawford, C., Mason, R.W., Wikstrom, R., and Shaw, E. (1988). The design of peptidyldiazomethane inhibitors to distinguish between the cysteine proteinases calpain II, cathepsin L, and cathepsin B. Biochem. J. 253:751-758.

Darbre, A. (1986). Analytical Methods. **Practical Protein Chemistry: A handbook.** (ed. A. Darbre); John Wiley and Sons, Ltd. New York. pp.248-249.

DeLuca-Flaherty, C., McKay, d.B., Parham, P. and Hill, B.L. (1990). Uncoating protein (hsc70) binds a conformationally labile domain of clathrin light chain LC_a to stimulate ATP hydrolysis. Cell 62:875-887.

Diment, S., Martin, K.J., and Stahl, P.D. (1989). Cleavage of parathyroid hormone in macrophage endosomes illustrates a novel pathway for intracellular processing of proteins. J. Biol. Chem. 264:13403-13406.

Dunn, K.W. and Maxfield, F.R. (1992). Delivery of ligands from sorting endosomes to late endosomes occurs by maturation of sorting endosomes. J. Cell Biol. 117:301-310.

Emans, N., Gorvel, J-P., Walter, C., Gerke, V., Kellner, R., Griffiths, G. and Gruenberg, J. (1993). Annexin II is a major component of fusogenic endosomal vesicles. J. Cell Biol. 120:1357-1369.

Farquhar, M.G. and Palade, G.E. (1981). The golgi apparatus (complex)-(1954-1981)-from artifact to centerstage. J. Cell Biol. 91:77-103.

Finkle, B.J. and Smith, E.L. (1958). Crystalline papain: number and reactivity of thiol groups; chromatographic behavior. J. Biol.Chem. 230:669-690.

Fischer, H.D., Gonzalea-Noriega, A., and Sly, W.S. (1980). β-gluccuronidase binding to human fibroblast membraane receptors. J. Biol. Chem. 255:5069-5074.

Fontana, A., and Gross, E. (1986). Fragmentation of polypeptides by chemical methods. Practical Protein Chemistry: A Handbook. (Ed. A. Darbre); John Wiley and Sons, Ltd. New York. p. 72.

Forgac, M. 1992a). Structure and properties of the coated vesicle (H^+)-ATPase. J. Bioener. Biomemb. 24:341-350.

Forgac, M. (1992b). Structure, function, and regulation of coated vesicle V-ATPase. J. Exp. Biol. 172:155-169.

Fox, T. deMiguel, E., Mort, J.S., and Storer, A.C. (1992). Potent slow-binding inhibition of cathepsin B by its propeptide. Biochemistry 31:12571-12576.

Gaete, V., Nunez, M.T., and Glass, J. (1991). Cl^-, Na^+ and H^+ fluxes during the acidification of rabbit reticulocyte endocytic vesicles. J Bioener. Biomem. 23:147-160.

Gal, S., and Gottesman, M.M. (1988) Isolation and sequence of a cDNA for human pro-(cathepsinL). Biochem. J. 253:303-306.

Gal, S., Willingham, M.C., and Gottesman, M.M.(1985). Processing and lysosomal localization of a glycoprotein whose secretion is transformation stimulated. J. Cell. Biol. 100:535-544.

Geuggenheim, E.A. (1926). Philos. Mag., 7th Series; 2:538-543.

Gilmore, R., Blobel, G., and Walter, P. (1982a). Protein translocation across the endoplasmic reticulum: detection in the microsomal membrane of a receptor for the signal recognition particle. J. Cell Biol. 95:463-469.

Gilmore,R., Walter, P., and Blobel, G. (1982b) Protein translocation across the endoplasmic reticulum: isolation and characteization of the SRP receptor. J. Cell Biol. 95:470-477.

Glickman, J.N., Conibear, E., and Pearse, B.M.F.(1989). Specificity of binding of clathriin adaptors to signals on the mannose 6-phosphate/insulin-like growth factor II receptor. EMBO J. 8:1041-1047.

Green, S.A., Zimmer, K-P., Griffiths, G., and Mellman, I. (1987). Kinetics of intracellular transport and sorting of lysosomal memrane and plasma membrane proteins. J. Cell Biol. 105:1227-1240.

Grinde, B. (1983). The thiol proteinase inhibitors Z-Phe-Phe-CHN_2, inhibit lysosomal protein degradation in isolated rat hepatocytes. Biochem. Biophys. Acta. 757:15-20.

Gruenberg, J. and Howell, K.E. (1989). Membrane traffic in endocytosis: insights from cell-free assays. Annu. Rev. Cell Biol. 5:453-481.

Hanada, K., Tamai, M., Yamagishi, M., Ohmura, S., Sawada, J., and Tanaka, I. (1978a). Isolation and characterization of E-64, a new thiol protease inhibitor. Agric. Biol. Chem. 42:523-528.

Hanada, K., Tamai, M., Ohmura, S., Sawada, J., Seki, T., and Tanaka, I. (1978b). Dtructure and synthesis of E-64, a new thiol protease inhibitor. Agric. Biol. Chem. 42:529-536.

Hanewinkel, H., Glossl, J., and Kresse, H. (1987). Biosynthesis of cathepsin B in normal and I-cell fibroblasts. J. Biol. Chem. 262:12351-1235.

Harter, C., and Mellman, I. (1992). Transport of the lysosomal membrane glycoprotein lpg120 (lpg-A) to lysosomes does not require appearance on the plasma membrane. J. Cell Biol. 117:311-325.

Hashida, S., Towatari, T., Kominami, E., and Katanuma, N. (1980). Inhibition by E-64 derivitives of rat liver cathepsin B and cathepsin L in vitro and in vivo. J. Biochem. 88:1805-1811.

Helenius, A., Mellman, I., Wall, D., and Hubbard, A. (1983) Endosomes. Trends. Biochem. Sci. 8:245-250.

Hoflack, B., Fujimoto, K., and Kornfeld, S. (1987). The interaction of phosphorylated oligosaccharides and lysosomal enzymes with bovine liver cation-dependent mannose 6-phosphate receptor. J. Biol. Chem. 262:123-129.

Hoflack, B., and Kornfeld, S. (1985). Lysosomal enzyme binding to mouse P388 D1 macrophage membrane lacking the 215-kDa mannose 6-phosphate receptor: evidence for the existence of a second mannose 6-phosphate receptor. Proc. Natl. Acad. Sci. USA 82:4428-4432.

Hoflack,B. and Lobel, P. (1993). Functions of the mannose 6-phosphate receptors. **In Advances in Cell and Molecular Biology of Membranes, vol.1: Endosomes and Lysosomes: A dynamic relationship.** (eds. A.M. Tartakoff, B.Storrie, and R.F. Murphy) JAI Press, Inc. pp.51-80.

Hubbard, S.C., and Robbins, P.W. (1979). Synthesis and processing of protein-linked oligosaccharides in vivo. J. Biol. Chem. 254:4568-4576.

Hunziker, W., whitney, J.A., and Mellman, I. (1992). Brefeldin A and the endocytic pathway: possible implications for membrane traffic and sorting. FEBS Lett. 307:93-96.

Ishidoh, K., Imajoh, S., Emori, Y., Ohno, S., Kawasaki, H., Minami, Y., Kominami, E., Katunuma, N., and Suzuki, K. (1987). Molecular clonong and sequencing of rat cathepsin H. FEBS Lett 226:33-37.

Johnson, K.F., and Kornfeld, S. (1992). The cytoplasmic tail of the mannose 6-phosphate/insulin-like growth factoe II receptor has two signals for lysosomal sorting in the golgi. J. Cell Biol. 119:249-257.

Joseph, L.J., Chang, L.C., Stamenkovich, D., and Sukhatme,V.P. (1988). Complete nucleotide sequence and deduced amino acid sequences of human and murine preprocathepsin L. J. Clin. Invset. 81:1621-1629.

Kamphius, I.G., Kalk, K.H., Swarle, M.B.A., and Drenth, J. (1985). Structure of papain at 1.65 Åresolution. J. Mol. Biol. 179:233-256.

Kiess, W., Blickenstaff, G.D., Sklar, M.M., Thomas, G.L., Nissley, S.P., and Sahagian, G.G. (1988). Biochemical evidence that the type II insulin-like growth factor receptor is identical to the cation-indepentent mannose 6-phosphate receptor. J. Biol. Chem. 263:9339-9344.

Kirschke, H., Schmidt, I., and Wiederanders, B. (1986). Cathepsin S: the cysteine proteinase from bovine lymphoid tissue is distinct from cathepsin L. Biochem. J. 240:455-459.

Kirschke, H., Wiederanders, B., Brömme, D., and Rinne, A. (1989). Cathepsin S from bovine spleen: purification, distribution, intracellular localization and action on proteins. Biochem J. 264:467-473.

Klumperman, J., Hille, A., Veenendaal, T., Oorschot, V., Stoorvogel, W., von Figura, K., and Geuze, H.J. (1993). Differences in the endosomal distributions of the two mannose 6-phosphate receptors. J. Cell Biol. 121:997-1010.

Knight, C.G. (1980). Human cathepsin B: inhibition by leupeptin. Biochem. J. 189:447-453.

Knight, C.G. (1986). The characterization of enzyme inhibition. In **Proteinase Inhibitors** (Eds. Barrett, A.J. and Salvesen, G.), Elsevier Science Publishers, Cambridgen UK. pp. 23-51.

Kominami, E., Tsukahara, T., Hara, K., and Katunuma, N. (1988). Biosynthesis and processing of lysosomal cysteinse proteinases in rat macrophages. FEBS Lett. 231:225-228.

Kornfeld, S. (1987). trafficking of lysosomal enzymes. FASEB J. 1:462-468.

Ktisiakis, N.T., Thomas, D.N., and Roth, M.C. (1990). Characteristics of the tyrosine recognition signal for internalization of transmembrane surface glycoproteins. J. Cell Biol. 111:1391-11407.

Laemmli, U.K. (1970). Cleavage of structural proteins during the assembly of the head of bacteriophage T4. Nature 227:680-685.

Lenhard, J.M., Kahn, R.A., and Stahl, P.D. (1992). Evidence for ADP-ribosylation factor (ARF) as a regulator of in vitro endosome-sndosome fusion. J. Biol. Chem. 267:13047-13052.

Lowe, G. and Williams, A. (1965). Dit=rect evidence for an acylated thiol as an intermediats in papain and ficin catalyzed hydrolyzes. Biochem. J. 96:189-193.

Ludwig, T., Griffiths, G., and Hoflack, B. (1991). Distribution of newly synthsized lysosomal enzymes in the endocytic pathway of normal rat kidney cells. J. Cell Biol. 115:1561-1572.

MacDonald, R.G., Pfeffer,S.R., Cassens, L., Tepper, M.A., Brocklebank, C.M., Mole, J.E., Anderson, J.K., Chen, E., Czech, M.P., and Ullrich, A. (1988). A singls receptor binds both insulin-like growth factor II and mannnose 6-phosphate. Science 239:1134-1137.

Mach, L., Mort, J.S., and Glössl, J. (1994). Maturation of human procathepsin B: proenzyme activation and proteolytic processing of the precursor to the mature proteinase, in vitor, are primarily unimolecular processes. J. Biol. Chem. 269:13030-13035.

Mach, L., Stüwe, K., Hagen, A., Ballaun, C., and Glössel, J. (1992). Proteolytic processing and glycosylation of cathepsin B: the role of the primary structure of the latent precursor and the carbohydrate moiety for cell-type-specific mollecular forms of the enzyme. Biochem J. 282:577-582.

Marquez-Sterling, N., Herman, I.M., Pesecreta, T., Arai, H., Terres, G., and Forgac, M. (1991). Immunolocalization of the vacuolar-type (H^+)-ATPase from clathrin-coated vesicles. Eur. J. Cell Biol. 56:19-33.

Marshall, R.D.(1972). Glycoproteins. Ann. Rev. Biochem. 41:673-702.

Mason, R.W. (1986). Species varients of cathepsin L and their immunological identification. Biochem. J. 240:285-288.

Mason, R.W., Wilcox, D., WIkstrom, P., and Shaw, E.N. (1989a). The identification of active forms of cysteine proteinases in Kirsten-virus transformed mouse fibroblasts by use of a specific radiolabelled inhibitor. Biochem. J. 257:125-129.

Mason, R.W., Bartholomew, L.T., and Hardwidk, B.S. (1989b). The use of benzyloxycarbonyl-[^{125}I]iodotyrosyl-alanyl-diazomethane as a probe for active cysteine proteinases in human tissues. Biochem. J. 263:945-949.

Mason, R.W., Gal, S., and Gottesman, M.M. (1987). The identification of the major excreted protein (MEP) from a transformed mouse cell line as a catalytically active precursor form of cathepsin L. Biochem. J. 248:449-454.

Mason, R.W., Greene, G.D.J., and Barrett, A.J. (1985). Human liver cathepsin L. Biochem. J. 226:233-241.

Mason, R.W. and Masey, S.D. (1992). Surfaace activation of Pro-cathepsin L. Biochem. Biophys. Res. Comm. 189:1659-1666.

Mason, R.W., Walker, J.E., and Northrop, D. (1986). The-N-terminal amino acid sequences of the heavy and light chains of human cathepsin L. Biochem. J. 240:373-377.

Mason, R.W. and Wilcox, D. (1993). Chemistry of lysosomal cysteine Proteinases. In **Advances in Cell and Molecular Biology of Membranes, Vol. 1: Endosomes and Lysosomes: A Dynamic Relationship.** (Eds. A.M. Tartakoff, B. Storrie, and R.F. Murphy) JAI Press, Inc., pp.81-116.

Mathews, P.M., Martinie, J.B., and Fambrough, D.M. (1992). The pathway and targetting signal for delivery of the integral membrane glycoprotein LEP100 to lysosomes. J. Cell Biol. 118:1027-1040.

Mayor, S., Presley, J.F., and Maxfield, F.R. (1993). Sorting of membrane components from ensosomes and subsequent recycling to the cell surface occurs by a bulk flow process. J. Cell Biol. 121:1257-1269.

Mayora, L.S., Diaz, r., and Stahl, P.D. (1989). Reconstitution of endosome proteolysis in a cell free system: transfer of immune complexes internalized via Fc receptors to an endosomal proteokytic compartment. J. Biol. Chem. 264:5392-5399.

McGowan, E.B., Becker, E., and Detwiler, T.C. (1989). Inhibition of calpain in intact platelets by hte thiol protease inhibitor E-64d. Biochem. Biophys. Res. Comm. 158:432-435.

Mehdi, S.(1991). Cell penettrating inhibitors of calpain. Trends Biochem, Sci. 16:150-153.

Meyer, D.L., Krause, E., and Dobbersteine, B. (1982). Secretory protein translocation across membranes- the role of the "docking protein". Nature 297:647-650.

Michalek, M.T., Benacerraf, B., and Rock, K.L. (1992). The class II MHC-restricted presentation of endogenously synthesized ovalbumin displays clonal variation, requires endosomeal/lysosomal processing, and is up-regulated by heat shock. J. Immunol. 148:1016-1024.

Miller, C. and Koeffler, H.P. (1986). Bioessays 5:18-21.

Morgan, D.O., Edman, J.C., Standring, D.N., Fried, V.A., Smith, M.C., Roth, R.A., and Rutter, W.J. (1987). Insulin-like growth faactor II receptor as a multifunvctional binding protein. Nature 329:301-307.

Musil, D., Zucic, D., Turk, D., Engh, R.A., Mayr, I., Huber, R., Popovic, T., Turk, V., Towatari, T., Katunuma, N., and Bode, W. (1991). The refined 2.15Å X-ray crystal structure of human liver cathepsin B: the structural basis for its specificity. EMBO J. 10:2321-2330.

Neefjes, J.J., and Ploegh, H.L. (1992). Inhibition of endosomal proteolytic activity by leupeptin blocks surface expression of MHC class II molecules and their conversion to SDS resistant αβ heterodimers in endosomes. EMBO J. 11:411-416.

Nishimura, Y., Furuno, K., and Kato, K. (1988). Biosynthesis and processing of lysosomal cathepsin L in primary cultures of rat hepatocytes. Arch. Biochem. Biophys. 263:107-116.

Nishimura, Y., and KAto, K. (987). Intracellular transport and processing of lysosomal cathepsin H. Biochem. Biophys. Res. Comm. 148:329-334.

Node, T., Isogai, K., Katunuma, N., Tarumoto, Y., and Ohzeki, M. (1981). Effects on cathepsin B, H, and D in pectoral muscle of dystrophic chickens (line 413) of in vivo administration of E-64c (N-[N-(L-3-transcarboxyoxirane-2-carbonyl)-L-leucyl]-3-methyl-butylamine). J Biochem. 90:893-896.

Oshima, A., Nolan, C.M., Kyle, J.W., Grubb, J.H., and Sly, W.S. (1988). The human cation-dependent mannose 6-phosphate receptor. Cloning and sequence of the full-length cDNA and expression of functional receptor in COS cells. J. Biol. Chem. 263:2553-2562.

Parks, J.E., Lopez, J.M., Cluett, E.B., and Brown, W.J. (1991). Identification of a membrane glycoprotein found primarily in the prelysosomal endosome compartment. J. Cell Biol. 112:245-255.

Pearse, B.M.F. (1988). Receptors compete for adaptors found in plasma membrane coated pits. EMBO. J. 7:3331-3336.

Pellham, H.R. (1989). Control of protein exit from the endoplasmic reticulum. Ann. Rev. Cell Biol. 5:1-23.

Portney, D.A., Erickson, A.H., Kochan, J., Ravetch, J.V., and Unkeless, J.C. (1986). Cloning and characterzation of a mouse cysteine proteinase. J. Biol. Chem. 261:14697-14703.

Polgar, L. (1973). Onthe mode of activation of the catalytically essential sulfhydryl group of papain. Eur. J. Biochem. 33:104-109.

Puri, J., and Factorovich, Y.(1988). Selective inhibition of antigen presentation to cloned T cells by protease inhibitors. J. Immunol. 141:3313-3317.

Rabinowitz, S., Horstmann, H., Gordon, S., and Griffiths, G. (1992). Immunocytochemical characterization of the endocytic and phagolysosomal compartments in peritoneal macrophages. J. Cell Biol. 116:95-112.

Racoosin, e.L., and Swanson, J.A. (1993). Macropinosome maturation and fusion with tubular lysosomes in macrophages. J. Cell Biol. 121:1011-1020.

Rauber, P., Angliker, H., Walker, B., and Shaw,E. (1986). The synthesis of peptidylfluoromethanes and their properties as inhibioters of serine proteinases and cysteine proteinases. Biochem. J. 239:633-640.

Reilly, J.J., Chen, P., Sailor, L.Z., Wilcox, D., Mason, r.W., and Chapman, H.A. (1991). Cigarette smoking induces an elastolytic cysteine proteinase in macrophages distinct form cathepsin L. Am. J. Physiol. 261:L41-L48.

Reilly, J.J., Mason, R.W., Chen, P., Joseph, L.J., Sukhatme, V.P., Yee, R., and Chapman, H.A. (1989). Ssynthesis and processing of cathepsinL, and elastase, by human alveolar macrophages. Biochem. J. 257:493-498.

Renfrew, C.A. and Hubbard, A.L. (1991). Sequential processing of epidermal growth factoe in early and late endosomes of rat liver. J. Biol. Chem. 266:4348-4356.

Rich, D.H. (1986). Inhibitors of cysteine proteinases. In **Proteinase Inhibitors** (Eds. A.J. Barrett and G. Salvesen) Science Publishers, Amsterdam. pp.153-178.

Rich, D.H., Brown, M.A., and Barrett, A.J. (1986). Purification of cathepsin B by a new form of affinity chromatography. Biochem. J. 235:731-734.

Rijnboutt, S., Stroorvogel, W., Geuze, H.J. and Strous, G.J. (1992). Identification of subcellular compartments involved in biosynthetic processing of cathepsin D. J. Biol. Chem. 267:15665-15672.

Rodman, J.S., Levy, M.A., Diment, S., and Stahl, P. (1990). Immunolocalization of endosomal cathepsin D in rabbit alveolar macrophages. J Leukocyte Biol. 48:116-122.

Roederer, M., Barry, J.R., Wilson, r.B., and Murphy, R.F. (1990). Endosomes can undergo an ATP-dependent density increase in the absence of dense lysosomes. J. Cell. Biol. 51:229-234.

Sahagian, G.G., Distter, J., and Jourdian, G.W. (1981). Characterization of a membrane-associated receptor from bovine liver that binds phosphomannosyl residues of bovine testicular beta-galactosidase, Proc. Natl. Acad. Sci. USA. 78:4289-4293.

Salminen, A., Gottesman, M.M (1990). Inhibitor studies indicate that active cathepsin L is probably essential to its own processing in cultures fibroblasts. Biochem. J. 272:39-44.

Santoro, L., Reboul, A., Journet, A.M., and Colomb, M.G. (1993). Major involvement of cathepsin B in the intracellular proteolytic processing of exogenous IgGs in U937 cells. Molec. Immunol. 30:1033-1039.

Schechter, I., and Berger, A. (1967). On the active site of proteinases. I. Papain. Biochem. Biophys. Res. Comm. 27;157-161.

Schnitzer, J.E., and Bravo, J. (1993). High affinity binding, endocytosis, and degredation of conformationally modified albumins: potential role of gp30 and gp18 as novel scavenger receptors. J. Biol. Chem. 268:7562-7570.

Schnitzer, J.E., Sung, A., Horvat, R., Bravo, J. (1992). Preferential interaction of albumin-binding proteins , gp30 and gp18, with conformationally modified albumins. J. Biol. Chem. 267:24544-24553.

Shaw, E. (1984). The selective inactivation of thiol proteinases by diazomethanes in vivo and in vitro. J. Protein Chem. 3:109-120.

Shaw, E., and Greene, G.D.J. (1981). Inactivation of thio; proteases with peptidyl diazomethyl ketones. Meth. Enzymol. 80:820-826.

Shi, G-P., Munger, J.S., Meara, J.P., Rich, D.H., and Chapman, H.A. (1992). Molecular cloning and expression of a human alveolar macrophage cathepsin S, an elstinolytic cysteins protease. J. Biol. Chem. 267:7258-7262.

Shoji-Kasai, Y., Senshu, M., Iwashita, S., and Imahori, K. (1988). Thiol protease-specific inhibitor E-64 arrests human epidermoid carcinoma A431 cells at mitotic metaphase. Proc. Natl. Acad. Sci. USA 85:146-150.

Simon, O., Bohley, P., Munchmeyer, R., Bergner, H., and Huckel, C. (1977). Studies on the in vivo action of leupeptin on the nitrogen retention in rats. Acta. Biol. Med. Germ. 36:1923-1925.

Smythe, E., Carter, L.L, and Schmid, S.L. (1992). Cytosol- and clathrin-dependent stimulation of endocytosis in vitro by purified adaptors. J. Cell Biol. 119:1163-1171.

Stoorvogel, W., Strous, G.J., Geuze, H.J., Oorschot, V., Schwartz, A.L. (1991). Late endosomes derive from early endosomes by maturation. Cell 65:417-427.

Tamai, M., Matsumoto, K., Omura, Ss., Koyama, I., Ozawa, Y., and Hanada, K. (1986). In vitro and in vivo inhibitoin of cysteine proteinases by EST, a new analog of E-64. J. Pharmacobio-Dyn. 9:672-677.

Thannhauser, T.W., Konishi, Y., and Scheraga, H.A. (1984). Sensitive quantitative analysis of disulfide bond in polypeptides and proteins. Anal. Biochem. 138:181-188.

Tian, W., and Tsou, C. (1982). Determination of the rate constant of enzyme modification by measuring the substrate reaction in the presence of the modifier. Biochem. J. 21:1028-1032.

Tong, P.Y., Gregory, W.W., and Kornfeld, S. (1989a). Ligand interactions of the cation-independent mannse 6phosphate receptor: the stoichiometry of mannose 6-phosphate binding. J. Biol. Chem. 264:7962-7969.

Tong, P.Y., and Kornfeld, S. (1989b). Ligand interactions of the cation-dependent mannose 6-phosphate receptor: comparison with the cation-independent mannose 6-phosphate receptor. J. Biol.Chem. 264:7970-7975.

Troen, B.R., Gal, S., and Gettesman, M.M. (1987). Sequence and expression of the cDNA for MEP (major excreted protein), a transformation-regulated sectrted protein. Biochem. J. 246:731-735.

Tsuchiya, S., Yamabe, M., Yamaguchi, Y., Kobayashi, Y., Konno, T., and Tada, K. (1980). Establishment and characterization of a human acute monocytic leukemia cell line (THP-1). Int. J. Cancer 26:171-176.

Twinning, S.S. (1984). Fluorescence isothiocyanate lacbeled casein assay for proteolytic enzymes. Anal. Biochem. 143:30-34.

Umezawa, H. (1972). **Enzyme Inhibitors of Microbial Origin.** University Park Press, Baltimore.

van der Sluijs, P., Hull, M., Webster, P., Mâle, P., Goud, B., and Mellman, I. (1992). The small GTP-binding protein rab4 controls an early sorting event on the endocytic pathway. Cell 70:720-740.

Varughese, K.I., Ahmed, F.r., Carey, P.R., Hasnain, S., Huber, C.P., and Storer, A.C. (1989). The crystal structure of a papain-E-64 complex. Biochemistry 28:1330-1332.

Vidard, L., Rock, K.L., and Benacerraf, B. (1992). Diversity in MHC class II ovalbumin T cell epitopes generated by distinct proteases. J Immunol. 149:498-504.

Waheed, A., Braulke, T., Junghans, U., amnd von Figura, K. (1989). Mannose 6-phosphate/insulin-like growth factor II receptor: the two types of ligands bind simultaneously to one receptor at sidderent sites. Biochem. Biophys. Res. Comm. 152:1248-1254.

Walter, P., and Blobel, G. (1980). Purification of a membrane-associated protein complex required for protein translocation across the endoplasmic reticulum. Proc. Natl. Acad. Sci. USA 77:7112-7116.

Ward, C.J., Crocker, J., Chen, S.J., Stockley, R.A., and Burnett, D, (1990). Changes in the expression of elastase and cathepsin B with differentiation of U937 promonocytes by Gmesf. Biochem. Biophys. Rev. 167:659-664.

Waxdal, M.J., Konigsburg, W.H., Henley, W.L., and Edelman, G.M. (1968). The covalent structure of a human γG-immunoglobulin. II. Isolation and characterization of the cyanogen bromide fragments. Biochemistry 7:1959-1966.

Wessling-Resnick, M., and Braell, W.A. (1990) Characterization of the mechanism of endocytic vesicle fusion in vitro. J. Biol. Chem. 265:16751-16759.

Wiederanders, B., Brömme, D., Kirschkee, H., Kalkkiner, N., Rinne, A., Paquette, T., and Toothman, P. (1991). Primary structure of bovine cathepsin S- comaprison to cathepsin L, cathepsin H, cathepsin B, and papain. FEBS Lett. 286:189-192.

Wilcox, D. The role of cathepsin L in elastin Degradation. Dissertation, 1990.

Wilcox, D. and Mason, R.W. (1992). Inhibition of cysteine proteinases in lysosomes and whole cells. Biochem. J. 285:495-502.

Xin. X-Q., Gunesekara, B., and Mason, R.W. (1992). The specificity and elastinolytic activities of bovine cathepsin S and H. Arch. Biochem. Biophys. 299:334-339.

Zupan, A.A., and Johnson, E.M. Jr. (1991). Evidence for endocytosis-dependent proteolysis in the generation of soluble truncated nerve growth factor receptors by A875 human melanoma cells. J. Biol. Chem. 266:15384-15390.

CURRICULUM VITAE

Adele K. Mountz

340 Hope Road
Stafford, VA 22554
(703) 720-0899

Apt. 3105
1300 University City Blvd.
Blacksburg, VA 24060
(703) 552-3720

EDUCATION:

Ph.D. in Biochemistry;
Virginia Polytechnic Institute and State University
Blacksburg, VA
QCA: 3.78/4.0
May, 1994

B.S. in Biochemistry and Nutrition
Virginia Polytechnic Institute and State University
Blacksburg, VA
QCA: 3.85/4.0
May 5, 1990 Summa cum laude

SCHOLARSHIPS:

Four Year Tuition Waiver, Department of Biochemistry and Nutrition, Virginia Polytechnic Institute and State University, 1990-94

J.L. Pratt Senior Research Grant, Department of Agriculture and Life Sciences, Virginia Polytechnic Institute and State University, 1989

Cyrus McCormick Scholarship, Department of Agriculture and Life Sciences, Virginia Polytechnic Institute and State University, 1988

Robert C. Byrd Scholarship, Department of Education, Commonwealth of Virginia, 1987

Elk's "Most Valuable Student", 1987

Virginia Polytechnic Institute and State University Women Alumni Scholarship, Tidewater Chapter, 1987

AWARDS:

Sigma Delta Epsilon / Graduate Women in Science Eli Lily and Company Travel Awards recipient, March 1992

Annual Awards, Department of Biochemistry and Nutrition, Virginia Polytechnic Institute and State University: "Scholarship Award", May 1990

American Chemical Society James Lewis Howe Award for Research and Scholastic Achievement, April 1990

Alpha Zeta National Agriculture Honorary Fraternity Outstanding Senior in Biochemistry, Virginia Polytechnic Institute and State University, May 1990

Selected to Who's Who Among Students in American Universities and Colleges, 1990

HONOR SOCIETIES:

Alpha Zeta National Agriculture Honorary Fraternity, Virginia Chapter, Fall 1988
Censor: Spring 1989 - May 1990
Pledge Master: Spring 1989

Phi Sigma Biological Sciences Honor Society, Spring 1989

Phi Kappa Phi, Spring 1989

Mortar Board National Senior Honor Society, Spring 1989

Phi Lambda Epsilon National Honorary Chemical Society, Spring 1989

Golden Key National Honor Society, Fall 1988

Gamma Beta Phi Society, Spring 1989

Phi Eta Sigma National Freshman Honor Society, Fall 1988

RESEARCH INTERESTS:

"The Synthesis, Characterization, and Use of a Protein-Cysteine Proteinase Inhibitor Complex for the Study of Endosome/Lysosome Fusio, Ph.D Dissertation research, Department of Biochemistry and Anaerobic Microbiology

(previously the Department of Biochemistry and Nutrition), Virginia Polytechnic Institute and State University, Blacksburg, VA 24061; June, 1990 - May, 1994.

"Mass Spectrometry of Lipid Peroxides", Department of Chemistry, Virginia Polytechnic Institute and State University. (undergraduate research for Dr. G. Sanzone, Spring 1988 - Spring 1990)
-rebuilding a double focusing mass spectrometer
-using the instrument to study lipid peroxidation products

Neurosciences, especially pathological development of Alzheimer's Disease and the possible role of proteinases

PRESENTATIONS:

"Synthesis, Characterization, and Use of a Protein-Cysteine Proteinase Inhibitor Complex for the Study of Endosome/Lysosome Fusion", Adele K. Mountz and Robert W. Mason; poster to be presented to the ASBMB meeting, Washington, D.C., May, 1994.

"Synthesis of a Protein/Cysteine Proteinase Inhibitor Complex for the Study of Endosome/Lysosome Fusion", Adele K. Mountz and Robert W. Mason; poster presented to the International Conference for Proteolysis and Protein Turnover, October 1992, Williamsburg, Virginia.

"Activation of Pro-Cathepsin L", Adele K. Mountz, Steven E. Massey, and Robert W. Mason; poster presented to the Virginia Biochemists Conference, November 1991, Wintergreen, Virginia.

"Methods of Extraction of Novel Cysteine Proteinases", Xue-Qin Xin, Adele K. Mountz, and Robert W. Mason; poster presented April 1991 FASAB Meeting, Atlanta, Georgia

EMPLOYMENT:

Junior Lab Technician: National Health Laboratories, Vienna, Virginia; May - July 1989.
- HDL measurements (Olympus Demand)
- operating four Tecan Ag automatic pipeters

Lab Technician B: Department of Biochemistry and Nutrition, Virginia Polytechnic Institute and State University, Blacksburg, Virginia; for Dr. H. Calvin, Columbia University, March - August, 1988.

- research and design assay for presence of lipid peroxides and hydrogen peroxide in twelve day old mouse lens
- inject nine to twelve day mice
- care for mouse colonies

Musician: Student Volunteer, The Tidewater Winds, Norfolk, Virginia; June 1986 - August 1987.